Aus der Klinik für Neurologie
der Medizinischen Fakultät Charité – Universitätsmedizin Berlin

DISSERTATION

# Regulation of human T cell properties by the micromilieu

zur Erlangung des akademischen Grades
Doctor medicinae (Dr. med.)

vorgelegt der Medizinischen Fakultät
Charité – Universitätsmedizin Berlin

von

Dominik Soll

aus Fulda

Datum der Promotion: 18. September 2020

Teilergebnisse der vorliegenden Arbeit wurden veröffentlicht in:

Matthias, J., Maul, J., Noster, R., Meinl, H., Chao, Y.-Y., Gerstenberg, H., Jeschke, F., Gasparoni, G., Welle, A., Walter, J., Nordström, K., Eberhardt, K., Renisch, D., Donakonda, S., Knolle, P., Soll, D., Grabbe, S., Garzorz-Stark, N., Eyerich, K., Biedermann, T., Baumjohann, D., Zielinski, C.E., 2019. Sodium chloride is an ionic checkpoint for human TH2 cells and shapes the atopic skin microenvironment. Sci. Transl. Med. 11, eaau0683.

Matthias, J., Heink, S., Picard, F., Zeiträg, J., Kolz, A., Chao, Y.Y., Soll, D., de Almeida, G.P., Glasmacher, E., Jacobsen, I.D., Riedel, T., Peters, A., Floess, S., Huehn, J., Baumjohann, D., Huber, M., Korn, T., Zielinski, C.E., 2020. Salt generates antiinflammatory Th17 cells but amplifies pathogenicity in proinflammatory cytokine microenvironments. J. Clin. Invest. 137786.

Das Wissen hat Grenzen, das Denken nicht.

–

Albert Schweitzer

**Table of content**

**List of figures and tables**

**Abstract**

T cells represent a central component of the human adaptive immune system. Among them, $CD4^+$ T helper cells and $CD8^+$ cytotoxic T cells can be distinguished which either mediate the actions of other immune cells or kill affected cells, respectively. Their proper function is dependent on an appropriate surrounding micromilieu, which classically includes other cell types as well as chemokines and cytokines. Interestingly, recent findings suggest that also the osmolarity of the microenvironment may have an influence. Since osmolarity is substantially higher in lymphatic tissue and other immunologically active compartments than in plasma, I investigated what kind of alterations this hypertonicity can evoke in different effector T cell species. Due to their relevance in autoimmune and tumor diseases, $T_h17$ and $CD8^+$ T cells have been in the focus of my studies.

To investigate phenotypical and metabolic changes, $T_h17$ cells and $CD8^+$ T cells have been cultured and stimulated in hypertonic medium and subsequently analyzed. Additionally, shRNA and molecular inhibitors were utilized to uncover possible underlying molecular pathways. Consequently, to analyze functional alterations in hypertonicity, $CD8^+$ T cells specific for MART-1 were purified and their cytolytic capability towards target cells presenting MART-1 was evaluated in a hypertonic environment.

Upon activation under hypertonic conditions, the $T_h17$ phenotype was significantly augmented within the $T_h17$ cell population, though this was going hand in hand with induction of anti-inflammatory markers such as FOXP3 and TGF-β expression. I was able to illustrate that both effects were mediated via the p38 MAP kinase pathway. Moreover, cytotoxic T cells showed significant increase of their cytolytic capability in hypertonic medium. It correlated with enhanced expression of granzyme B, perforin and TNF-α as well as alternative cytolytic molecules such as TRAIL. Similarly, the cytotoxic T cells demonstrated augmented cell activation and cell metabolism in a hyperosmotic microenvironment.

Concurrence of the upregulation of pro- and anti-inflammatory features in $T_h17$ cell subsets in a hypertonic microenvironment indicates a relevant role in $T_h17$-mediated autoimmune diseases. Moreover, enhanced cytotoxic activity of $CD8^+$ T cells in higher osmolarity may represent a vital part of the defense system protecting the human body from pathogens and preventing tumor growth. These findings may bring about therapeutic innovations in the highly investigated field of adoptive T cell therapies, making the deployed $CD8^+$ T cells even more effective. Lastly, considering osmolarity when investigating T cell functionality will become essential in future to obtain reliable, relevant and translational findings.

**Zusammenfassung**

T-Zellen stellen einen zentralen Bestandteil des Immunsystems des menschlichen Körpers dar. Man unterscheidet $CD4^+$ T-Helferzellen und $CD8^+$ zytotoxische T-Zellen, deren jeweilige Funktionen vom jeweils umgebenden Mikromilieu beeinflusst werden, das sich klassischerweise aus anderen Zellen, Pathogenen und Zytokinen zusammensetzt. Neue Erkenntnisse zeigen jedoch, dass auch die Osmolarität der Umgebung einen Einfluss auf die Zellen haben kann. Die Osmolarität in lymphatischem Gewebe und anderen immunologisch aktiven Kompartimenten ist signifikant höher als im Blutplasma. Daher habe ich die Veränderungen untersucht, die diese Hyperosmolarität in verschiedenen Effektor-T-Zellen hervorrufen. Im Fokus meiner Untersuchungen standen $T_h17$- und zytotoxische $CD8^+$ T-Zellen, da sie im Rahmen von Autoimmun- und Tumorerkrankungen eine klinisch relevante Rolle spielen.

Zur Untersuchung phänotypischer und metabolischer Veränderungen wurden $T_h17$- und $CD8^+$ T-Zellen in hypertonischem Medium kultiviert, stimuliert und anschließend analysiert. Der zugrundeliegende Mechanismus wurde mithilfe von shRNA sowie molekularen Inhibitoren untersucht. Zur Analyse funktioneller Veränderungen wurden MART-1-spezifische $CD8^+$ T-Zellen isoliert, deren zytolytisches Potenzial anschließend in Zytotoxizitätstests untersucht wurde.

$T_h17$-Zellen zeigten einen verstärkten $T_h17$-Phänotyp sowie antiinflammatorische Eigenschaften wie FOXP3- und TGF-β-Expression, wenn sie unter hypertonischen Bedingungen aktiviert wurden. Beide Veränderungen wurden durch den p38-MAP-Kinase-Signalweg einschließlich NFAT5 und SGK1 reguliert. Hingegen zeigten zytotoxische T-Zellen in hypertonischem Medium signifikant verbesserte zytolytische Fähigkeiten, die durch verstärkte Expression von Granzyme B, Perforin, und TNF-α sowie weiterer zytolytischer Moleküle wie TRAIL vermittelt wurden. Ebenso wiesen zytotoxische T-Zellen auch eine gesteigerte Aktivierung und erhöhte Stoffwechselleistung unter hypertonischen Bedingungen auf.

Die Verstärkung sowohl von pro- als auch antiinflammatorischen Charakteristiken in $T_h17$-Zellen in hypertonischer Umgebung deutet auf eine mögliche Relevanz dieser Ergebnisse in der Pathogenese von $T_h17$-vermittelten Autoimmunerkrankungen hin. Die gesteigerte Aktivität von $CD8^+$ T-Zellen in hypertonischer Umgebung könnte Teil der gesunden Immunabwehr sein, die den menschlichen Körper vor Pathogenen oder bösartigem Tumorwachstum schützt. Darüber hinaus ergeben sich aus diesen Ergebnissen möglicherweise praktische Anwendungen auf dem Gebiet der adoptiven T-Zelltherapie. Letztlich zeigen meine Ergebnisse, dass die Berücksichtigung von osmotischen Faktoren bei Untersuchungen zu T-Zellfunktionen relevant ist.

# 1. Introduction

## 1.1. From infection to adaptive immune responses

Microorganisms that penetrate the physical barriers of the human body quickly encounter its highly potent immune system. Common classification of the immune system discriminates between innate and adaptive immunity. The innate immune system represents the body's first response towards a potential pathogen. Classically, it involves many different cell species producing an unspecific and generalized inflammatory response towards the intruding microbes. Macrophages, already present in the tissue, recognize certain fragments of microorganisms that lead to their activation. Consequently, macrophages phagocyte extracellular pathogens and release small inflammatory molecules, chemokines and cytokines. In combination with activation of the complement system, these molecules recruit other inflammatory cells like granulocytes and monocytes towards the infection site. Neutrophil granulocytes, that engulf and destruct the intruders, represent the principal effector cells in this early phase of inflammation. Responses of the innate immune system are rapid and broad means to clear pathogens. However, these unspecific defense mechanisms are not sufficient to fight off every kind of infection. Therefore, as a second line of defense, a highly specific reaction towards the microorganisms is necessary. It can be provided only by lymphocytes that constitute the adaptive immune system. Noteworthy, adaptive immune reactions lead to an immunological memory so that future infections with the same pathogen result in accelerated and specific immune response. (Janeway et al., 2001a, 2001b) The importance of adaptive immunity can be better understood by considering immunological disorders in which lymphocyte function is impaired. For example, in severe combined immunodeficiency or advanced human immunodeficiency virus (HIV) infection, hindrance of the immune system leads to numerous opportunistic infections (Allenspach et al., 1993; Huang and Crothers, 2009).

In order to ignite adaptive immune processes, antigen-presenting cells, most notably dendritic cells, have to ingest and degrade the pathogen. Subsequently, they migrate to a nearby lymph node to present the processed antigens to naïve T lymphocytes on major histocompatibility complex (MHC) II surface molecules. Due to almost infinite diversity in the T cell receptor repertoire, the encounter with a T cell specifically recognizing the presented epitope is highly probable. Cognate recognition of the antigen leads to clonal proliferation of the specific T cell as well as cell activation and differentiation into an effector T cell. These activated T cells will migrate to the primary infection site to exert their function. (Abbey and O'Neill, 2007)

The T lymphocyte population diverges in terms of expression of certain clusters of differentiation (CD) on the cell surface and can be subdivided in $CD4^+$ and $CD8^+$ T cells. $CD4^+$ T cells are stimulated by antigens presented on MHC II complexes by antigen-presenting cells and activate macrophages or B lymphocytes in order to eliminate intracellular and extracellular bacteria and viruses. On the other hand, $CD8^+$ cells can be stimulated by all body cells which present peptides via their MHC I molecules. MHC I molecules are surface protein complexes that are utilized by almost all body cells to present antigens to immune cells. Upon activation, $CD8^+$ deploy several cytolytic mechanisms to kill the target cell with the recognized epitope, making them essential for clearance of viral infections as well as mutated tumor cells. In accordance with their respective classical functions, $CD4^+$ cells are called T helper ($T_h$) cells while $CD8^+$ T cells are known as cytotoxic T lymphocytes (CTL). (Janeway et al., 2001a) The distinct functions of the different mature T cell species will be dealt with in the next chapters. After successful clearance of the infection, most effector T cells will disappear while some remain to form memory T cells (Pepper and Jenkins, 2011).

### 1.2. T helper cell functions in health and disease and the role of the micromilieu

Upon antigen presentation by a dendritic cell, epitope-specific naïve $CD4^+$ T cells will start to proliferate and differentiate into effector $T_h$ cells. Noticeably, there are several different classes of $T_h$ cells, each exerting distinct functions during an immune reaction. Classically, they were distinguished between $T_h1$ and $T_h2$ cells that differ in their typical cytokine profile as well as the recruitment of different supporter cells. $T_h1$ cells characteristically produce Interferon-γ (IFN-γ) and activate majorly macrophages by increasing their phagocytic functions and supporting them in overcoming intracellular bacterial infections. Conversely, $T_h2$ cells produce mostly interleukin (IL)-4 and IL-5 and activate B cells to promote antibody production, an essential step in order to fight toxins, viruses and extracellular bacteria. (Raphael et al., 2015)

Our understanding of the different T cell species has immensely increased and new functional features are continuously being discovered. In 2005, a novel distinct lineage within the $T_h$ cell population has been described, the $T_h17$ cells (Harrington et al., 2005). Among other things, they produce IL-17 and IL-22 as well as express the surface marker chemokine receptor (CCR) 6 and transcription factor RAR-related orphan receptor-γt (RORγt) (Acosta-Rodriguez et al., 2007; Annunziato and Romagnani, 2009; Oestreich and Weinmann, 2012). They represent crucial players in host defense against extracellular pathogens including fungi and eukaryotes (Curtis and

Way, 2009). Gradually, other new T helper cell species that did not fit into the classical schema have been characterized; most prominent examples are $T_h9$ and $T_h22$ cells which – similar to $T_h17$ cells – are also named after the principal effector interleukins that they produce. However, the discovery of $T_h17$ cells is of special interest, because IL-17 has been associated with several autoimmune diseases such as psoriasis, rheumatoid arthritis and multiple sclerosis (MS) (Kotake et al., 1999; Lock et al., 2002; Wong et al., 2008).

The frequency of $T_h17$ cells has been shown to be increased in skin lesions and peripheral blood of patients suffering from psoriasis (Kagami et al., 2010; Lowes et al., 2008). In rheumatoid arthritis, peripheral $T_h17$ cell levels have been shown to correlate with the severity of clinical symptoms and their activity appears to be involved in bone destruction (Kim et al., 2013; Sato et al., 2006). However, the picture is more complex in MS. MS is a chronic autoimmune neurological disorder, during which neurons in the central nervous system are being demyelinated, which disrupts the function of the underlying nervous tissue. Symptoms often include visual, physical and psychiatric problems, although almost every functional system can potentially be affected. $T_h17$ cells are not only more abundant in the peripheral blood of MS patients, but they are also detected at higher frequency in the cerebrospinal fluid with even greater numbers during an acute episode (Li et al., 2011; Matusevicius et al., 1999). Furthermore, they are able to disrupt tight junctions within the blood-brain barrier, what may contribute to subsequent immune reactions inside the central nervous system (Kebir et al., 2007).

Besides their role in health and disease, there is another feature in $T_h17$ cells that makes them highly relevant in research: their close connection to regulatory T ($T_{reg}$) cells. The principal function of $T_{reg}$ cells is the maintenance of tolerance to self-antigens, which they achieve by the release of the anti-inflammatory cytokines IL-10, transforming growth factor β (TGF-β) as well as by cytolysis of other immune cells, induction of IL-2 deprivation and suppression of dendritic cells function (Vignali et al., 2008).

Even though $T_h17$ cells and $T_{reg}$ cells appear very different, they share many similarities such as their priming cytokine milieu. Differentiation of naïve T cells into effector and memory T cells can be modelled *in vitro* by exposition to a certain cytokine mix. To produce $T_h17$ or $T_{reg}$ cells, TGF-β is a necessary factor, among other things. The only difference is the absence of additional IL-6 to generate $T_{reg}$ cells as this interleukin is essential for the creation of $T_h17$ cells (Kimura and Kishimoto, 2010; Zheng, 2013). These similar formation conditions suggest a tight bond between these two subsets. In fact, the lineage frontiers between $T_h17$ and $T_{reg}$ cells are not as impermeable

as originally proposed for other T cell species. It is defined by a phenomenon called T cell plasticity. Dependent on changes in their micromilieu effector T cells of one class can obtain the phenotype and potentially the function of another. This feature is especially prominent between $T_h17$ and $T_{reg}$ cells (Zhou et al., 2009). Some T cells have been described as co-producing the hallmark cytokines of both, $T_h17$ and $T_{reg}$ cells, as well as co-expressing both their master transcription factors, RORγt and Forkhead box P3 (FOXP3), respectively (Voo et al., 2009; Zhou et al., 2009). These cells are in plastic interstate between the $T_h17$ and regulatory phenotype and have been found in several pathological settings. Interestingly, they combine functional features of both classes, producing high levels of $T_h17$ associated pro-inflammatory cytokines like IL-17 as well as exerting suppressive function on other immune cells (Chellappa et al., 2015). Additionally, anti-inflammatory features in $T_h17$ cells have also been shown in another context. Discussing the effect of the cytokine milieu on $T_h17$ functions, Zielinski et al. have shown that $T_h17$ cells can co-produce either the pro-inflammatory IFN-γ or the anti-inflammatory IL-10 and TGF-β depending on the pathogens used for the stimulation (Gutcher et al., 2011; Zielinski et al., 2012). This effect was subsequently pinpointed to the presence or absence of IL-1β in the environment. Consistently, the ability in $T_h17$ cells to suppress proliferation of other T cells depends on the presence of IL-1β in the environment. Since IL-1β seems to induce pro-inflammatory features, only $T_h17$ cells induced in the absence of it are successfully able to exert regulatory functions. (Noster et al., 2016, 2015)

These studies emphasize the relevance of the composition of the micromilieu for the differentiation of T cells as well as for potential plastic changes and interphases between the T cell subsets. Furthermore, the respective microenvironment of the T cells appears to determine their acute functionality. Their two-headed nature, their relevance in conditions of health and disease within the adaptive immune system and in autoimmune diseases, as well as their functional dependence on factors in their micromilieu make $T_h17$ cells especially interesting targets of research.

### 1.3. The functionality of cytotoxic T cells and the role of the micromilieu

As mentioned before, $CD8^+$ cytotoxic T cells have their own distinct set of skills to exert their specific functions. Presentation of deformed antigens on malfunctioning body cells' MHC I complex leads to activation of antigen-specific $CD8^+$ cytotoxic T cells. Activated T cells can be identified by surface expression of CD69 and PD-1, which are established activation markers of memory T cells upon polyclonal αCD3/CD28 stimulation. CD69 is one of the earliest activation

markers being expressed already after only a few hours. (Agata et al., 1996, p. 1; Ziegler et al., 1994, p. 69)

Upon activation, effector T cells undergo vast changes in their cell metabolism. Resting T cells produce ATP predominantly by fatty acid β-oxidation and oxidative phosphorylation. Upon activation as the demand for energy increases, fatty acid β-oxidation is downregulated while oxidative phosphorylation remains engaged and the more rapid aerobic glycolysis becomes the predominant ATP supplier. (Pearce et al., 2013)

The activation leads to CTL-mediated killing by disruption of the epitope-presenting body cells. Classically, this disruption is caused by programmed cell death, also known as apoptosis. Apoptosis represents a suicidal program that can be conducted by almost all cells of the human body. (Janeway et al., 2001c) A recent study using *in vivo* imaging techniques has shown that cell death in these target cells happens mostly within 20 to 120 minutes after the first contact between the CTL and the affected target cell (Halle et al., 2016).

Several mechanisms are known today, by which CTLs evoke apoptosis in target cells. Release of pro-inflammatory cytokines is one of these techniques. It is mainly supporting the general immune response and, thus, supplying assistance in further inflammatory reactions. IFN-γ and tumor necrosis factor α (TNF-α) are the most significant among the released cytokines. IFN-γ is fundamental for anti-viral reactions, such as inducing upregulation of the expression of MHC I molecules in surrounding potentially infected cells. Among other things, it leads to activation of macrophages, which help to clear the infection and remove cell remains. TNF-α has two distinct effects on target cells. On the one hand, it leads to expression of NFκB in other immune cells, consequently boosting inflammatory response, host defense, and cell proliferation. On the other hand, it can activate a caspase cascade in target cells which results in cell death via apoptosis. (Boehm et al., 1997; Kalliolias and Ivashkiv, 2016) However, the cytolysis directly induced by TNF-α takes more than 18 hours and is not the primary pathway during acute lysis reactions (Ratner and Clark, 1993).

The perforin/granzyme pathway represents the most prominent and important mechanism employed by CTLs to eliminate cells. CTLs carry granules containing perforin, granzymes and other cytolytic mediators that can be released upon activation by a target cell presenting the correct antigen via its MHC I complex. When the granules fuse with the cell membrane the expression levels of the granules' glycoprotein CD107a (LAMP1) are increased on the cell surface, which makes it a reliable marker for degranulation (Aktas et al., 2009). Even though the exact interactions

of perforin and granzymes are still under investigation, the classical view already gives a large insight into the mechanism. Upon release in the vicinity of a target cell, perforin generates a pore in the target cell's plasma membrane, enabling the granzymes to enter. Subsequently, the granzymes will initiate the programmed cell death. However, other modes of entry have been shown for granzymes and their intracellular functionality also appears to depend on the presence of perforin. (Pinkoski et al., 1998) The consequent cascade leading to cell death is better understood. Among the cytolytic mediators, granzyme B represents the most potent player. Through a series of reactions, mainly based on proteolytic cleavage and including the activation of initiator caspases, it provokes certain irreversible effects such as DNA fragmentation and mitochondrial disruption. This will ultimately culminate in the death of the cell. (Barry and Bleackley, 2002) Other cytolytic proteins that exist within the granules, including granzyme A or granulysin, can also support this process in different ways, including caspase-independent pathways. (Voskoboinik et al., 2015) Expression of the effector molecules granzyme B, perforin and IFN-γ is regulated by the transcription factor RUNX3, among others (Cruz-Guilloty et al., 2009, p. 3).

A third pathway of cytotoxicity is mediated by interaction of so-called death receptors on the target cell's surface and their ligands expressed on the surface of CTLs. Among the better known death receptor ligands, the most intensively studied are Fas ligand (FasL) and TNF-related apoptosis-inducing ligand (TRAIL). Upon binding of the ligand, the death receptors will activate intracellular cell death effector molecules such as the aforementioned caspases. Consequently, the apoptosis program is initiated. (Guicciardi and Gores, 2009) Of note, some non-cytotoxic functions of the death receptor signaling have recently been discovered – among others, activation of NFκB which conversely is able to increase resistance to apoptosis (Falschlehner et al., 2007; Legembre et al., 2004). Nevertheless, the cell death inducing pathways appear to be dominant over any anti-apoptotic effects (Ishimura et al., 2006).

Noteworthy, recent studies demonstrate that effector and memory $CD8^+$ T cells are also influenced by the cytokine milieu in which they act (Kim and Harty, 2014). For instance, Richer et al. were able to show that pro-inflammatory cytokines such as IL-12 enhance signaling of the T cell receptor resulting in increased antigen sensitivity (Richer et al., 2013). This finding demonstrates that the micromilieu is not only important for T helper cell functions but also for the functionality of CTLs. When investigating the role of the micromilieu on T cell functions, the focus has mainly been on cell-cell-contacts, cytokine composition and presence of certain pathogens. However, there is another important factor of the cells' microenvironment which has been shown to vary

greatly between different body compartments and whose effects on T cells are consequently highly relevant to uncover: the osmolarity.

### 1.4. Variations in osmolarity in the human body and their implications on T cell functions

Osmolarity is the quantitative measure of the amount of particles in solution in a certain volume of a liquid. Tonicity is a qualitative measure to describe the osmotic pressure gradient between two solutions separated by a semipermeable membrane such as the cell membrane. (Lombard, 2014)

It has long been believed that the osmolarity within the human body is quite stable and resembles the one in plasma – except for the kidney where very high osmolarity levels have been known already for some time (Sands and Layton, 2009). However, recent research has found the osmolarity to vary widely between different compartments of the human body. The changes in osmolarity can be appreciated by understanding the body's sodium homeostasis. Long-term studies on subjects for future Mars missions revealed that the daily sodium intake and output only rarely match: even though their intake was the same every day, their sodium excretion did not resemble their consumption. Interestingly, rather weekly or monthly than daily phases were found to determine the sodium excretion. (Rakova et al., 2013; Titze et al., 2002) This finding suggests that there is a storage of excess sodium inside the body. In 2004, Go et al. demonstrated that, in mice, the sodium concentration is significantly increased in lymphoid organs to levels between 160 and 250 mmol/l (Go et al., 2004). Parallelly, Titze et al. found that, after feeding rats with a high-salt diet, the excess body sodium was stored within the skin increasing the sodium concentration to up to 190 mmol/l compared to 140 mmol/l in plasma (Titze, 2004). A novel technique, the magnetic resonance imaging of $^{23}Na$, allows visualizing the sodium contents in all compartments and organs of the human body, revealing sodium accumulation not only in skin, but also in muscle and brain (Inglese et al., 2010; Kopp et al., 2013, 2012).

Since lymphoid tissue accommodates a broad range of immune processes, analysis of the effects of the hyperosmolarity predominant in lymphoid organs (e.g. the thymus and lymph nodes) on immune cells is crucial. Naïve T cells mature in the thymus to emigrate into the periphery, circulate and enter the lymph nodes awaiting to be activated. In addition, T cell differentiation may take place under hyperosmotic conditions. Kleinewietfeld et al. have investigated the effects of hyperosmolarity on T cell differentiation and found that the generation of $T_h17$ cells was highly boosted, whereas other T helper cell lineages remained less affected (Kleinewietfeld et al., 2013).

(Fig. 1.1) The discovered effect correlated with more severe forms of experimental autoimmune encephalomyelitis (EAE) in mice fed a high-salt diet. Mechanistically, the p38 mitogen-activated protein (MAP) kinase pathway involving the nuclear factor of activated T cells 5 (NFAT5) and further downstream the serum and glucocorticoid-regulated kinase 1 (SGK1) were identified as relevant mediators of the effects of the hypertonicity on naïve $CD4^+$ T cells (Kleinewietfeld et al., 2013; Wu et al., 2013). p38 MAP kinase was already known to control IL-17 production in T helper cells as well as severity of EAE (Noubade et al., 2011), while NFAT5 – the only known osmosensitive transcription factor in mammals – has been described before to be essential for survival and appropriate immune response of T cells in hypertonicity (Go et al., 2004). Another study investigated the effect of hyperosmolarity on regulatory T cell functions and demonstrated that $T_{reg}$ cells show reduced suppressive capability in a hypertonic environment (Hernandez et al., 2015).

However, sodium accumulation does not only occur in physiological lymphoid tissue, but does also happen in tissues during pathological, especially inflammatory and neoplastic processes. Schwartz et al. have shown that infection with Bacillus Calmette–Guérin (BCG) doses induced local extracellular hyperosmolarity in mice with values of up to 600 mosmol/l. In addition, they demonstrated that cytokine production and secretion upon stimulation of a human T24 cell line was proportional to osmolarity levels in its microenvironment. (Schwartz et al., 2009) Consistently, sodium content in the skin has been shown to be increased during infections in humans (Jantsch et al., 2015). Analogously, increased sodium concentrations within MS lesions have been recently confirmed (Paling et al., 2013).

Likewise, the tumor microenvironment appears to be characterized by increased osmolarity levels. Due to vascular fenestration, tumor vessels are highly permeable to plasma proteins such as albumin, which exerts extracellular hyperosmotic stress on all cells in the tumor microenvironment (Feng et al., 2000). Additionally, solid tumor cells are permanent targets of physical stress generated by the growth of the tumor itself. The mechanical stress causes sodium efflux in the tumor elevating the osmolarity levels in its microenvironment (McGrail et al., 2015).

Thus, inflammation and tumor sites have increased levels of osmolarity. They accommodate many immune reactions of effector T cells such as $T_h17$ cells and CTLs. The effects of hypertonicity – as an important factor of the micromilieu for immune cells – on T cell differentiation have already been described in past studies, the effect of hypertonicity on the functions of effector T cells remains less well investigated (Fig. 1.1).

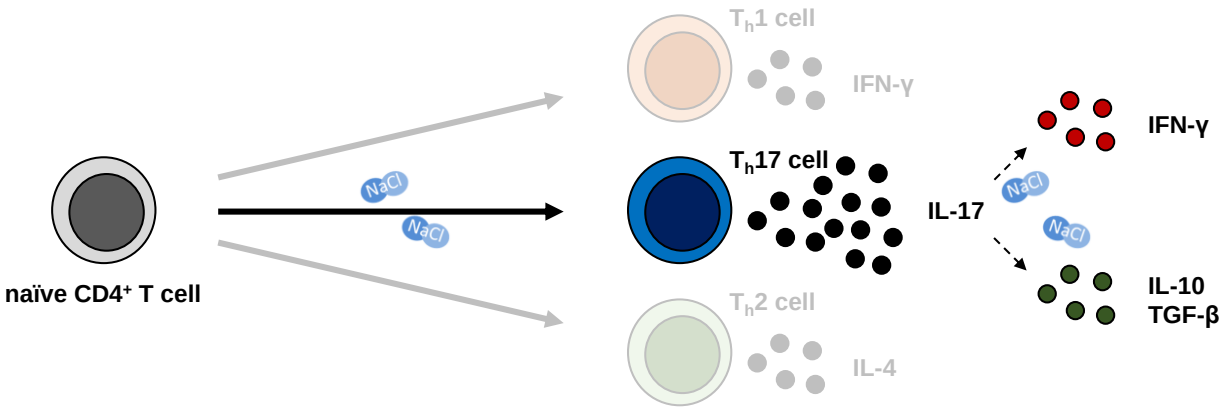


**Figure 1.1. Effects of hyperosmolarity on T helper cell differentiation and plasticity.** Kleinewietfeld et al. have shown that the differentiation of $T_h17$ cells is highly induced, if naïve $CD4^+$ T cells are stimulated under hypertonic conditions, while $T_h1$ and $T_h2$ differentiation is less affected. The $T_h17$ cells can develop a pro- or anti-inflammatory phenotype producing either pro- or anti-inflammatory cytokines.

## 1.5. Aims of the study

Most of the *in vitro* studies about human immune responses are conducted in an isotonic environment. However, in the human body many immune reactions take place under conditions of increased osmolarity, such as during inflammation and at tumor sites. It is the aim of this study to investigate if the hypertonic milieu affects the functionality of different effector T cell classes. Effector T cells – fundamental players within the adaptive immune system – have a pivotal role in the coordination of inflammation as well as in tumor control.

$T_h17$ cells are one of the most relevant types of effector T cells and have been shown to be of major importance in the pathophysiology of various autoimmune diseases. They are especially prone to plastic changes and can develop a pro- or anti-inflammatory phenotype. Thus, in the first part of my thesis, I have analyzed the influence of a hypertonic environment on the cells' phenotype and subsequently investigated the molecular mediators of these effects in primary human $T_h17$ cells.

In the second part, I have focused on how the hypertonic environment could shape the functionality of cytotoxic T cells. They play central roles in the restraint of viral infections as well as in tumor control. To explore the significance of hypertonicity herein, I have investigated its effects on the activation level, phenotype, metabolism and killing efficiency of primary human cytotoxic T cells. Since $CD4^+$ T cells can exert certain cytotoxic functions, too, these cells were investigated with respect to certain cytotoxic functions, as well (Takeuchi and Saito, 2017).

## 2. Materials and Methods

### 2.1. Materials

#### 2.1.1. Plastics and commodities

| Item | Company |
|---|---|
| 384-well Assay Plate | Corning |
| CELLSTAR® Tubes 15ml, 50ml | Greiner bio-one |
| Electrophoresis cuvettes | Mirus Biotech® |
| E-Plate 96 | ACEA Biosciences |
| F96 MaxiSorp NUNC-Immuno Plate | Thermo Scientific |
| Falcon® 24-well Microplate | Corning |
| Falcon® 96 Well Round Bottom | Corning |
| FrameStar® 384 | 4titude |
| Minisart® filter (0,45 µm) | Sartorius |
| PCR Strips of 8 caps | Brand |
| PCR Strips of 8 tubes | Brand |
| Safe-Lock Tubes 1.5 ml | Eppendorf |
| VWR® Tissue Culture Flask, 75 $cm^2$ | VWR |
| XF96 cell culture microplate | Agilent Technologies |
| $XF^e96$ extracellular flux assay kit | Agilent Technologies |

#### 2.1.2. Equipment

| Type of Equipment | Model | Company |
|---|---|---|
| Balance | CP 124 S | Sartorius |
| Cell separator | autoMACS® Pro Separator | Miltenyi Biotec |
| Centrifuges | Biofuge fresco<br>Centrifuge 5810R<br>Multifuge 3 S-R<br>Sorvall RC 6+ | Heraeus<br>Eppendorf<br>Heraeus<br>Thermo Scientific |
| Electroporator | Nucleofector IIb | Lonza |
| Flow cytometer | CytoFLEX<br>FACSAria™ IIIu | Beckman Coulter<br>BD Biosciences |

| | | |
|---|---|---|
| | MoFlo Legacy Cell Sorter | Beckman Coulter |
| Hemocytometer | Neubauer improved | Marienfeld Superior |
| Incubator | HERAcell 240 | Heraeus |
| Laminar flow hood | HERAsafe | Heraeus |
| Metabolic assay platform | Seahorse XFe96 Analyzer | Agilent Technologies |
| Microscope | Axiovert 25 | Carl Zeiss |
| PCR detection system | CFX384 Touch™ | Bio-Rad |
| pH meter | Routine meter pH 526 | Sigma-Aldrich |
| Pipette | Pipetman P10, 20, 200, 1000 | Gilson |
| Pipettor | Stripettor™ Plus | Corning |
| Radiation source | OB 29 | Buchler |
| Real-time cell analyzer | xCELLigence RTCA MP | ACEA Biosciences |
| Thermal cycler | T3000 Thermocycler | Biometra |
| Water bath | Typ 1013 | GFL |
| Electrolyte measuring unit | Cobas® 8000 | Roche |

### 2.1.3. Chemicals and reagents

| **Chemical / Reagent** | **Company** |
|---|---|
| 1-Bromo-3-chloropropane | Sigma |
| 2-Mercaptoethanol | Gibco® by Life Technologies |
| 2-Propanol | Roth |
| Ampicillin | Roth |
| Antimycin A | Sigma |
| Biocoll Seperating Solution | Merck |
| Bovine Serum Albumin | Serva |
| Brefeldin A | Sigma |
| Calcium chloride | Merck |
| CCCP | Sigma |
| CFSE | Thermo Scientific |
| DMEM (1x) | Gibco® by Life Technologies |
| DMSO | Sigma |
| Dulbecco's PBS | Sigma |

| | |
|---|---|
| Dulbecco's PBS (with Ca & Mg) | PAA |
| EDTA | Roth |
| Ethanol | Roth |
| Fetal Bovine Serum (FCS) | Merck |
| Ficoll-Paque™ PLUS | GE Healthcare |
| Glucose | Sigma |
| GlutaMAX™ (100x) | Gibco® by Life Technologies |
| GSK650394 (SGK1 inhibitor) | R&D Systems |
| Human Serum (HS) | Pool of 12 donors, Munich |
| IL-2 | in-house preparation |
| Ionomycin | Sigma |
| LB Broth | Roth |
| MART-1 peptide (26-35; A27L)<br>*ELAGIGILTV* | Biosyntan GmbH |
| MEM NEAA (100x) | Gibco® by Life Technologies |
| Oligomycin A | Sigma |
| Penicillin / Streptomycin<br>(10 000 U/ml / 10 000 µg/ml) | Merck |
| Phorbol 12-myristate 13-acetate (PMA) | Sigma |
| Phytohemagglutinin (PHA) | Thermo Scientific |
| pMHC complex | Busch lab, TU Munich |
| Propidium iodide | eBioscience |
| Puromycin | Sigma |
| RNase-free water | Roth |
| Rotenone | Sigma |
| RPMI 1640 (1x) | Gibco® by Life Technologies |
| RPMI 1640 with 20 mM Hepes | Merck |
| SB202190 (p38 inhibitor) | Sigma |
| Sodium chloride | Sigma |
| Sodium Pyruvate (100x) | Gibco® by Life Technologies |
| Streptavidin-APC | Biolegend |
| Streptavidin-BV421 | Biolegend |
| TaqMan® Fast Universal PCR Master Mix | Applied Biosystems |

| | |
|---|---|
| Transposase SB100X | Busch lab, TU Munich |
| Transposon coding for MART-1-specific TCR | Busch lab, TU Munich |
| TRI Reagent® | Sigma |
| Trypsin-EDTA Solution | Sigma |
| Unbuffered RPMI 1640 | Sigma |

### 2.1.4. Buffers and media

| **Medium** | | **Composition** |
|---|---|---|
| Cell line growth medium | | DMEM (1x) |
| | 1 % | Sodium Pyruvate (100x) |
| | 1 % | MEM NEAA (100x) |
| | 1 % | GlutaMAX™ (100x) |
| | 1 % | Penicillin / Streptomycin |
| | 10 % | FCS |
| Complete medium (FCS) / Complete medium (HS) | | RPMI 1640 (1x) |
| | 1 % | Sodium Pyruvate (100x) |
| | 1 % | MEM NEAA (100x) |
| | 1 % | GlutaMAX™ (100x) |
| | 1 % | Penicillin / Streptomycin |
| | 0,1 % | 2-Mercaptoethanol |
| | 10 % | FCS or |
| | 5 % | HS |
| MACS buffer | | PBS |
| | 5 % | FCS |
| | 2 mM | EDTA |
| NaCl stock | | PBS |
| | 2,7 M | NaCl |
| Seahorse assay medium | | Unbuffered RPMI 1640 |
| | 1 % | GlutaMAX™ (100x) |
| | 2 g/l | Glucose |
| T cell assay medium | | Complete medium (HS) |
| | 50 U/ml | IL-2 |

| | | |
|---|---|---|
| Wash buffer | 1 % | RPMI 1640 with 20 mM Hepes<br>FCS |

### 2.1.5. Antibodies

| **Antibodies used for flow cytometry** | **Clone** | **Company** |
|---|---|---|
| αCCR4-PECy7 | TG6 | Biolegend |
| αCCR6-PE | 11A9 | BD |
| αCD107a-APC | H4A3 | Biolegend |
| αCD19-ECD | J3-119 | Beckman Coulter |
| αCD3-FITC | UCHT1 | Biolegend |
| αCD45RA-FITC | ALB11 | Beckman Culter |
| αCD4-PECy7 | A161A1 | Biolegend |
| αCD69-PECy7 | FN50 | Biolegend |
| αCD8-APC | HIT8a | Biolegend |
| αCXCR3-APC | 1C6 | BD Biosciences |
| αFOXP3-FITC | PCH101 | eBioscience |
| αGranulysin-PE | DH2 | Biolegend |
| αGrzA-PB | CB9 | Biolegend |
| αGrzB-FITC | GB11 | Biolegend |
| αIFN-γ-PECy7 | 4S.B3 | Biolegend |
| αIL-10-APC | Jes3-19F1 | BD Biosciences |
| αIL-17-APCCy7 | BL168 | Biolegend |
| αIL-22-PE | 2G12A41 | Biolegend |
| α-mouse-TCR β-chain-APC | H57-597 | Biolegend |
| αPD-1-BV421 | EH12.2H7 | Biolegend |
| αPerforin-PB | B-D48 | Biolegend |
| αRORγt-PE | AFKJS-9 | eBioscience |
| αTGF-β-BV421 | TW4-9E7 | BD Biosciences |
| αTNF-α-FITC | 2-179-E11 | DRFZ |

| **Antibodies used for stimulation** | **Clone** | **Company** |
|---|---|---|
| αCD28 | CD28.2 | BD Biosciences |

| | | |
|---|---|---|
| αCD3 | TR66 | Enzo |

### 2.1.6. TaqMan® primers/probes

| **Target Gene** | **all by Thermo Scientific** |
|---|---|
| *FASLG* | Hs00181225_m1 |
| *FOXP3* | Hs01085834_m1 |
| *NFAT5* | Hs00232437_m1 |
| *RNA18S5* | Hs03928990_g1 |
| *RORC* | Hs01076122_m1 |
| *RUNX3* | Hs00231709_m1 |
| *SGK1* | Hs00985033_g1 |
| *TNFSF10* | Hs00921974_m1 |

### 2.1.7. Kits

| **Kit** | **Company** |
|---|---|
| BD Cytofix/Cytoperm™ | BD Biosciences (554714) |
| CD4 MicroBeads, human | Miltenyi |
| FOXP3/Transcription Factor Fixation/Permeabilization Concentrate and Diluent | eBioscience (00-5521-00) |
| High Capacity cDNA Reverse Transcription Kit | Applied Biosystems |
| MaxiPrep | QIAGEN |
| PureYield™ MidiPrep | Promega |
| Zombie Yellow™ Fixable Viability Kit | Biolegend |

### 2.1.8. Cell lines

| **Cell line** | **Company** |
|---|---|
| A-375 | ATCC® CRL-1619 |
| HEK-293 | ATCC® CRL-1573 |

### 2.1.9. Bacterial stocks and plasmids

| **Plasmid** | **Supplier** |
|---|---|
| psPAX2 (packaging plasmid) | Gift from Didier Trono (Addgene plasmid #12260) |
| pMD2.G (envelope plasmid) | Gift from Didier Trono (Addgene plasmid #12259) |
| shNFAT5<br>*TRCN0000437810*<br>(CCGGGTGGACTGCGTAGGGATATTGCTCGAGCAATATCCCTACGCAGTCCACTTTTTTG)<br>*TRCN0000020021*<br>(CCGGCCGAACTCAATTTCTCCACTTCTCGAGAAGTGGAGAAATTGAGTTCGGTTTTT)<br>*TRCN0000020022*<br>(CCGGGCAGCAGATTTCATCAAATATCTCGAGATATTTGATGAAATCTGCTGCTTTTT)<br>*TRCN0000020023*<br>(CCGGCGGACAACAAAGGCAACTCAACTCGAGTTGAGTTGCCTTTGTTGTCCGTTTTT)<br>*TRCN0000020019*<br>(CCGGGCCCAGATTCAGTCAGAGTTACTCGAGTAACTCTGACTGAATCTGGGCTTTTT) | Mission® by Sigma-Aldrich |
| shSGK1<br>*TRCN0000196562*<br>(CCGGGCAATCTTATTGCACACTGTTCTCGAGAACAGTGTGCAATAAGATTGCTTTTTTG)<br>*TRCN0000194957*<br>(CCGGCTGGAAGCTTAGCAATCTTATCTCGAGATAAGATTGCTAAGCTTCCAGTTTTTTG)<br>*TRCN0000040175*<br>(CCGGCGGAATGTTCTGTTGAAGAATCTCGAGATTCTTCAACAGAACATTCCGTTTTTG) | Mission® by Sigma-Aldrich |

| | |
|---|---|
| *TRCN0000040177* (CCGGCATGTCTTCTTCTCCTTAATTCTCGAG AATTAAGGAGAAGAAGACATGTTTTTG) *TRCN0000010432* (CCGGCAATTCTCATCGCTTTCATGACTCGA GTCATGAAAGCGATGAGAATTGTTTTTG) | |

### 2.1.10. Software

| **Software** | **Company** |
|---|---|
| Bio-Rad CFX Manager | Bio-Rad, Hercules, USA |
| Excel 2013 | Microsoft, Redmond, USA |
| FlowJo 10.1 | Treestar, Ashland, USA |
| Powerpoint 2013 | Microsoft, Redmond, USA |
| Prism 5 for Windows | GraphPad Software, La Jolla, USA |
| Wave 2.2.0 | Seahorse Bioscience |
| Word 2013 | Microsoft, Redmond, USA |

## 2.2. Methods

### 2.2.1. Ethics approval

The ethics approval was obtained from the Institutional Review Board of the Charité Universitätsmedizin Berlin, Germany, with the study number EA1/221/11. All experiments were conducted in accordance with the Declaration of Helsinki.

### 2.2.2. Electrolyte measurement

Media were produced following the respective formulas (see 2.1.4). Subsequently, sodium, chloride and potassium ions concentrations in Complete medium with and without additional NaCl were measured using a Cobas® 8000 electrolyte measuring unit. For Complete medium + NaCl, additional 60 mM NaCl were added to the medium by using a 1:44 dilution of NaCl stock.

### 2.2.3. Ficoll density gradient separation and PBMC preparation

Peripheral blood mononuclear cells (PBMCs) were isolated by Ficoll gradient centrifugation of heparinized blood from healthy volunteers. Separated PBMCs were washed once in PBS and twice in wash buffer. Subsequently, cells were counted using a Neubauer hemocytometer and adjusted to the desired cell density.

### 2.2.4. T cell purification

For obtainment of $T_h17$ enriched cells, $CD4^+$ cells were purified from isolated PBMCs by autoMACS-based magnetic cell separation of the isolated PBMCs using CD4 MicroBeads. Purified $CD4^+$ cells were stained with antibodies in MACS buffer at 4 °C for 30 minutes. Antibodies used for staining were αCD45RA-FITC, αCXCR3-APC, αCCR4-PECy7, αCCR6-PE. Cell sorting was carried out at FACSAria$^{TM}$ IIIu and MoFlo Legacy Cell Sorter (Gating strategy: lymphocytes, single cells, $CD45RA^-$, $CCR6^+$, $CXCR3^-$, $CCR4^+$, as described previously to be an appropriate sorting strategy) (Acosta-Rodriguez et al., 2007; Zielinski et al., 2012). After sorting, cells were washed twice and rested in wash buffer for at least 30 minutes at 4 °C before they were counted and adjusted to the desired density.

For obtainment of $CD4^+$ and $CD8^+$ memory T cells, isolated PBMCs were stained with antibodies in MACS buffer at 4 °C for 30 minutes. Antibodies used for staining were αCD45RA-FITC, αCD4-PECy7, αCD8-APC. Cell sorting was carried out at FACSAria and MoFlo (Gating strategy: lymphocytes, single cells, $CD45RA^-$, $CD4^+$ or $CD8^+$). After sorting, cells were washed twice and rested in wash buffer for at least 30 minutes at 4 °C before they were counted and adjusted to the desired density. The purity of sorted cell populations was usually more than 98 %.

For obtainment of nucleofected MART-1-specific T cells, nucleofected PBMCs were stained with antibodies in MACS buffer at 4 °C for 30 minutes. Antibodies used for staining were αCD3-FITC and α-mouse-TCR β-chain-APC. For exclusion of dead cells, propidium iodide was used. Cell sorting was carried out at MoFlo (Gating strategy: lymphocytes, single cells, $CD3^+$, mouse-TCR β-$chain^+$ or mouse-TCR β-$chain^-$) into an αCD3/αCD28-coated (see 2.2.6.) MaxiSorp NUNC-Immuno Plate.

For obtainment of MART-1-specific $CD8^+$ T cells from the natural repertoire, isolated PBMCs of an HLA-A2-seropositive donor were stained with tetramers and antibodies in MACS buffer at 4 °C for 30 minutes. Tetramers were assembled the day before by incubating pMHC complex loaded

with MART-1 peptide with Streptavidin-APC or with Streptavidin-BV421 overnight at 4 °C. Tetramers used for staining were pMHC-Streptavidin-BV421 and pMHC-Streptavidin-APC. Antibodies used for staining were αCD3-FITC, αCD8-PE and αCD19-ECD. For exclusion of dead cells, propidium iodide was used. Single cell sorting was carried out at MoFlo (Gating strategy: lymphocytes, single cells, $PI^-/CD19^-$, $CD8^+$, $CD3^+$, pMHC-Streptavidin-$APC^+$/pMHC-Streptavidin-$BV421^+$) into a 384-well assay plate. pMHC complexes loaded with MART-1 peptide had been refolded by Manuel Effenberger as described previously (Altman et al., 1996; Busch et al., 1998; Garboczi et al., 1996b, 1996a).

### 2.2.5. Nucleofection of PBMCs

1 x $10^7$ freshly isolated PBMCs were washed twice in PBS and resuspended in pre-equilibrated nucleofection buffer 1SM (Chicaybam et al., 2013). 20 µg transposon coding MART-1-specific TCR/0,5 µg transposase SB100X solution was added to the cell suspension and subsequently transferred into an electrophoresis chamber. Nucleofection was performed by Manuel Effenberger using the program U-14 for human T lymphocytes on Lonza nucleofector IIb. After nucleofection, the cell suspension was transferred into a 24-well microplate containing complete medium (HS) with 50 U/ml IL-2. After 24 hours, successfully nucleofected T cells were purified from cell suspension (see 2.2.4.).

### 2.2.6. Cell culture and stimulation

After isolation, $T_h17$ enriched cells, $CD4^+$ or $CD8^+$ memory T cells were stimulated polyclonally with αCD3/αCD28. For this purpose, MaxiSorp NUNC-Immuno Plates were coated with 1 µg/ml αCD3 and 1 µg/ml αCD28 in PBS (with Ca & Mg) at 50 µl per well and incubated overnight at 4 °C. Subsequently, the antibody suspension was aspirated and wells were washed twice with wash buffer. Cells were seeded into wells in duplicates numbering 5 x $10^4$ cells per well in complete medium (FCS) and cultured at 37 °C and 5 % $CO_2$. Where indicated, additional 60 mM NaCl were added to the cultures by using a 1:44 dilution of NaCl stock in the respective medium. In some experiments, the inhibitors SB202190 and GSK650394 were added to the cultures at concentrations of 5 µM or 1 µM, respectively. On day 2 after stimulation, cells were transferred to 96-well round bottom plate and rested for another 3 days before analysis.

Sorted T cells after nucleofection were stimulated polyclonally with αCD3/αCD28 for 2 days and rested for another 5 days. Subsequently, 1 x $10^5$ cells were expanded in complete medium (HS) containing 50 U/ml in 24-well microplates, co-cultured with 5 x $10^5$ irradiated, allogenic PBMCs in the presence of PHA at a concentration of 1 µg/ml.

Single cell sorted MART-1-specific $CD8^+$ T cells were cultured in complete medium (HS) containing 50 U/ml of IL-2 in 384-well assay plates. Single cells were co-cultured with 5 x $10^4$ irradiated (45 Gy), allogenic PBMCs in the presence of PHA at a concentration of 1 µg/ml. Clone populations were expanded in complete medium (HS) containing 50 U/ml in 24-well microplates, co-cultured with 5 x $10^5$ irradiated, allogenic PBMCs in the presence of PHA at a concentration of 1 µg/ml.

Cell lines were cultured in cell line growth medium in 75 $cm^2$ tissue culture flasks at 37 °C and 5 % $CO_2$. They were regularly split at 70-80 % confluence and subsequently re-cultured.

For cytotoxicity assays, sorted MART-1-specific $CD8^+$ T cell clones or nucleofected T cells were taken from expansion. 5 x $10^4$ cells were seeded per well in duplicates in an αCD3/αCD28-coated MaxiSorp NUNC-Immuno Plate, stimulated for 2 days and subsequently rested for another 3 days (see above) until used for cytotoxicity assays. Where indicated, additional 60 mM NaCl were added to the cultures by using a 1:44 dilution of NaCl stock in the respective medium.

### 2.2.7. Lentiviral gene silencing

Bacterial stocks carrying plasmids (see 2.1.9) were amplified in LB Broth containing Ampicillin at a concentration of 100 µg/ml. Plasmid DNA was purified using the QIAGEN Maxiprep (for psPAX2 and pMD2.G) or the PureYield™ Midiprep (for shNFAT5 and shSGK1) according to the manufacturers' protocols.

For production of lentiviral particles, HEK-293 cells were incubated together with purified DNA (10.5 µg psPAX2 + 3,5 µg pMD2.G + 14µg shNFAT5 or 10.5 µg psPAX2 + 3,5 µg pMD2.G + 14µg shSGK1 or 10.5 µg psPAX2 + 3,5 µg pMD2.G) solute in 0,25 M calcium chloride at 37 °C and 5 % $CO_2$. After 24 hours, the supernatant was discarded and fresh cell line growth medium was added. Supernatants containing the lentiviruses were collected and filtered 30 – 32 hours later. Lentiviruses were stored at -80 °C until being used for transduction of T cells.

$T_h17$ enriched T cells or nucleofected MART-1-specific T cells (see 2.2.4.) were seeded into αCD3/αCD28-coated wells in duplicates numbering 5 x $10^4$ cells per well in complete

medium (FCS) and cultured at 37 °C and 5 % $CO_2$ (see 2.2.6). After 12 hours of activation, transduction with supernatants containing pooled lentiviral particles against *SGK1* (shSGK1), *NFAT5* (shNFAT5) or without shRNA insertion (shCtrl) was performed. After another 36 hours, cells were transferred to a 96-well round bottom plate, washed and resuspended in fresh complete medium (FCS) containing Puromycin at a concentration of 1,5 µg/ml for selection of successfully transduced cells. Gene expression was measured by qPCR on day 5 of cell culture. All conditions were set up in duplicates.

### 2.2.8. Intracellular cytokine and surface staining and FACS analysis

When not indicated otherwise, stainings and analyses were performed on day 5 of cell culture. Antibodies used for cell staining were diluted in concentrations as tested in titrations or as recommended by the manufacturer.

For surface staining, T cells were stained with antibodies in MACS buffer at 4 °C for 30 minutes. Antibodies used for surface staining were αPD-1-BV421, αCD69-PECy7 and αCCR6-PE.

For intracellular cytokine staining for IFN-γ, TNF-α, IL-17, IL-22, IL-10 and TGF-β, T cells were stimulated for 5 hours with PMA and Ionomycin at concentrations of 0,2 µM and 1 µg/ml in complete medium (FCS), respectively. For the last 2,5 hours of stimulation Brefeldin A was added to cultures at a concentration of 10 µg/ml. Cells were then fixed and permeabilized using the BD Cytofix/Cytoperm$^{TM}$ Kit. Permeabilized cells were stained with antibodies in PermWash at 4 °C for 30 minutes. Antibodies used for staining were αIFN-γ-PECy7, αIL-10-APC, αIL-17-APCCy7, αIL-22-PE, αTGF-β-BV421, αTNF-FITC.

For intracellular cytokine staining for Granzyme A, Granzyme B, Perforin and Granulysin, T cells were fixed and permeabilized using the BD Cytofix/Cytoperm$^{TM}$ Kit. Permeablized cells were stained with antibodies in PermWash at 4 °C for 30 minutes. Antibodies used for staining were αGranulysin-PE, αGrzA-PB, αGrzB-FITC, αPerforin-PB.

For staining of transcription factors, T cells were fixed and permeabilized using the FOXP3/Transcription Factor Fixation/Permeabilization Concentrate and Diluent Kit. Permeabilized cells were stained with antibodies in permeabilization buffer at 4 °C for 30 minutes. Antibodies used for staining were αFOXP3-FITC and αRORγt-PE.

For staining of CD107a, T cells were stimulated for 5 hours with PMA and Ionomycin (see above) in complete medium (FCS) containing the staining antibody αCD107a-APC.

For proliferation measurements, T cells were labelled directly after purification with CFSE at a concentration of $5 \times 10^{-7}$ M at room temperature for 8 minutes. Then, cells were washed and seeded into αCD3/αCD28-coated wells numbering $5 \times 10^4$ in complete medium (FCS) and cultured at 37 °C and 5 % $CO_2$ for 5 days (see 2.2.6). Proliferation was assessed by CFSE dilution.

For live/dead discrimination, Zombie Yellow™ Fixable Viability Kit was used.

After all staining steps, cells were washed twice in MACS buffer. Flow cytometric analysis was performed using a CytoFLEX flow cytometer and FlowJo 10.1. Whenever distinct populations were identifiable, results were represented in percentages while otherwise the mean fluorescence intensity (MFI) was shown.

### 2.2.9. RNA isolation, cDNA Reverse Transcription and qPCR

For RNA isolation, respective cells were washed twice in PBS at room temperature and resuspended in Tri Reagent®. 1-Bromo-3-chloropropane were added and samples were centrifuged at 12 000 g for 15 minutes at 4 °C. RNA was precipitated by addition of 2-propanol and incubation for 10 minutes at room temperature. Samples were centrifuged at 12 000 g for 10 minutes at 4 °C, washed in 75 % ethanol and centrifuged under the same conditions again. Subsequently, RNA pellets were resuspended in RNase-free water.

For conversion to cDNA, the High Capacity cDNA Reverse Transcription Kit was used according the manufacturer's protocol.

For quantitative real-time PCR (qPCR), master mixes were prepared containing cDNA samples, the TaqMan® Fast Universal PCR Master Mix and the respective TaqMan® primer/probe. Reactions were performed in triplicates on a CFX384 Touch™ PCR detection system. Values are represented as the difference in $C_t$ values normalized to RNA18S5 for each sample as per the following formula: relative RNA expression = $2^{-\Delta Ct} \times 10^6$. For lentiviral gene silencing data, all results were normalized to the value of the sample without NaCl treatment and without shRNA insertion (shCtrl).

### 2.2.10. ECAR and OCR measurements

For measurements of the extracellular acidification rate (ECAR) and oxygen consumption rate (OCR) of T cells, the Seahorse XFe96 Analyzer was used. $CD4^+$ and $CD8^+$ memory T cells were

cultured as described in 2.2.6 and resuspended in Seahorse assay medium (pH adjusted to 7,4-7,45). Where indicated, additional 60 mM NaCl were added to the media by using a 1:44 dilution of NaCl stock in respective medium during the culture and measurements. T cells were seeded into a XF96 cell culture microplate numbering 2,5 x $10^5$ per well in at least 4 replicates. T cell attachment was enhanced by centrifugation up to 40 g and then immediate stopping without brake. The metabolic pathways can be investigated by analysis of the media containing the cells: extracellular acidification is a marker for aerobic glycolysis, while increased oxygen consumption suggests increased oxidative phosphorylation and metabolic throughput (Divakaruni et al., 2014). Using XF$^e$96 extracellular flux assay kits, metabolic pathways were analyzed by addition of oligomycin, carbonyl cyanide 3-chlorophenyl hydrazine (CCCP), antimycin A (AA) and rotenone at concentrations of 2 x $10^{-6}$ M, 1,5 x $10^{-6}$ M, 2 x $10^{-6}$ M and 2 x $10^{-6}$ M, respectively.

Metabolic parameters were measured in four different settings: unaltered (labelled as none), after inhibition of ATP synthase by oligomycin ('oligomycin'), after mitochondrial uncoupling by CCCP ('CCCP') and after inhibition of mitochondrial respiration by antimycin A and rotenone ('AA+rotenone'). For statistical analysis, all measurements per donor in one setting were averaged.

Basal ECAR is the initial rate measured and corresponds to ECAR(none). Maximal ECAR is the rate following treatment with oligomycin and thus corresponds to ECAR(oligomycin).

OCR values were calculated as per the following formulas:
Basal OCR = OCR(none) – OCR(AA+rotenone)
Maximal OCR = OCR(CCCP) – OCR(AA+rotenone).

Interpretation of the data was conducted in accordance with published approaches (Divakaruni et al., 2014).

### 2.2.11. Cytotoxicity Assay

Specific effector T cells were cultured as described in 2.2.6. For baseline measurements, 100 µl of cell line growth medium were added to a 96-well E-plate. A375 melanoma cells were seeded onto E-plate in duplicate wells numbering 5 x $10^3$ in 100 µl of cell line growth medium. Cell attachment and growth were monitored on the xCELLigence System over 24 hours at 37 °C and 5 % $CO_2$. After 24 hours, 100 µl of the medium were removed and 100 µl of fresh cell line growth medium containing $10^{-7}$ M MART-1 peptide were added for 1 hour. MART-1 is a peptide regularly found

on the surface of malignant melanoma cells (Busam et al., 1998). The high frequency of MART-1-specific cells among the cytotoxic T cells made it an ideal target epitope (Pittet et al., 1999). Subsequently, 100 µl of the growth medium were removed and 100 µl T cell assay medium, containing specific effector T cells at a 1:1 ratio to original cell seeding number (when not indicated otherwise) or no T cells, were added. All conditions were set up in duplicates. Cell indices were monitored every 15-30 minutes for another 24-48 hours on the xCELLigence System by measurement of concurrent impedance. Where indicated, additional 60 mM NaCl were added to the media by using a 1:44 dilution of NaCl stock in respective medium.

Values are represented as cell indices (CI) as given by the xCELLigence System, cell indices normalized to the start of the co-culture (nCI) or as cell lysis calculated per the following formula: $\text{Cell lysis} = \frac{\text{nCI(A-375 only)} - \text{nCI(A-375 + CTLs)}}{\text{nCI(A-375 only)}}$. (Peper et al., 2014)

### 2.2.12. Statistical analysis

When not indicated otherwise, bars and lines represent mean values and error bars represent the standard error of the mean. When not indicated otherwise, dots represent individual healthy donors. When not indicated otherwise, p-values and significance were determined by paired two-tailed t-test for comparison of two groups or ANOVA for comparison of three or more groups using GraphPad Prism 5 (for ANOVA: *: $p < 0,05$; **: $p < 0,01$; ***: $p < 0,001$; ns: $\geq 0,05$).

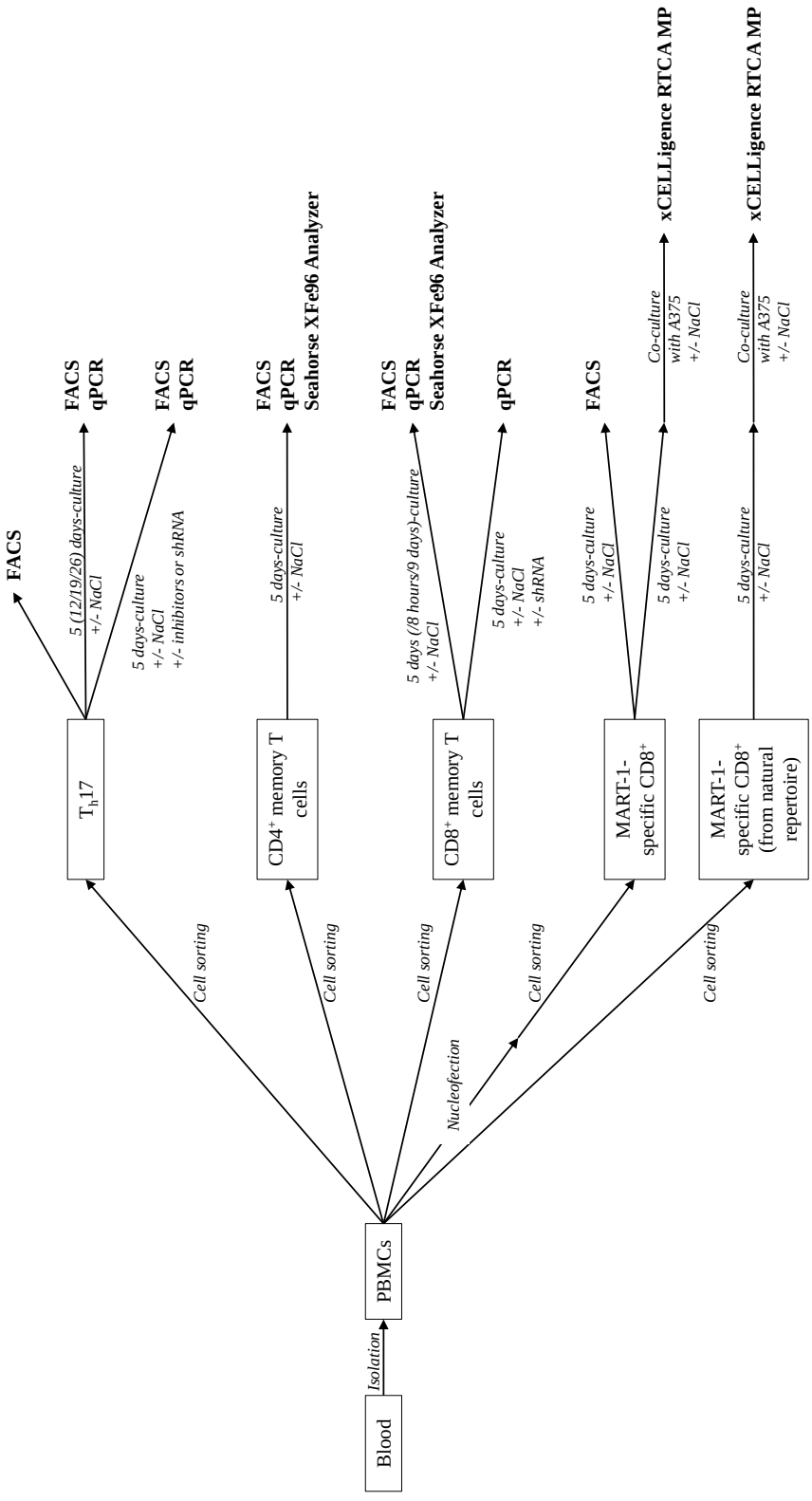


**Figure 2.1. Methodological summary in a workflow diagram.**
Cells are printed in regular, *Methods* in italics, **Analyses** in bold.

## 3. Results

In order to study the human body's T cell responses, the physiological conditions have to be recreated *in vitro* as thoroughly as possible. Thus, for the *in vitro* experiments of this study, a medium resembling the hyperosmotic conditions in inflammatory and tumor sites (complete medium + NaCl) was composed to have an increased osmolarity and a sodium concentration of approximately 200 mmol/l while normal medium (complete medium) contains approximately 140 mmol/l. The electrolyte concentrations of the respective media have been measured confirming prior calculations (Table 3.1).

### 3.1. Effects of hypertonicity on survival and proliferation in memory T cells

To mimic the reaction of epitope-specific T cells in the tissue, T cells in the culture were stimulated using monoclonal antibodies (mAbs) for 2 days and rested for another 3 days under either isosmotic (none) or hyperosmotic conditions (NaCl) before analysis. To outline the general effects that a hypertonic milieu exerts on memory T cells, the cell proliferation (Fig. 3.1A) as well as the frequency of dead cells (Fig. 3.1B) of primary $CD4^+$ $CD45RA^-$ and $CD8^+$ $CD45RA^-$ cells were quantified using flow cytometric measurements of CFSE dilution and Zombie live/dead staining, respectively. Here, no relevant differences were found (Fig. 3.1). Hence, survival and proliferation of memory T cells were comparable between iso- and hypertonic conditions.

### 3.2. Effects of hypertonicity on the $T_h17$ phenotype in $T_h17$ cells

Subsequently, functional alterations in $T_h17$ cells by the hypertonic environment of their effector sites were investigated. Since $T_h17$ cells are highly plastic, the first step was to determine whether these cells maintain or change their $T_h17$ phenotype. To assess this, primary $CD4^+$ memory T cells were enriched for $T_h17$ cells and stimulated under iso- and hypertonic conditions. In a hypertonic milieu, production of IL-17 and IL-22 and expression of CCR6 were significantly upregulated, while changes in the expression of RORγt were indeed significant but only marginal (Fig. 3.2). These findings support the idea, that the $T_h17$ phenotype in a hypertonic environment is not only maintained, but also promoted.

Since $T_h17$ can develop either a pro- or anti-inflammatory phenotype, the primary $T_h17$ enriched cells were assessed for expression of anti-inflammatory hallmarks. The fraction of $FOXP3^+$ cells

| Complete medium | mmol/l |
|---|---|
| [$Na^+$] | 143 |
| [$Cl^-$] | 106 |
| [$K^+$] | 5,81 |
| **Complete medium + NaCl** | |
| [$Na^+$] | 203 |
| [$Cl^-$] | 168 |
| [$K^+$] | 5,79 |

**Table 3.1. Sodium chloride-enriched medium is hyperosmotic relative to standard T cell culture medium.**
Complete medium (FCS) was enriched with sodium chloride by addition of NaCl stock in an 1:44 dilution. Electrolyte concentrations were measured using the Cobas® 8000.

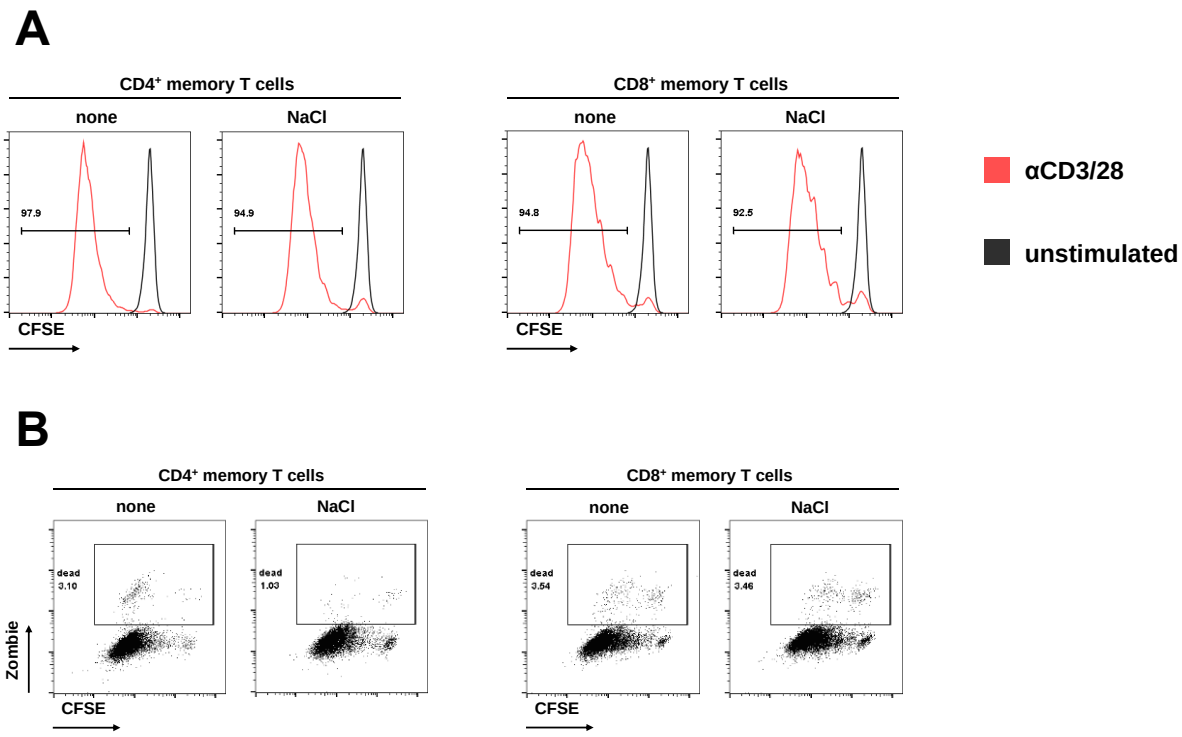


**Figure 3.1. Physiological hypertonicity does not affect survival or proliferation of memory T cells.**
Purified primary $CD4^+$ or $CD8^+$ memory T cells were isolated, stained with CFSE and subsequently stimulated for 2 days with αCD3/αCD28 mAbs and rested for 3 days in the presence or absence of a higher concentration of NaCl (see Table 1). **(A)** On day 5, CFSE dilution was measured by FACS. As a neg ative control T cells were stained with CFSE, but not stimulated by mAbs. One representative FACS histogram out of 3 healthy donors is shown. **(B)** On day 5, cells were stained using the Zombie Yellow™ Fixable Viability Kit and measured by FACS. One representative FACS dot blot out of 6 healthy donors is shown.

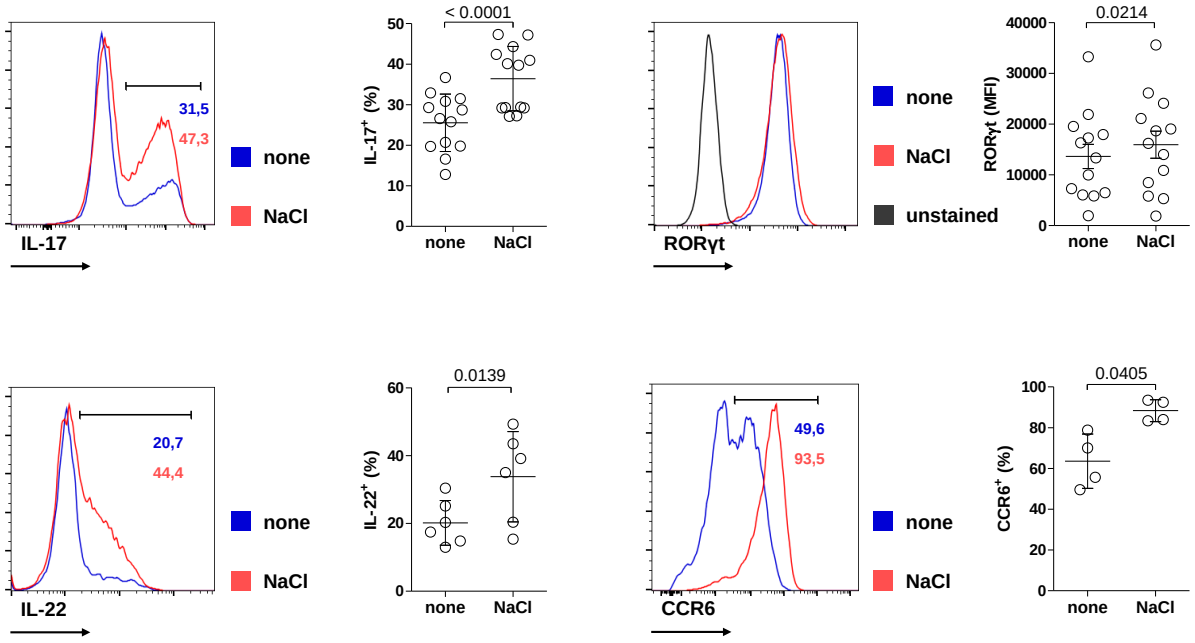


**Figure 3.2. Hypertonicity promotes the $T_h17$ phenotype in $T_h17$ enriched memory T helper cells.**

Purified primary $T_h17$ enriched T cells were isolated and stimulated for 2 days with αCD3/αCD28 mAbs and rested for 3 days in the presence or absence of a higher concentration of NaCl. On day 5, cells were stained and expression of IL-17, RORγt, IL-22 and CCR6 was measured by FACS. Data show mean ± SEM of 13 (for IL-17 and RORγt), 6 (for IL-22) or 4 (for CCR6) healthy donors.

was below 20 % if stimulated in an isotonic environment and as high as 40 % under hypertonic conditions (Fig. 3.3A). The difference was particularly prominent in the IL-17$^+$ FOXP3$^+$ fraction. This suggests that hypertonicity may favor the anti-inflammatory phenotype in $T_h17$ cells. To investigate whether the stimulation in a hypertonic milieu leads to an increase or whether the stimulation in an isotonic environment leads to a decrease in FOXP3 expression, the levels of FOXP3 after stimulation were compared to those in $T_h17$ enriched cells *ex vivo*. The data show that stimulation of the cells in isotonicity did not considerably affect FOXP3 expression after 5 days, while stimulation in hypertonicity boosted FOXP3 expression (Fig. 3.3B). Subsequently, the effect of higher osmolarity on the production of pro- and anti-inflammatory cytokines was analyzed. $T_h17$ enriched cells that were stimulated in a hypertonic milieu expressed higher levels of TGF-β, but were less likely to produce IL-10 and showed a minimal increase in IFN-γ production (Fig. 3.3C). In summary, the precise orientation of the cytokine profile of $T_h17$ cells in hypertonicity remains ambiguous.

Plastic changes in memory T cells can be permanent or transient, therefore the durability of the effects of hypertonicity on the memory $T_h17$ cells needed to be determined. To do so, the $T_h17$ enriched cells were divided into three groups and assessed over a longer period of time. The first group was kept under isotonic conditions for the whole duration of culture, the second group was stimulated once in a hypertonic environment and after 5 days transferred into isotonic conditions, the third group was continuously kept under hypertonic conditions. All cells were stimulated as described previously, rested, and re-stimulated every 7 days for a total of 26 days. The results show that the increased IL-17 production of $T_h17$ cells in hypertonicity remained high even after the cells returned into an isotonic environment for at least one week before aligning with the cells that were not exposed to hypertonicity at all. On the contrary, elevated FOXP3 expression in hypertonicity quickly returned to normal expression levels after the $T_h17$ cells had entered an isotonic environment. Furthermore, it appears that constant hypertonic conditions led to progressive increase of FOXP3 expression in $T_h17$ cells suggesting that the described promotion of the $T_h17$ phenotype but not of the anti-inflammatory phenotype represent a lasting alteration. (Fig. 3.4)

### 3.3. Molecular mechanisms mediating the effects of hypertonicity on $T_h17$ cells

In order to understand the effects that a hypertonic environment exerts on T cells, it is necessary to understand how the cells sense changes in osmolarity. The aforementioned p38 MAP kinase

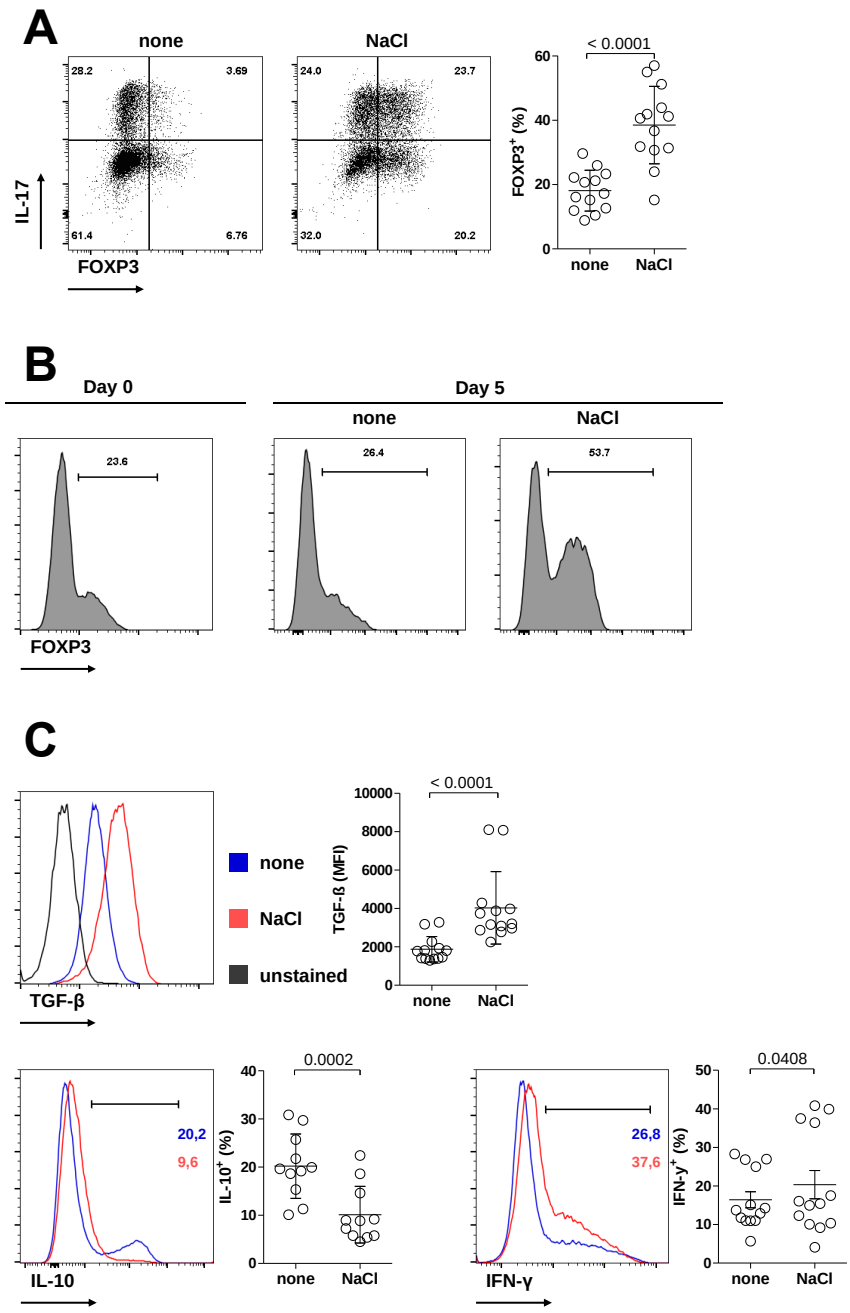


**Figure 3.3. Hypertonicity enhances anti-inflammatory features in $T_h17$ enriched memory T helper cells.**

Purified primary $T_h17$ enriched T cells were isolated and stimulated for 2 days with αCD3/αCD28 mAbs and rested for 3 days in the presence or absence of a higher concentration of NaCl. **(A)** On day 5, cells were stained and expression of IL-17 and FOXP3 was measured by FACS. Data show mean ± SEM of 13 healthy donors. **(B)** *Ex vivo* as well as on day 5, cells were stained and expression of FOXP3 was measured by FACS. One representative FACS histogram out of 2 healthy donors is shown. **(C)** On day 5, cells were stained and expression of TGF-β, IL-10 and IFN-γ was measured by FACS. Data show mean ± SEM of 13 (for TGF- β and IFN- γ) or 11 (for IL-10) healthy donors.

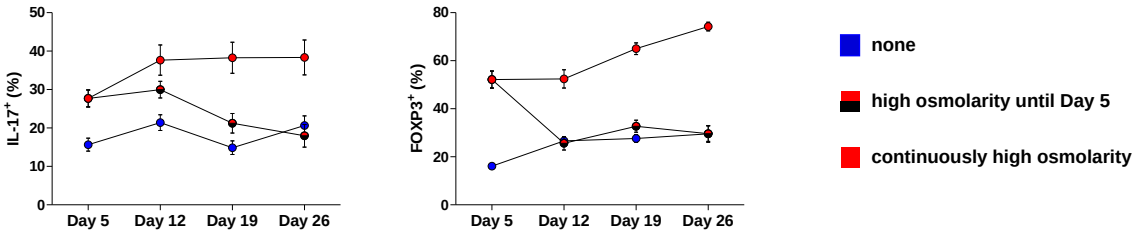


**Figure 3.4. The regulation of FOXP3 depends on continuously hypertonic environment while the increase in IL-17 expression is more durable.**
Purified primary $T_h17$ enriched T cells were isolated and stimulated for 2 days with αCD3/αCD28 mAbs and rested for 5 days in the presence or absence of a higher concentration of NaCl. After 7 days, cells were counted and restimulated for 2 days with αCD3/αCD28 mAbs and rested for another 5 days in the presence or absence of a higher concentration of NaCl. This cycle was repeated until day 26. On day 5, 12, 19 and 26, cells were stained and expression of IL-17 and FOXP3 was measured by FACS. Dots represent mean ± SEM of 4 healthy donors.

pathway was in the focus of this mechanistic work. Thus, in a first step it was investigated whether memory T cells show changes in the expression of *NFAT5* and *SGK1* in a hypertonic environment.

$CD4^+$ $CD45RA^-$ cells were stimulated under isotonic or hypertonic conditions and subsequently analyzed by qPCR. *NFAT5* and *SGK1* were expressed at significantly higher levels when the cells were stimulated under hypertonic conditions (Fig. 3.5). This result suggests that the p38 MAP kinase pathway may also play a role in enhancing the anti-inflammatory features in $T_h17$ cells.

To identify the explicit roles of p38 MAP kinase, NFAT5 and SGK1, molecular inhibitors and shRNA were used to suppress their expression or function. First, primary $T_h17$ enriched cells were incubated in either the presence or absence of the p38 MAP kinase inhibitor SB202190, stimulated as described before and afterwards analyzed for IL-17 and FOXP3 protein expression by flow cytometry. Both markers were significantly downregulated in the presence of the inhibitor affirming that not only the enhancement of the $T_h17$ phenotype but also the induction of anti-inflammatory characteristics is regulated by p38 MAP kinase (Fig. 3.6).

Secondly, *NFAT5* was silenced in primary $T_h17$ enriched cells using a shRNA approach. Subsequently, these cells were stimulated as described above and analyzed via qPCR and flow cytometry. The analysis of *NFAT5* and *SGK1* by qPCR showed that the usage of the shRNA construct is effective and the expression of *NFAT5* is successfully downregulated (Fig. 3.7A). The significant downregulation of the mRNA expression of *SGK1*, when *NFAT5* is silenced, confirms that SGK1 is a downstream kinase of NFAT5 as it has been described before (Fig. 3.7A). Similarly, mRNA expression levels of *RORC* and *FOXP3* – representing the master regulators for $T_h17$ and $T_{reg}$ cells, respectively – were significantly reduced when *NFAT5* was silenced (Fig. 3.7B). These findings were confirmed by flow cytometry data, showing that the increase in IL-17 and FOXP3 protein expression by hypertonicity was suppressed by silencing *NFAT5* (Fig. 3.7C). However, there was no substantial difference in the protein expression of TGF-β whether *NFAT5* was silenced or not pointing out that the osmotic regulation of TGF-β cannot be explained by activation of NFAT5 alone (Fig. 3.7D).

Lastly, the role of SGK1 was determined, as well. Primary $T_h17$ enriched cells were incubated in either the presence or absence of the SGK1 inhibitor GSK650394, stimulated as described above and analyzed by flow cytometry. The upregulation of IL-17 and FOXP3 by hypertonicity was reduced by inhibiting SGK1 (Fig. 3.8A). In addition, *SGK1* was silenced using shRNA (Fig. 3.8B). Accordingly, the mRNA expression of *FOXP3* was diminished by silencing *SGK1* while a

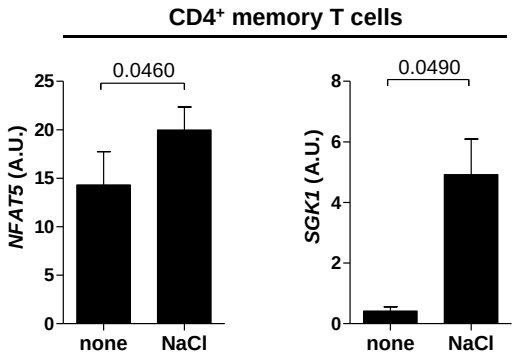


**Figure 3.5. The hypertonic environment affects possible mediators, the transcription factor NFAT5 and the kinase SGK1, in memory T helper cells.**
Purified primary $CD4^+$ memory T cells were isolated and stimulated for 2 days with αCD3/αCD28 mAbs and rested for 3 days in the presence or absence of a higher concentration of NaCl. On day 5, cells were analysed by qPCR for *NFAT5* and *SGK1*. Data show mean ± SEM of 6 healthy donors.

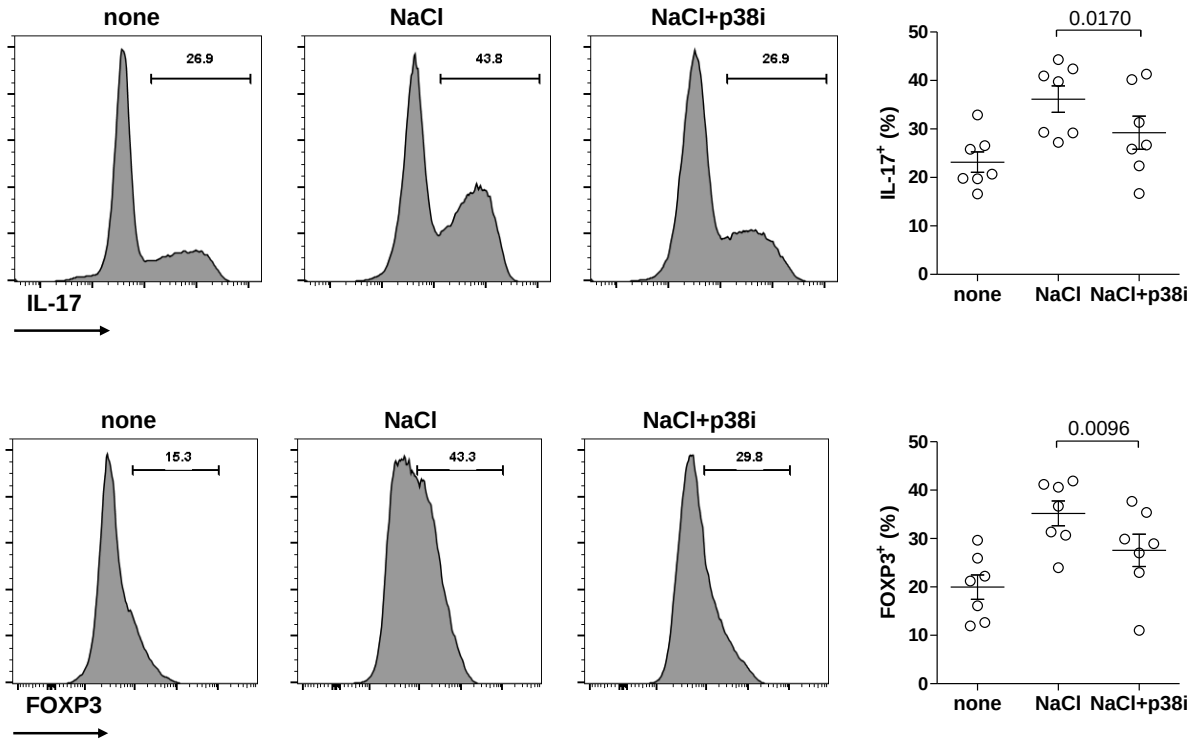


**Figure 3.6. Effects of hypertonicity on $T_h17$ enriched memory T helper cells are mediated by p38 MAP Kinase.**

Purified primary $T_h17$ enriched T cells were isolated and stimulated for 2 days with αCD3/αCD28 mAbs and rested for 3 days in the presence or absence of a higher concentration of NaCl. At least 1 h before stimulation, cells were incubated in the presence or absence of the p38 inhibitor SB202190 (p38i) at a concentration of 5 x $10^{-6}$ M. On day 5, cells were stained and expression of IL-17 and FOXP3 was measured by FACS. Data show mean ± SEM of 7 healthy donors.

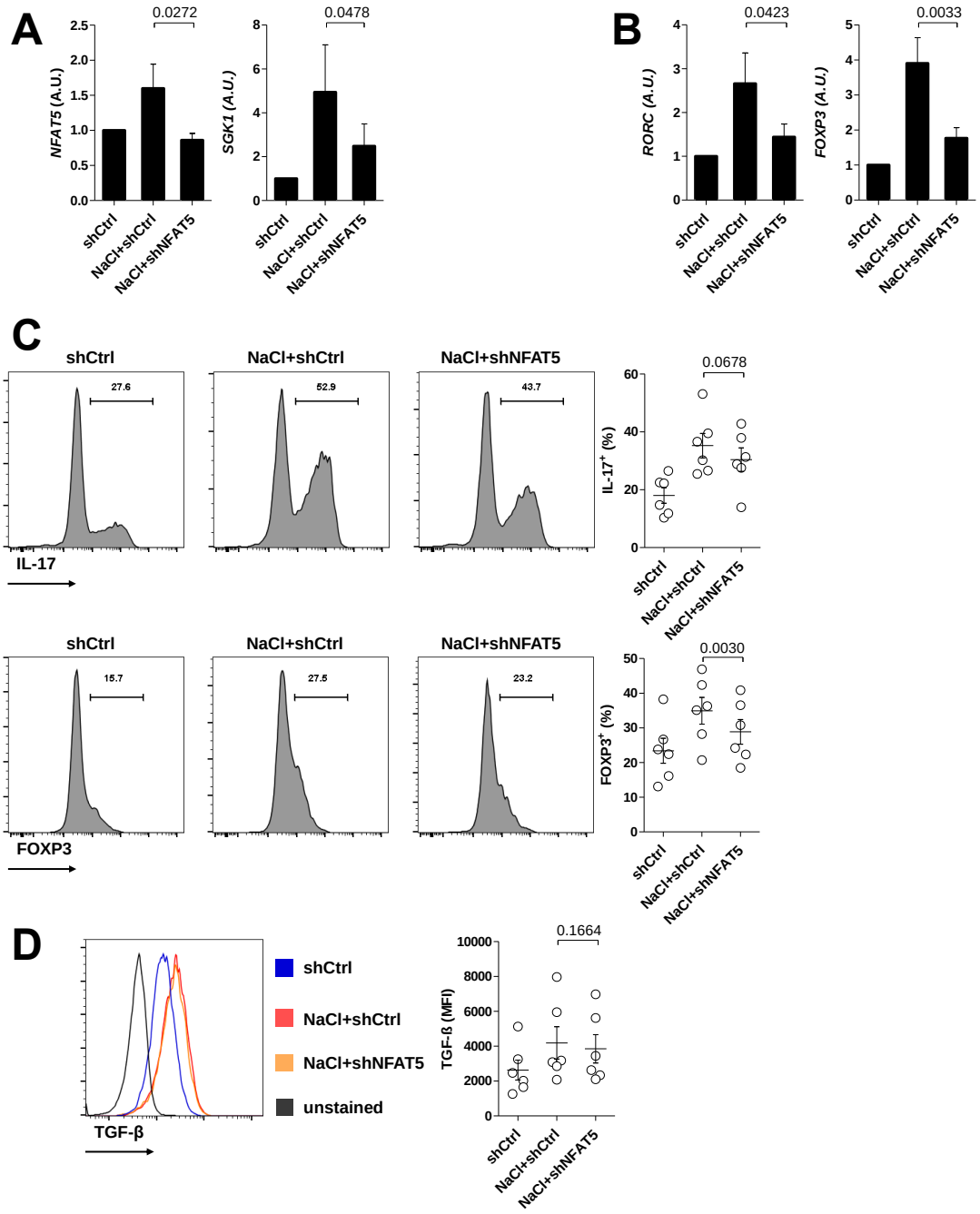


**Figure 3.7. Effects of hypertonicity on $T_h17$ enriched memory T helper cells are mediated by the transcription factor NFAT5.**

Purified primary $T_h17$ enriched T cells were isolated and stimulated for 2 days with αCD3/αCD28 mAbs and rested for 3 days in the presence or absence of a higher concentration of NaCl. Cells were transduced with NFAT5 specific (shNFAT5) or empty control shRNA(shCtrl). **(A-B)** On day 5, cells were analysed by qPCR for *NFAT5*, *SGK1*, *RORC* and *FOXP3*. Data show mean ± SEM of 6 healthy donors. **(C-D)** On day 5, cells were stained and expression of IL-17, FOXP3 and TGFβ was measured by FACS. Data show mean ± SEM of 6 healthy donors.

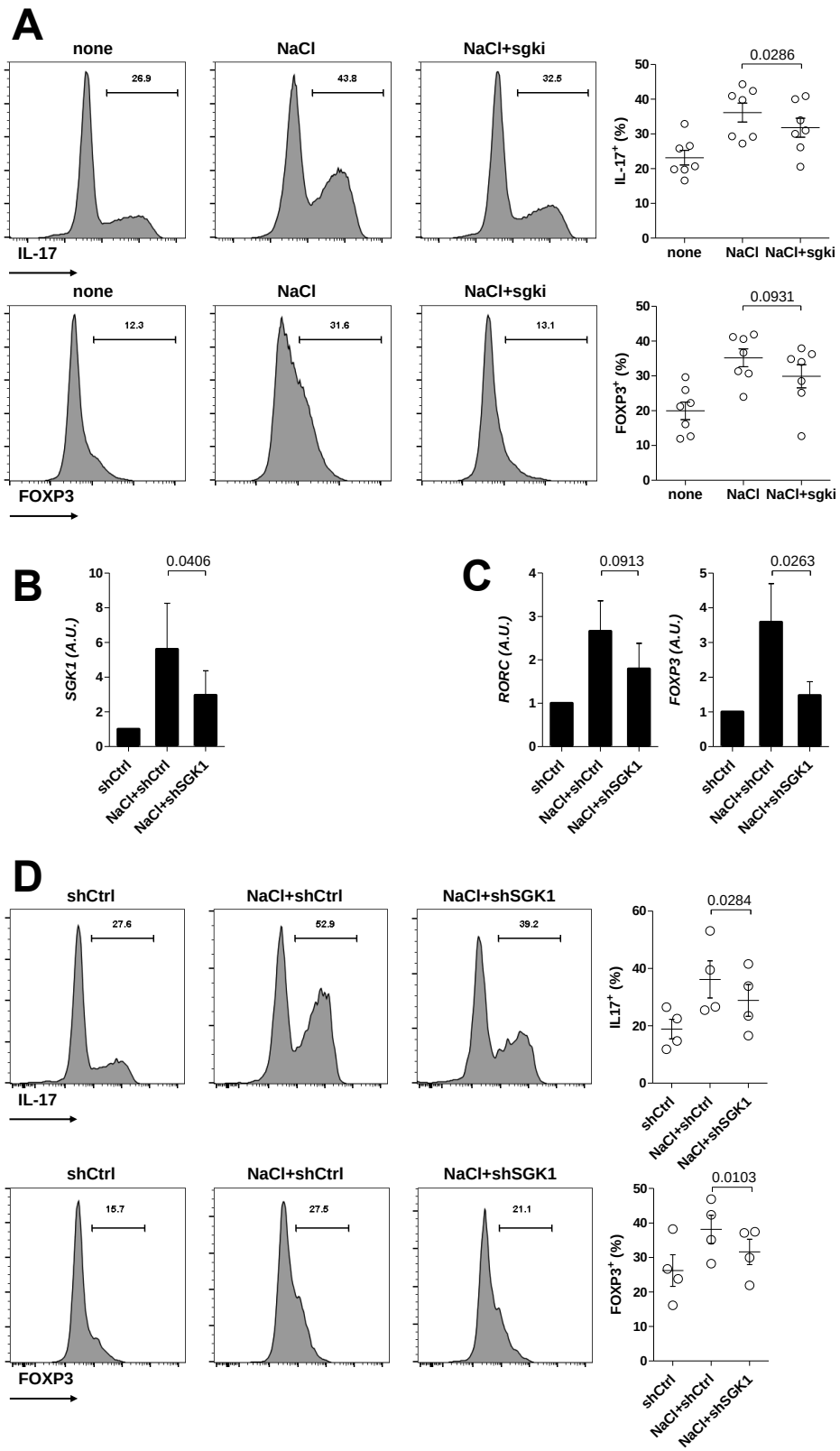
A
none
NaCl
NaCl+sgki
26.9
43.8
32.5
IL-17
0.0286
IL-17+ (%)
none
NaCl
NaCl+sgki
12.3
31.6
13.1
FOXP3
0.0931
FOXP3+ (%)
B
SGK1 (A.U.)
0.0406
shCtrl
NaCl+shCtrl
NaCl+shSGK1
C
RORC (A.U.)
0.0913
FOXP3 (A.U.)
0.0263
D
shCtrl
NaCl+shCtrl
NaCl+shSGK1
27.6
52.9
39.2
IL-17
0.0284
15.7
27.5
21.1
FOXP3
0.0103

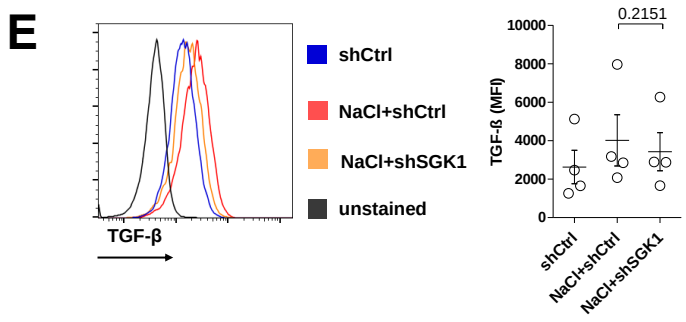


**Figure 3.8. Effects of hypertonicity on $T_h17$ enriched memory T helper cells are mediated by the kinase SGK1.**

**(A)** Purified primary $T_h17$ enriched T cells were isolated and stimulated for 2 days with αCD3/αCD28 mAbs and rested for 3 days in the presence or absence of a higher concentration of NaCl. At least 1 h before stimulation, cells were incubated in the presence or absence of the SGK1 inhibitor GSK650394 (sgki) at a concentration of 1 x $10^{-6}$ M. On day 5, cells were stained and expression of IL-17 and FOXP3 was measured by FACS. Data show mean ± SEM of 7 healthy donors. **(B-F)** Purified primary $T_h17$ enriched T cells were isolated and stimulated for 2 days with αCD3/αCD28 mAbs and rested for 3 days in the presence or absence of a higher concentration of NaCl. Cells were transduced with SGK1 specific (shSGK1) or empty control shRNA(shCtrl). **(B-C)** On day 5, cells were analysed by qPCR for *SGK1*, *RORC* and *FOXP3*. Data show mean ± SEM of 4 healthy donors. **(D-E)** On day 5, cells were stained and expression of IL-17, FOXP3 and TGFβ was measured by FACS. Data show mean ± SEM of 4 healthy donors.

connection between *SGK1* and *RORC* could not be determined by qPCR (Fig. 3.8C). Nevertheless, flow cytometry data confirmed that the hypertonicity-induced increases in the expression of both, IL-17 and FOXP3, were regulated by SGK1 (Fig. 3.8D). However, expression of TGF-β appeared not to be affected, consistent with the results from the *NFAT5* silencing experiments (Fig. 3.8E).

These findings emphasize, that the induction of the $T_h17$ phenotype in memory $T_h17$ cells is regulated via the p38 MAP kinase pathway including NFAT5 and SGK1, while the shift towards a more anti-inflammatory phenotype seems to be only partly mediated by it.

## 3.4. Effects of hypertonicity on the activation, metabolism and effector phenotype in cytotoxic T cells

Just as the $T_h17$ cells' reaction to hypertonicity may be highly relevant to understand autoimmune diseases, the same holds true for cytotoxic $CD8^+$ T cells in the context of immunological control of tumor diseases. Thus, the second part of my thesis comprises the analysis of the behavior of CTLs in hypertonic environments.

In a first step, the general effect of hyperosmolarity on the activation of cytotoxic T cells was analyzed. Accordingly, CTLs were stimulated under isosmotic or hyperosmotic conditions and analyzed for early and late protein expression of CD69 and PD-1 by flow cytometry. After 8 hours, cells under both conditions showed no significant differences in CD69 expression levels. However, after 5 days CD69 levels were much higher in CTLs kept in hyperosmotic culture (Fig. 3.9A). In case of PD-1 expression, the CTLs showed significantly higher levels after 5 days when they were stimulated under hypertonic conditions that decreased at later time point (Fig. 3.9B). In contrast to CTLs, $CD4^+$ memory T cells, gave a less consistent picture with CD69 expression not being affected by hyperosmolarity and PD-1 levels significantly increased (Fig. 3.9C). These results emphasize that a hyperosmotic environment boosts T cell activation in CTLs with the effects of hypertonicity taking some relevant time to have an impact. Of note, the increased activation does not appear to be linked to higher exhaustion of the T cells, which would be demonstrated by prolonged expression of PD-1: after 9 days, PD-1 expression levels have aligned again (Fig. 3.9B). Noticeably, the expression levels of the activation markers showed a high variance within the different populations, especially when measured after only a few hours.

In order to understand whether memory T cells adapt their metabolic profile to their higher activation levels in hypertonicity, metabolic analyses were conducted using the Seahorse XFe96

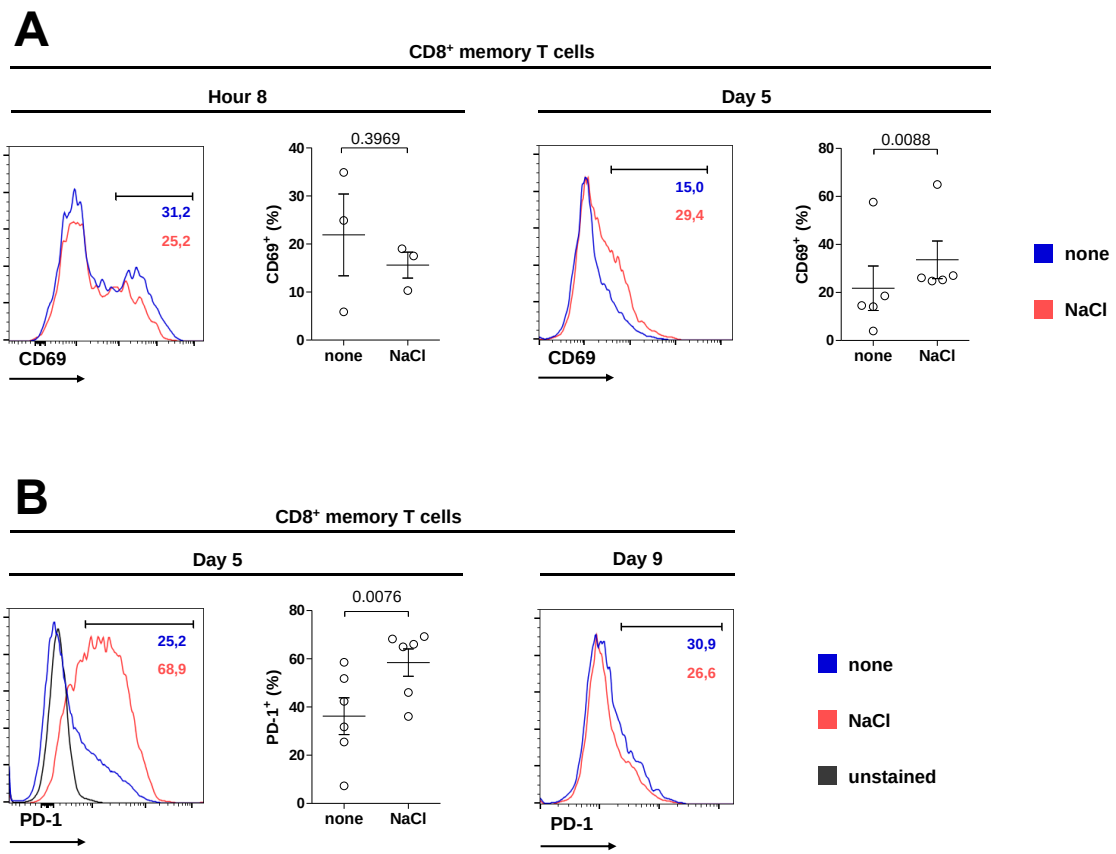


**Figure 3.9. Hypertonicity promotes memory T cell activation in cytotoxic T cells and possibly in T helper cells.**
Purified primary CD4⁺ or CD8⁺ memory T cells were isolated and stimulated for 2 days with αCD3/αCD28 mAbs and rested for 3-7 days in the presence or absence of a higher concentration of NaCl. **(A)** After 8 hours or on day 5, CD8⁺ memory T cells were stained and expression of CD69 was measured by FACS. Data show mean ± SEM of 3 (after 8 hours) or 5 (after 5 days) healthy donors. **(B)** On day 5 and day 9, CD8⁺ memory T cells were stained and expression of PD-1 was measured by FACS. Data show mean ± SEM of 6 healthy donors (after 5 days) or an representative FACS dot blot of 2 healthy donors (after 9 days). **(C)** On day 5, CD4⁺ memory T cells were stained and expression of CD69 and PD-1 was measured by FACS. Data show mean ± SEM of 5 (for CD69) or 3 (for PD-1) healthy donors.

Analyzer. CTLs were stimulated under either isosmotic or hyperosmotic conditions as described above. On day 5, the metabolic pathways were investigated. Basal values for the ECAR and the OCR were measured before adding any interfering reagents, the maximum values were measured after addition of oligomycin or the ionophore CCCP, respectively. Addition of Oligomycin, an ATP synthase inhibitor, allows assessment of the glycolytic capacity, while CCCP renders the inner mitochondrial membrane permeable to protons and thus uncouples the rate of electron transport and ATP production (see 2.2.10). CTLs showed significantly increased rates for extracellular acidification and oxygen consumption when they were stimulated under hypertonic conditions (Fig. 3.10AB). $CD4^+$ T cells, however, did not show significant changes in their metabolic profiles (Fig. 3.10C). Thus, it can be concluded that CTLs in hypertonicity adjust their metabolic profile to their higher activation levels by switching to the more rapidly working glycolysis and increasing their metabolic throughput. These results lead to the important question, whether the increased activation and the modulation of the metabolism in CTLs are linked to an improved effector function.

In this regard, the expression of relevant transcription factors and typical effector cytokines were evaluated. To examine potential effects of hyperosmolarity on the expression of the transcription factor RUNX3 as well as on the principal effector molecules TNF-α and IFN-γ, CTLs were stimulated in an isotonic or hypertonic environment and analyzed by qPCR and flow cytometry. In a hypertonic environment CTLs expressed higher levels of *RUNX3* and TNF-α while the level of IFN-γ remained almost unaltered suggesting an increased overall effector function (Fig. 3.11A).

Subsequently, both principal mechanisms inducing target cell death were investigated: the perforin/granzyme-mediated and the death receptor-mediated apoptosis. In hypertonic culture, CTLs significantly increased their granzyme B and perforin production while decreasing granzyme A expression. For granulysin, only a trend towards increased expression was observed (Fig. 3.11B). Investigation of effects on the death receptor pathways under hypertonic conditions gave a concordant picture with the *TNFSF10* (coding for TRAIL) expression being strongly boosted and the *FASL* expression non-significantly increased (Fig. 3.11C). Consistently, the expression of CD107a remained in line with perforin and granzyme B expression levels and was intensively induced representing a higher rate of degranulation upon activation (Fig. 3.11D).

Noticeably, $CD4^+$ T cells showed a similar pattern for TNF-α and CD107a and significant increase in IFN-γ production, but due to low overall expression levels roughly no changes in the production of granzymes and perforin (Fig. 3.11E).

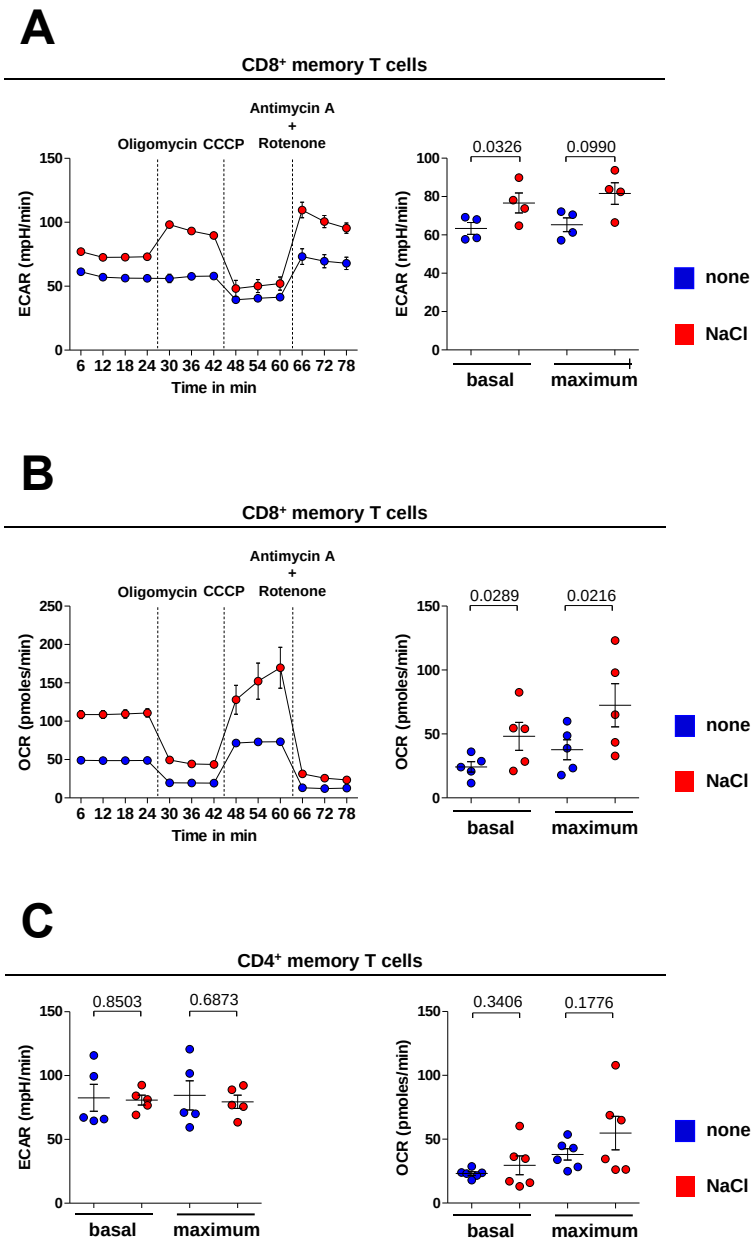


**Figure 3.10. Hypertonicity augments the metabolic throughput in cytotoxic memory T cells but not in memory T helper cells.**
Purified primary CD8$^+$ **(A-B)** or CD4$^+$ **(C)** memory T cells were isolated and stimulated for 2 days with αCD3/αCD28 mAbs and rested for 3 days in the presence or absence of a higher concentration of NaCl. On day 5, XF$^e$96 extracellular flux assay was performed. Metabolic pathways, represented by the extracellular acidification rate (ECAR) and the oxygen consumption rate (OCR), were analysed upon addition of oligomycin, CCCP, antimycin A and rotenone at concentrations of 2 x $10^{-6}$ M, 1,5 x $10^{-6}$ M, 2 x $10^{-6}$ M and 2 x $10^{-6}$ M, respectively. Data show one representative graph and mean ± SEM of at least 4 healthy donors.

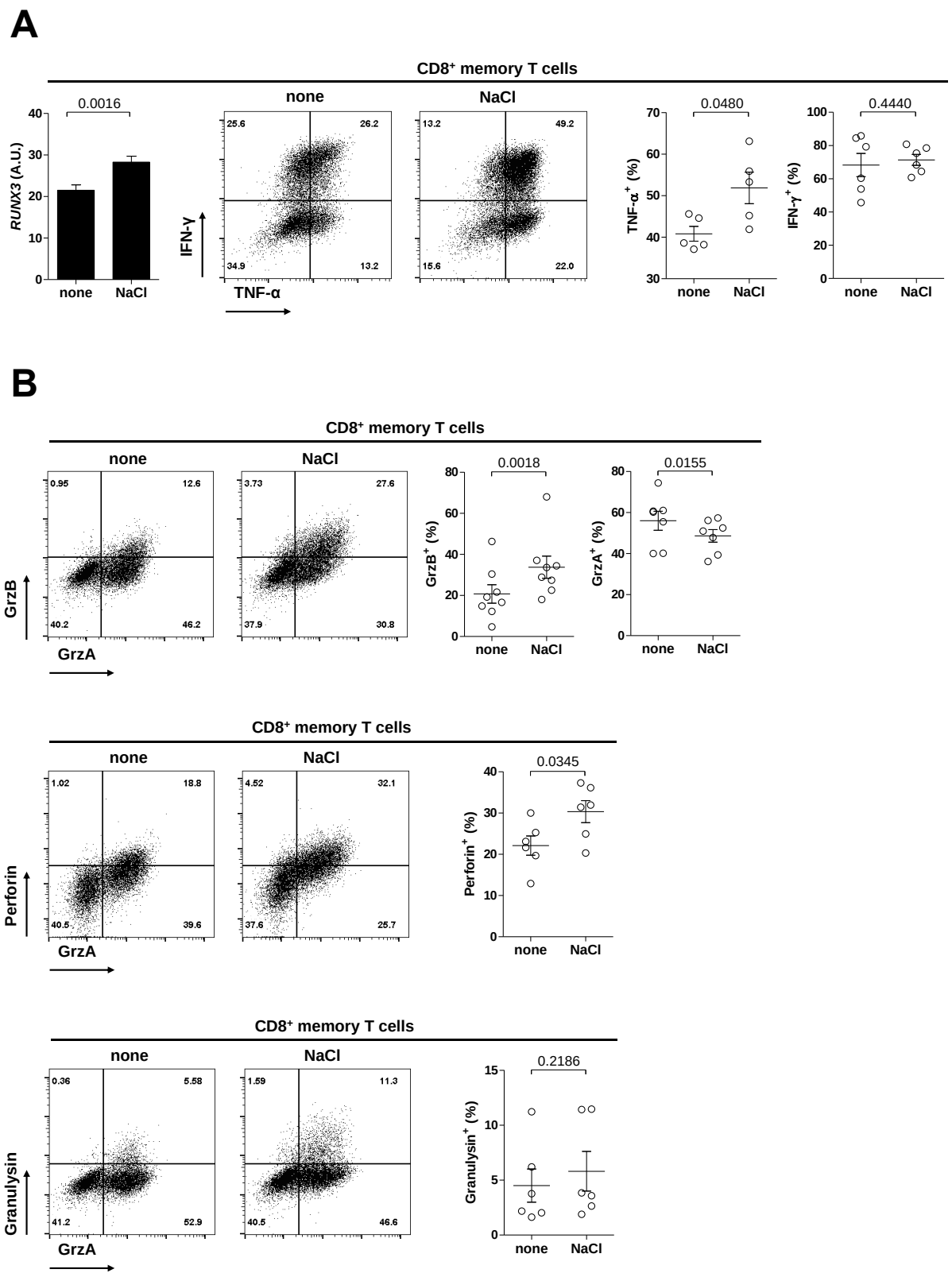
A
CD8+ memory T cells
0.0016
RUNX3 (A.U.)
none
NaCl
IFN-γ
TNF-α
25.6
26.2
34.9
13.2
13.2
49.2
15.6
22.0
0.0480
TNF-α+ (%)
0.4440
IFN-γ+ (%)
B
CD8+ memory T cells
0.95
12.6
40.2
46.2
3.73
27.6
37.9
30.8
GrzB
GrzA
0.0018
GrzB+ (%)
0.0155
GrzA+ (%)
CD8+ memory T cells
1.02
18.8
40.5
39.6
4.52
32.1
37.6
25.7
Perforin
0.0345
Perforin+ (%)
CD8+ memory T cells
0.36
5.58
41.2
52.9
1.59
11.3
40.5
46.6
Granulysin
0.2186
Granulysin+ (%)

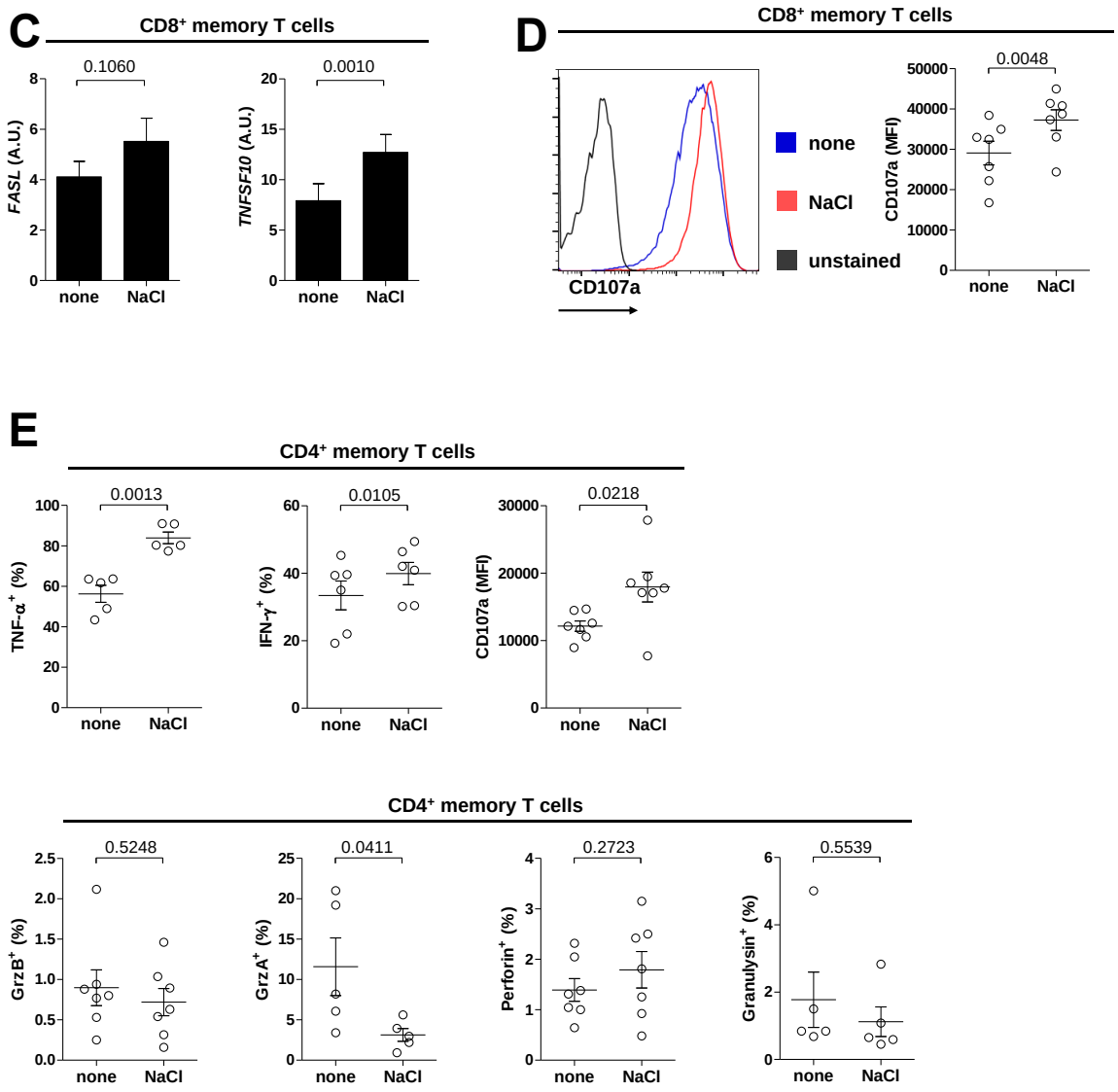


**Figure 3.11. Hypertonicity promotes expression of cytolytic effector molecules in cytotoxic memory T cells as well as in memory T helper cells.**
Purified primary CD8⁺ or CD4⁺ memory T cells were isolated and stimulated for 2 days with αCD3/αCD28 mAbs and rested for 3 days in the presence or absence of a higher concentration of NaCl. **(A)** On day 5, CD8⁺ memory T cells were analysed by qPCR for *RUNX3* or stained and expression of TNF-α and IFN-γ was measured by FACS. Data show mean ± SEM of 7 (for *RUNX3*), 5 (for TNF-α) or 6 (for IFN-γ) healthy donors. **(B)** On day 5, CD8⁺ memory T cells were stained and expression of GrzA, GrzB, Perforin and Granulysin was measured by FACS. Data show mean ± SEM of 8 (for GrzB), 7 (for GrzA) or 6 (for Perforin and Granulysin) healthy donors. **(C)** On day 5, CD8⁺ memory T cells were analysed by qPCR for *FASL* and *TNFSF10*. Data show mean ± SEM of 7 healthy donors. **(D)** On day 5, CD8⁺ memory T cells were stained and expression of CD107a was measured by FACS. Data show mean ± SEM of 7 healthy donors. **(E)** On day 5, CD4⁺ memory T cells were stained and expression of TNF-α, IFN-γ, CD107a, GrzB, GrzA, Perforin and Granulysin was measured by FACS. Data show mean ± SEM of at least 5 healthy donors.

These results demonstrate that CTLs stimulated in hypertonicity show a more aggressive and cytotoxic phenotype by producing more membrane-poring perforin, shifting the granzyme A : B ratio inside the granules towards the more effective granzyme B, increasing the cells' degranulation speed, inducing alternative cytolytic pathways and evoking a broader immune response via TNF-α.

### 3.5. Effects of hypertonicity on the cytolytic function in cytotoxic T cells

To investigate whether this phenotypical enhancement of CTLs is correlated with functional alterations, *in vitro* cytotoxicity assays were performed. xCELLigence devices were used for this purpose providing a close-to-live monitoring of cytolysis via frequent concurrent impedance measurements. Growth and proliferation of adherent cells on the well bottom will increase the impedance measured while cell lysis leads to decreased impedance. The impedance measurements are issued as cell index values; a schematic representation of the assay's setting is shown in Fig. 3.13A.

A375 is a human malignant melanoma cell line that has regularly been used in tumor analysis studies. Being adherent, it represents an ideal target cell line. For analysis of the cytolytic function of CTLs, their target cells' MHC complexes were loaded with MART-1 peptide. To gain reliable and reproducible effector cells, T cells were nucleofected with DNA coding for a MART-1-specific TCR. The introduced TCR contained a murine TCR β-chain, to enable enrichment for successfully nucleofected T cells by targeting the murine β-chain (Fig. 3.12A). The resulting populations demonstrated an expression of the introduced TCR of approximately 75 % for the isotonic and 70 % for the hypertonic condition and a $CD8^+$ purity of 90 % in both conditions (Fig. 3.12B). In one experiment the expression of the introduced TCR was noticeably lower in both groups (Fig. 3.12B).

To perform the cytotoxicity assay, A375 melanoma cells were seeded into the wells and co-culture with sorted nucleofected T cells was started 24 hours afterwards. Before, the T cells were stimulated for 5 days as described before. Conditions included an isosmotic environment for all cells in all steps, a hyperosmotic environment for all cells in all steps, a hyperosmotic environment only for the T cells just during their stimulation before isosmotic co-culture or an isosmotic environment during prior T cell stimulation but a hyperosmotic environment during co-culture (for schematic representation see Fig. 4.3).

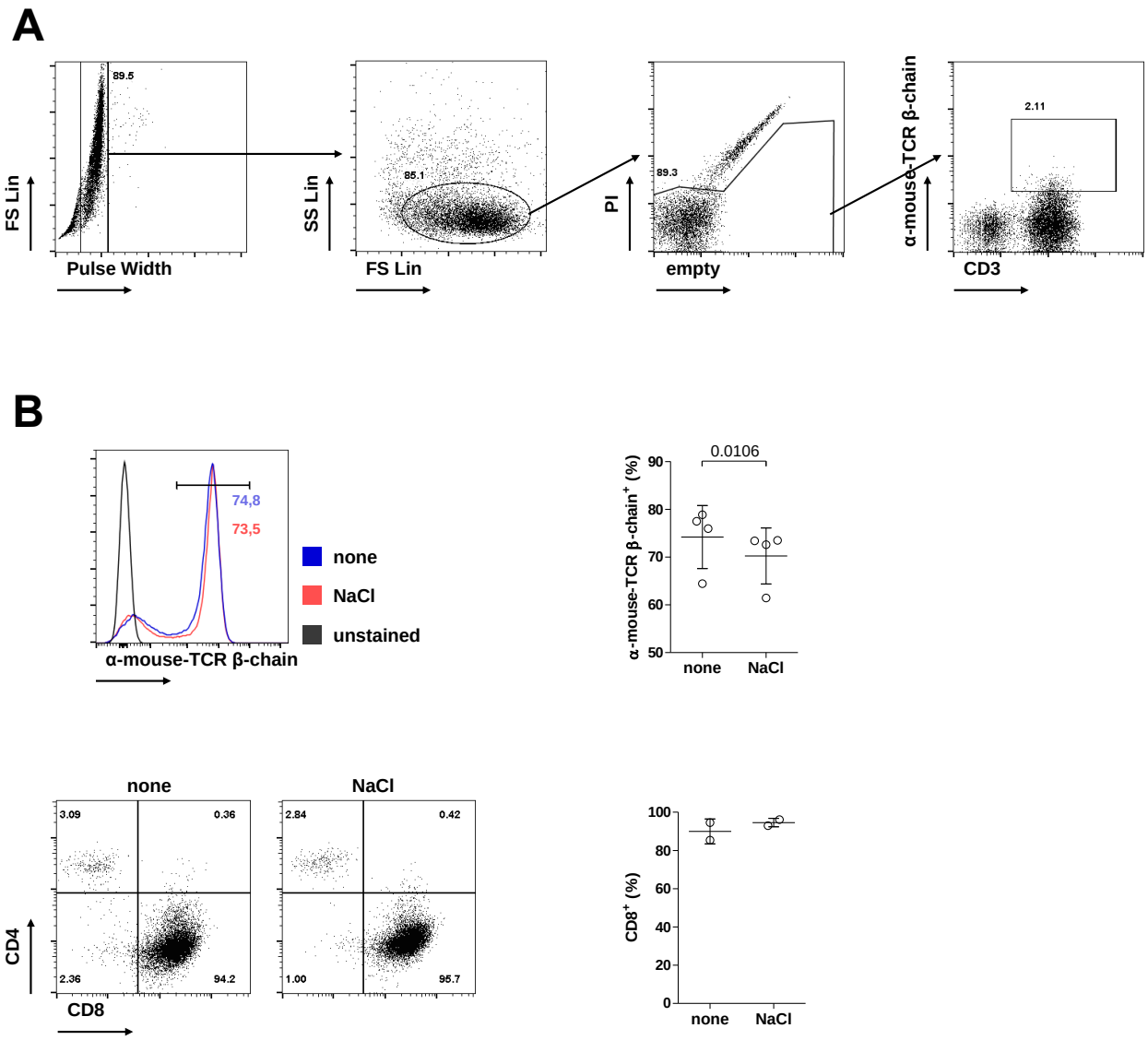


**Figure 3.12. Nucleofected T cells can be purified and show stable expression of the MART-1-specific TCR and persistent CD8⁺/CD4⁺ ratio irrespective of environmental osmolarity.**

Primary PBMCs were nucleofected with DNA coding for MART-1-specific TCR. **(A)** On day 1 after nucleofection, PBMCs were stained and sorted depending on the expression of CD3 and α-mouse-TCR β-chain. FACS dot blots including gates for the sorting strategy are shown. **(B)** Sorted nucleofected T cells were expanded and subsequently stimulated for 2 days with αCD3/αCD28 mAbs and rested for additional 3 days in the presence or absence of a higher concentration of NaCl. On day 5, cells were stained and expression of α-mouse-TCR β-chain, CD4 and CD8 was measured by FACS. Data show mean ± SEM of 4 (for α-mouse-TCR β-chain) or 2 (for CD8) experiments with cells from the culture from one healthy donor.

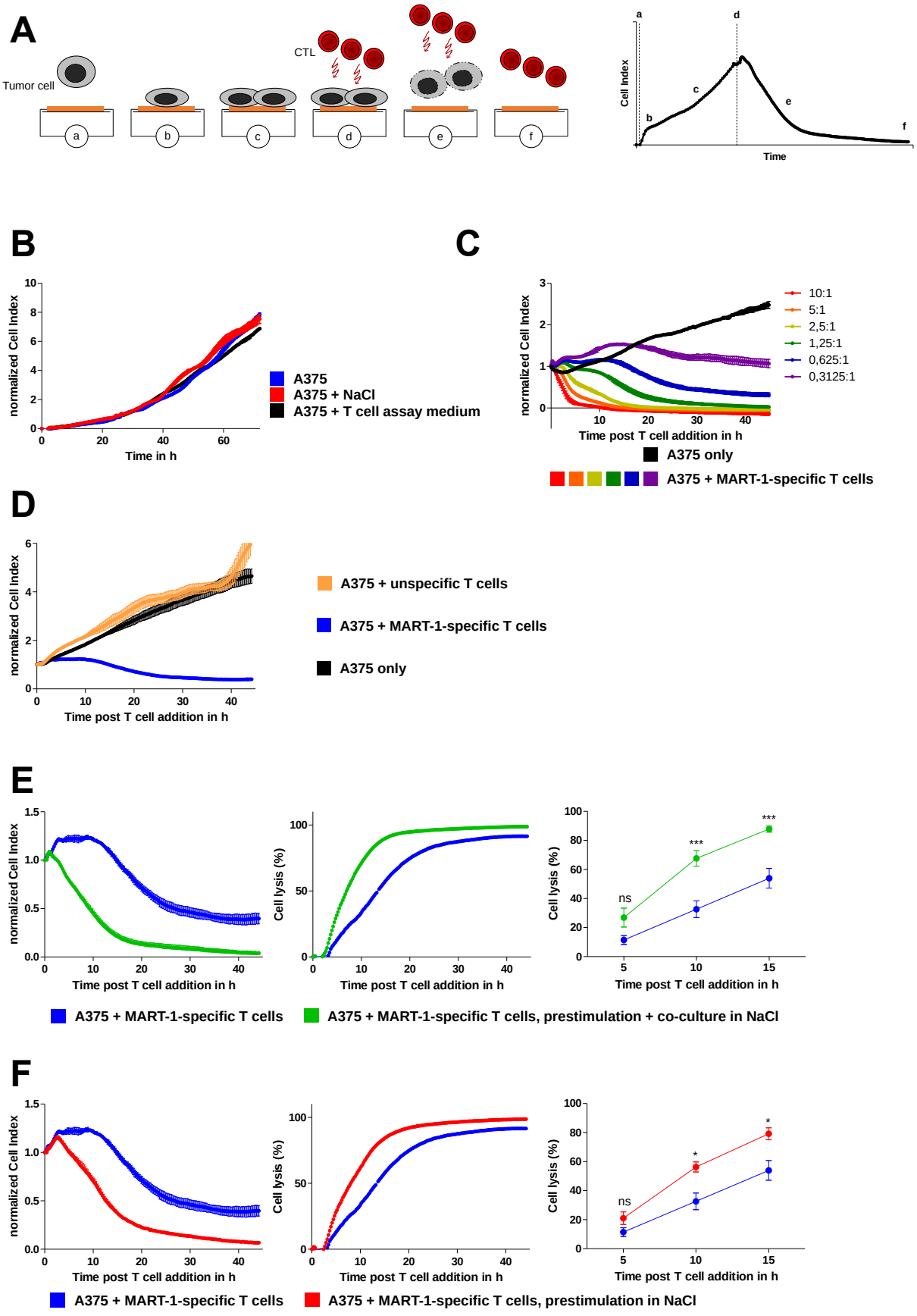
A
Tumor cell
CTL
a
b
c
d
e
f
Cell Index
Time
B
normalized Cell Index
Time in h
A375
A375 + NaCl
A375 + T cell assay medium
C
normalized Cell Index
Time post T cell addition in h
10:1
5:1
2,5:1
1,25:1
0,625:1
0,3125:1
A375 only
A375 + MART-1-specific T cells
D
normalized Cell Index
Time post T cell addition in h
A375 + unspecific T cells
A375 + MART-1-specific T cells
A375 only
E
normalized Cell Index
Time post T cell addition in h
Cell lysis (%)
Time post T cell addition in h
Cell lysis (%)
ns
***
***
Time post T cell addition in h
A375 + MART-1-specific T cells
A375 + MART-1-specific T cells, prestimulation + co-culture in NaCl
F
normalized Cell Index
Time post T cell addition in h
Cell lysis (%)
Time post T cell addition in h
Cell lysis (%)
ns
*
*
Time post T cell addition in h
A375 + MART-1-specific T cells
A375 + MART-1-specific T cells, prestimulation in NaCl

**Figure 3.13. Hypertonicity boosts the cytolytic effector function of nucleofected cytotoxic T cells.**

**(A)** Schematic representation of the impedance-based real-time cytotoxicity assay using xCELLigence. (a) Adhesive target tumor cells are added to the wells, (b) attach to the bottom of the wells and (c) proliferate and reproduce. (d) Specific T cells are added to the wells and (e) start to kill the target cells until all target cells are eliminated (f). **(B)** A375 melanoma cell line cells were seeded on E-plates and growth was monitored over 72 h. One representative graph of 4 experiments is shown. **(C)** A375 melanoma cell line cells (target cells) were seeded on E-plates as in (B). After 24 h, target cells were pulsed with MART-1 peptide for 1 h at a concentraton of $10^{-7}$ M. Sorted nucleofected MART-1-specific T cells (effector cells) were expanded in feeder-based cultures. Co-culture of target and effector cells was started directly after pulsing at indicated effector : target ratios. **(D)** After expansion, sorted nucleofected T cells were stimulated for 2 days with αCD3/αCD28 mAbs and rested for 3 days in the absence of additional NaCl. On day 4, A375 melanoma cell line cells were seeded and later pulsed as in (B, C). On day 5, co-culture of target and effector cells was started directly after pulsing at an effector : target ratio of 1:1. Effector cells were T cells sorted to be successfully nucleofected (MART-1-specific) or T cells sorted to be not nucleofected (unspecific) (see Figure 3.12A). **(E)** After expansion, sorted nucleofected MART-1-specific T cells were stimulated for 2 days with αCD3/αCD28 mAbs and rested for 3 days in the presence or absence of a higher concentration of NaCl. On day 4, A375 melanoma cell line cells were seeded and later pulsed as in (B, C), but in the presence or absence of a higher concentration of NaCl. On day 5, co-culture of target and effector cells was started directly after pulsing at an effector : target ratio of 1:1 in the presence or absence of a higher concentration of NaCl. Shown is one representative plot and a summary. Dots represent mean ± SEM of 3 experiments with nucleofected MART-1-specific T cells from the culture from one healthy donor. **(F)** After expansion, sorted nucleofected MART-1-specific T cells were stimulated for 2 days with αCD3/αCD28 mAbs and rested for 3 days in the presence or absence of a higher concentration of NaCl. On day 4, A375 melanoma cell line cells were seeded and later pulsed as in (B, C) in the absence of a higher concentration of NaCl. On day 5, co-culture of target and effector cells was started directly after pulsing at an effector : target ratio of 1:1 in the absence of a higher concentration of NaCl. Shown is one representative plot and a summary. Dots represent mean ± SEM of 3 experiments with the nucleofected MART-1-specific T cells from the culture from one healthy donor.

To evaluate whether the planned setting worked reliably, some establishing experiments analyzing the behavior of the tumor cells as well as the sorted nucleofected MART-1 specific T cells were conducted. Growth and proliferation of A375 tumor cells were not affected by the tonicity of the medium or by a change of medium like it would occur at the start of co-culture (Fig. 3.13B). When the sorted nucleofected MART-1 specific T cells were added to the wells, rapid killing of the adherent target cells occurred dependent on the indicated effector to target cell ratio (Fig. 3.13C). In all subsequent experiments, T cells and target cells were co-cultured at a ratio of 1:1. To evaluate whether this result represented an off-target TCR-mediated killing, T cells not expressing the MART-1-specific TCR were set in co-culture with target cells (Fig. 3.13D). There was no measurable cell death in the target cell population for the unspecific T cells. Thus, an effective design of the experiment with specific TCR-mediated killing of the target cells can be assumed.

If the growth of the target cell line, the stimulation of the MART-1-specific T cells and the co-culture of both cell types took place under hyperosmotic conditions, the measured cell index dropped at a higher rate than under isosmotic conditions, indicating a significantly higher lysis of target cells in hyperosmolarity (Fig. 3.13E). The difference in cell lysis was more than 30 % after 15 hours. To evaluate whether this effect was due to the T cells' or the target cells' reaction to a hypertonic environment, the MART-1-specific T cells were stimulated under hyperosmotic conditions while the growth of the target cell line as well as the subsequent co-culture took place under isosmotic conditions. Interestingly, these MART-1-specific T cells that were stimulated in hypertonicity only before co-culture still induced lysis of the target cells at a higher rate with the difference in lysis after 15 hours being 25 % (Fig. 3.13F). These results suggest that cytotoxic T cells feature a much higher cytolytic potential when they are stimulated under hypertonic conditions.

To confirm this finding and rule out that the observed effects in CTLs were influenced by the nucleofection, MART-1-specific cytotoxic T cells were purified directly from the natural repertoire of a healthy donor (Fig. 3.14A). Out of 1 x $10^8$ PBMCs, 67 cells were sorted to be MART-1-specific. They were cultured individually as clone populations to be able to subsequently rule out dissimilar growth behavior of different clones in iso- or hyperosmolarity. The most efficient clones could be identified for the cytotoxicity assay. Out of the 67 clones, 20 grew a population of which 12 populations were proliferating well enough to perform cytotoxicity assays. Of the 12 clone populations tested for cytotoxic potential by the described xCELLigence-based approach, the two most potent clones (Clone 1 + 7) were selected for cytotoxicity assays in iso- and hyperosmolarity. (Fig. 3.14B)

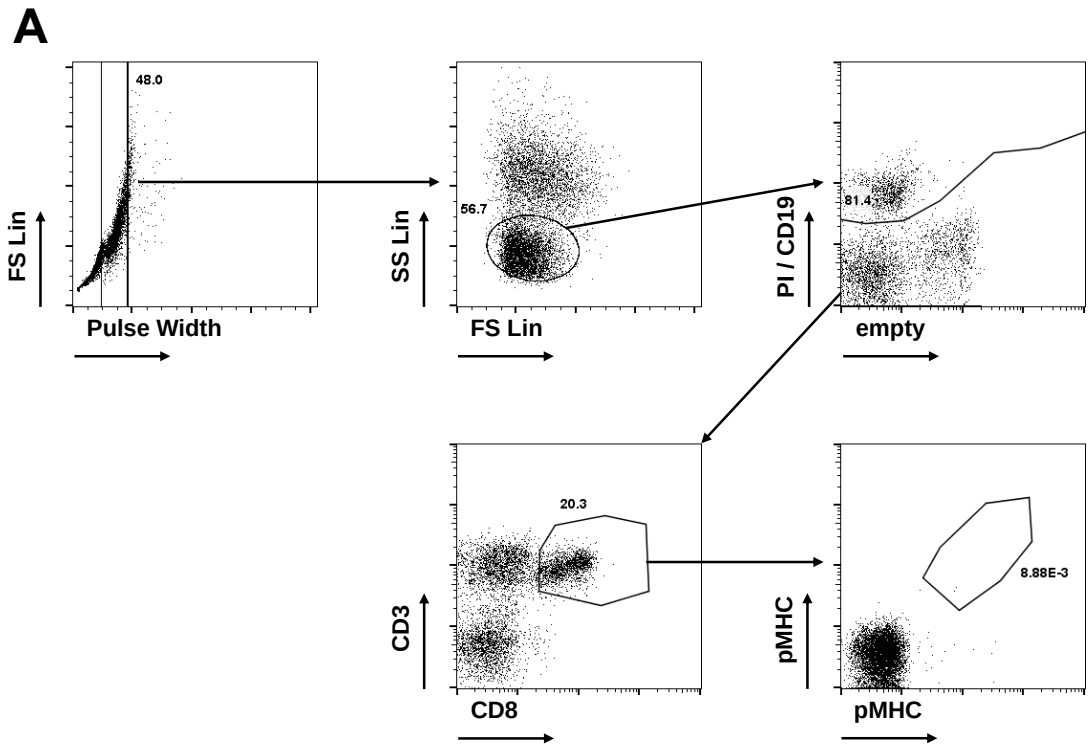


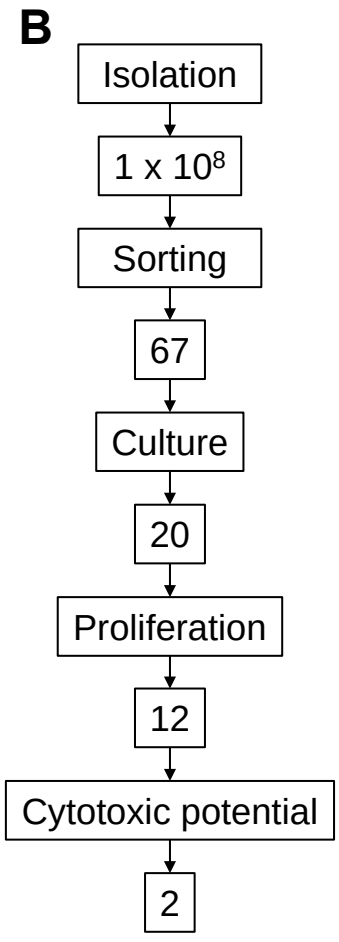


**Figure 3.14. MART-1-specific cytotoxic T cells from the natural repertoire can be isolated and expanded.** **(A)** Primary PBMCs were stained and sorted depending on the expression of CD3, CD8, CD19 and binding to pMHC tetrameric complexes loaded with MART-1 peptide. FACS dot blots including gates for the sorting strategy are shown. Cells were sorted as single cells into a 384-well plate and subsequently feeder-based expanded. **(B)** Schematic representation of handling of the MART-1-specific $CD8^+$ T cells from the natural repertoire.

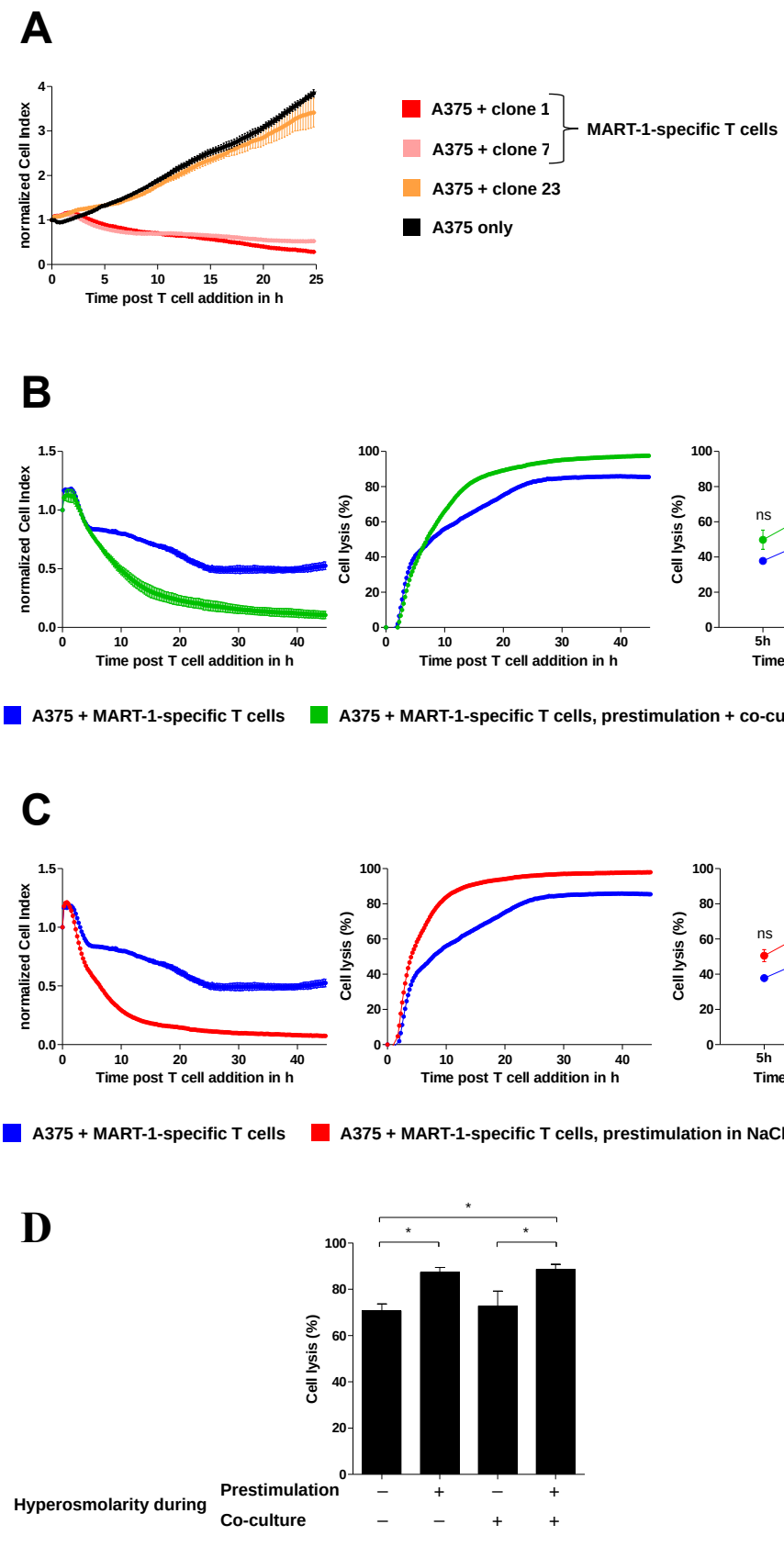
A
normalized Cell Index
Time post T cell addition in h
A375 + clone 1
A375 + clone 7
MART-1-specific T cells
A375 + clone 23
A375 only
B
normalized Cell Index
Time post T cell addition in h
Cell lysis (%)
Time post T cell addition in h
Cell lysis (%)
ns
5h
10h
15h
Time post T cell addition in h
A375 + MART-1-specific T cells
A375 + MART-1-specific T cells, prestimulation + co-culture in NaCl
C
normalized Cell Index
Time post T cell addition in h
Cell lysis (%)
Time post T cell addition in h
Cell lysis (%)
ns
5h
10h
15h
Time post T cell addition in h
A375 + MART-1-specific T cells
A375 + MART-1-specific T cells, prestimulation in NaCl
D
Cell lysis (%)
Hyperosmolarity during
Prestimulation
Co-culture

**Figure 3.15. Cytotoxic T cells from the natural repertoire show augmented cytolytic effector function in a hypertonic environment.**
**(A)** A375 melanoma cell line cells were seeded and later pulsed as previously described. Two MART-1-specific T cell clone populations (Clones 1 and 7) that expanded sufficiently and showed highest capacity in eliminating the tumor cells and 1 clone population of T cells sorted to be $CD3^+$ and $CD8^+$ but not $pMHC^+$ (Clone 23) (see Figure 3.14A) were selected. Co-culture of target and effector cells was started directly after pulsing at an effector : target ratio of 1:1. **(B)** After expansion, MART-1-specific T cell clone populations were stimulated for 2 days with αCD3/αCD28 mAbs and rested for 3 days in the presence or absence of a higher concentration of NaCl. On day 4, A375 melanoma cell line cells were seeded in the presence or absence of a higher concentration of NaCl. On day 5, co-culture of target and effector cells was started directly after pulsing with MART-1 peptide at an effector : target ratio of 1:1 in the presence or absence of a higher concentration of NaCl. Shown is one representative plot and a summary. Dots represent mean ± SEM of 2 experiments with the clones 1 and 7 from one healthy donor. **(C)** After expansion, MART-1-specific T cell clone populations were stimulated for 2 days with αCD3/αCD28 mAbs and rested for 3 days in the presence or absence of a higher concentration of NaCl. On day 4, A375 melanoma cell line cells were seeded in the absence of a higher concentration of NaCl. On day 5, co-culture of target and effector cells was started directly after pulsing with MART-1 peptide at an effector : target ratio of 1:1 in the absence of additional NaCl. Shown is one representative plot and a summary. Dots represent mean ± SEM of 2 experiments with the clones 1 and 7 from one healthy donor. **(D)** After expansion, MART-1-specific T cell clone populations were stimulated for 2 days with αCD3/αCD28 mAbs and rested for 3 days in the presence or absence of a higher concentration of NaCl. On day 4, A375 melanoma cell line cells were seeded in the presence or absence of a higher concentration of NaCl. On day 5, co-culture of target and effector cells was started directly after pulsing with MART-1 peptide at an effector : target ratio of 1:1 in the presence or absence of a higher concentration of NaCl. Data show mean ± SEM at 15 hours after starting the co-culture of 2 experiments with the clones 1 and 7 from one healthy donor.

As a control, cytotoxic T cells were selected that would not bind MART-1 (Clone 23). While the MART-1-specific T cells showed an effective killing of the target cells, the unspecific T cells did not affect growth of the target cells (Fig. 3.15A). Similar to the previous setting, growth of the target cells, stimulation of the MART-1-specific T cells and the co-culture were conducted either under iso- or hyperosmotic conditions and analyzed for cell lysis. In line with the findings from the nucleofected cells, cell lysis was significantly higher under hypertonic conditions with a difference of 18 % after 15 hours (Fig. 3.15B). Furthermore, stimulation of the MART-1-specific T cells under hypertonic conditions with target cell growth and subsequent co-culture taking place under isotonic conditions was sufficient to accelerate the cell lysis significantly (Fig. 3.15C). The lysis was found to be 17 % higher after 15 hours when only the T cells were stimulated under hypertonic conditions beforehand. These findings demonstrate consistently that a hypertonic environment induces the cytotoxic potential of T cells. Fig. 3.15D demonstrates that prestimulation of cytotoxic T cells under hypertonic conditions is sufficient to establish higher cytolytic capacity in the T cells independent of the milieu where the killing may take place.

### 3.6. Analysis of potential molecular mechanisms mediating the effects of hypertonicity on cytotoxic T cells

To investigate the underlying molecular mechanism behind this enhancement of cytotoxic T cell functions, the shNFAT5-shSGK1-model was employed again as a significant increase of the expression levels of *NFAT5* and *SGK1* in CTLs in hypertonicity was found (Fig. 3.16A). Similar to my previous approach, *NFAT5* and *SGK1* were silenced in primary cytotoxic $CD8^+$ T cells using shRNA introduced by lentiviruses. Analysis of *NFAT5* and *SGK1* suggest that the silencing was conducted successfully (Fig. 3.16B). However, the control conditions with an empty vector (shCtrl) did not behave like the conditions without any lentiviral manipulation when it comes to effects of hypertonicity on expression of *FASL* and *TNFSF10* (Fig. 3.16C). Thus, the employed model seems inappropriate to investigate the roles of NFAT5 and SGK1 in the mediation of the effects of hypertonicity on cytotoxic T cells.

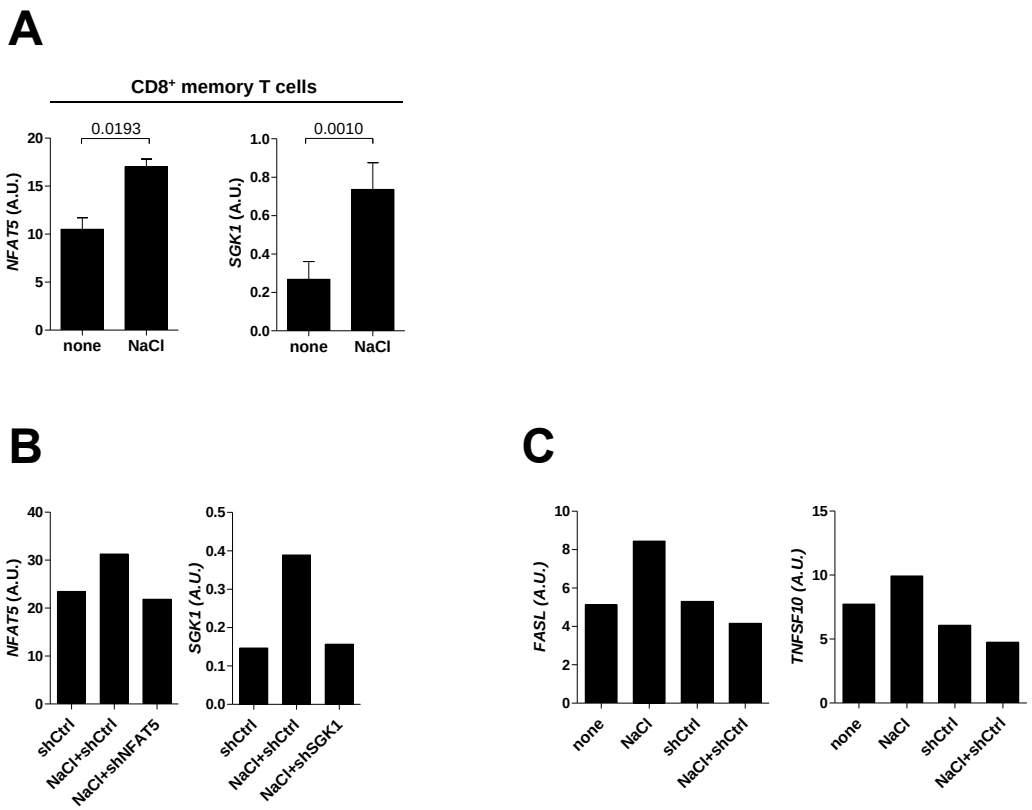


**Figure 3.16. Potential mediation of hypertonicity induced promotion of cytolytic functions in cytotoxic T cells by NFAT5 and SGK1 remains to be determined.**
Purified primary CD8$^+$ memory T cells were isolated and stimulated for 2 days with αCD3/αCD28 mAbs and rested for 3 days in the presence or absence of a higher concentration of NaCl. (**A**) On day 5, cells were analysed by qPCR for *NFAT5* and *SGK1*. Data show mean ± SEM of 5 healthy donors. (**B-C**) Cells were transduced with shRNA as described before to create the conditions shCtrl, shNFAT5 and shSGK1. On day 5, cells were analysed by qPCR for *NFAT5*, *SGK1*, *FASL* and *TNFSF10*. Data from one healthy donor is shown.

## 4. Discussion

The relevance of hypertonicity as an important factor in the lymphoid microenvironment has been demonstrated already in 2004 by Go et al. They showed that the osmosensitive transcription factor NFAT5 is essential for the survival of murine T cells under hyperosmotic conditions as well as for a complete T cell immune response (Go et al., 2004). This already emphasized the influence of hyperosmolarity on T cell activation. In 2011, it has been shown that the $Na^+$-sensitive p38 MAP kinase pathway and production of IL-17 are closely connected (Noubade et al., 2011). More recently, Kleinewietfeld et al. and Wu et al. analyzed the behavior and differentiation characteristics of naïve T cells in a hyperosmotic environment (Kleinewietfeld et al., 2013; Wu et al., 2013). Considering that many of the T cells' effector functions are conducted in the hypertonic milieu, the focus of my thesis was on the effects that hyperosmolarity exerts on memory T helper cells and cytotoxic T cells.

In the first part of my thesis, primary $T_h17$ cells have been cultured and their response to a hypertonic milieu has been investigated. I found the $T_h17$ phenotype induced in hypertonicity with increased production of characteristic $T_h17$ cytokines. Notably, the $T_h17$ cells showed increased expression of the anti-inflammatory transcription factor $FOXP3^+$ with ambiguous changes in pro- or anti-inflammatory cytokine production. While the $T_h17$ phenotype remained augmented even after the return to an isosmotic milieu, the induction of FOXP3 in $T_h17$ cells was directly dependent on a sustained hyperosmotic environment. I could demonstrate that the boost of this potential anti-inflammatory phenotype was regulated by the p38 MAP kinase pathway with NFAT5 and SGK1 being relevant mediators. A graphical synopsis of the results can be found in Fig. 4.1.

In the second part of my thesis, the activation level, the metabolic state and the cytolytic profile of primary cytotoxic $CD8^+$ T cells under hypertonic conditions have been analyzed. Moreover, the effects of hypertonicity on the immediate cytotoxic competence have been examined using specific killing assays. I found that CTLs reached higher levels of activation when stimulated under hypertonic conditions. This activation came along with increased metabolic throughput and increased expression of cytolytic effector molecules such as TNF-α, granzyme B and perforin as well as death receptor ligands. Furthermore, under hyperosmotic conditions, CTLs demonstrated enhanced antigen-specific killing capability and faster elimination of target cells. Graphical synopses of the results can be found in Fig. 4.2 and 4.3.

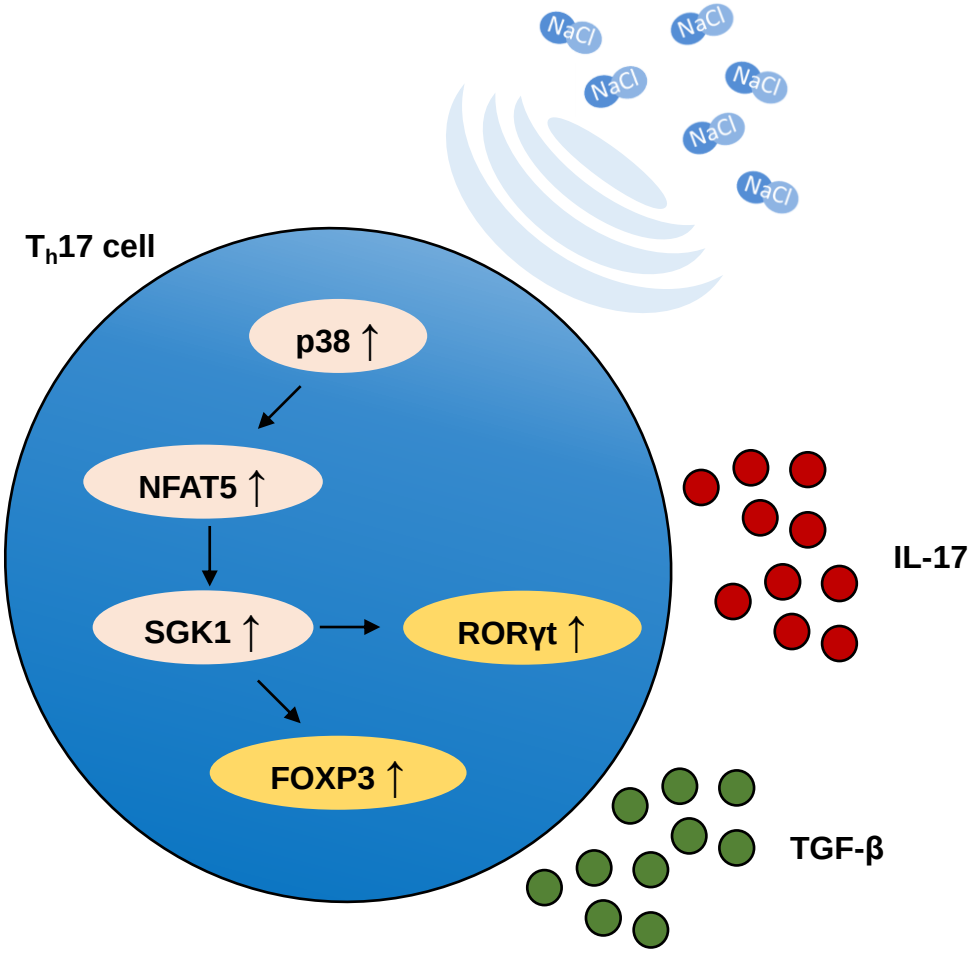


**Figure 4.1. Schematic representation of the changes in the phenotype of $T_h17$ cells in hyperosmotic environments and the mediating pathway.**
Hyperosmolarity induces many phenotypical changes in $T_h17$ cells. Induction of IL-17 and TGF-β are among the most prominent. Together with the phenotypical changes of the cell, certain transcription factors are being activated that play a role in defining the function of $T_h17$ cells: RORγt and FOXP3. The activation of these transcription factors is mediated via the p38 MAP kinase pathway including NFAT5 and SGK1.

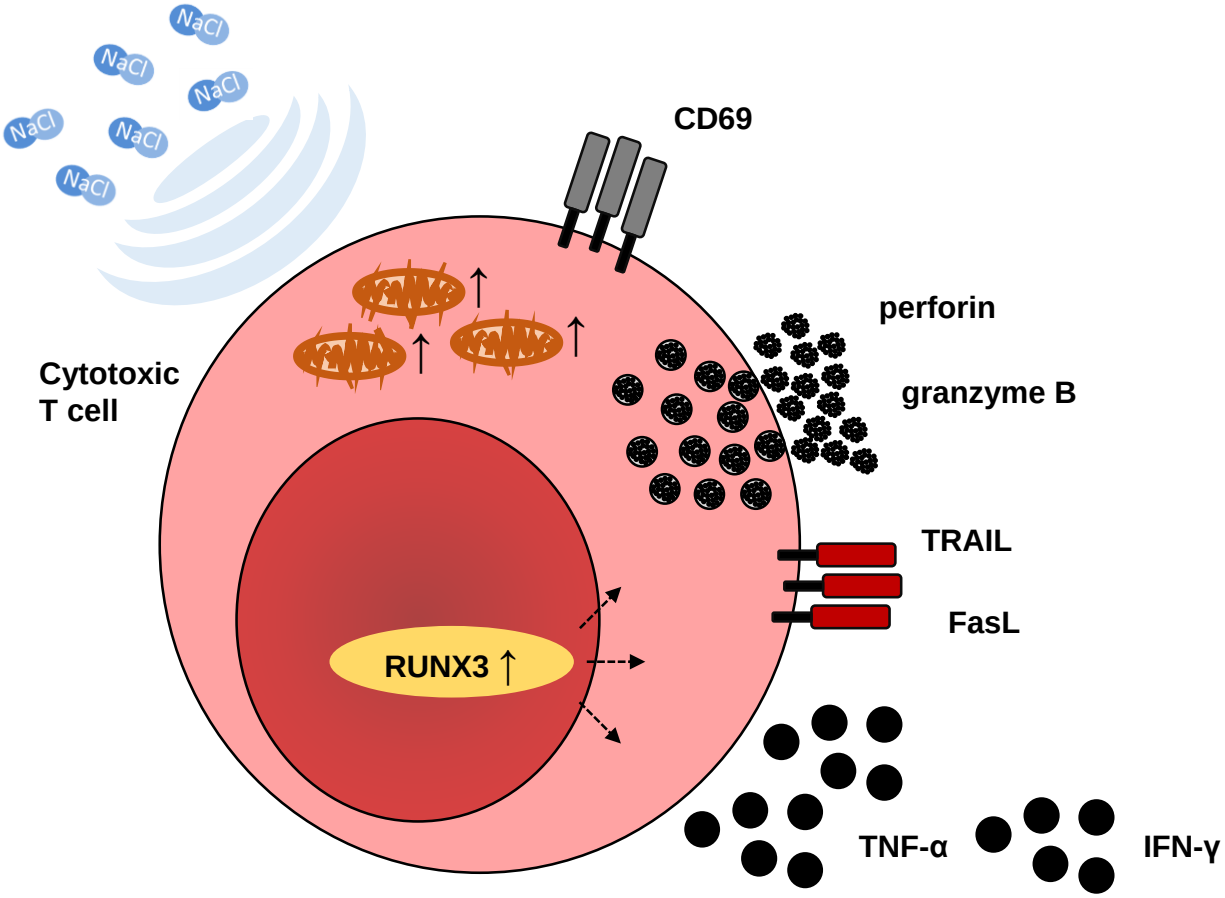


**Figure 4.2. Schematic representation of the changes in the phenotype of cytotoxic T cells in hyperosmotic environments.**
Upon stimulation in hypertonicity, cytotoxic T cells undergo several changes. Along with higher expression of CD69 and boost of the cell metabolism including glycolysis and oxidative phoshorylysis, the cells express higher levels of RUNX3 strengthening the cytotoxic profile: Increased production of TNF-α (with unchanged IFN-γ expression), intensified expression of death receptor ligands such as TRAIL and FasL on the cell surface, faster degranulation as well as higher levels of perforin and granzyme B in the cytotoxic granules can be observed.

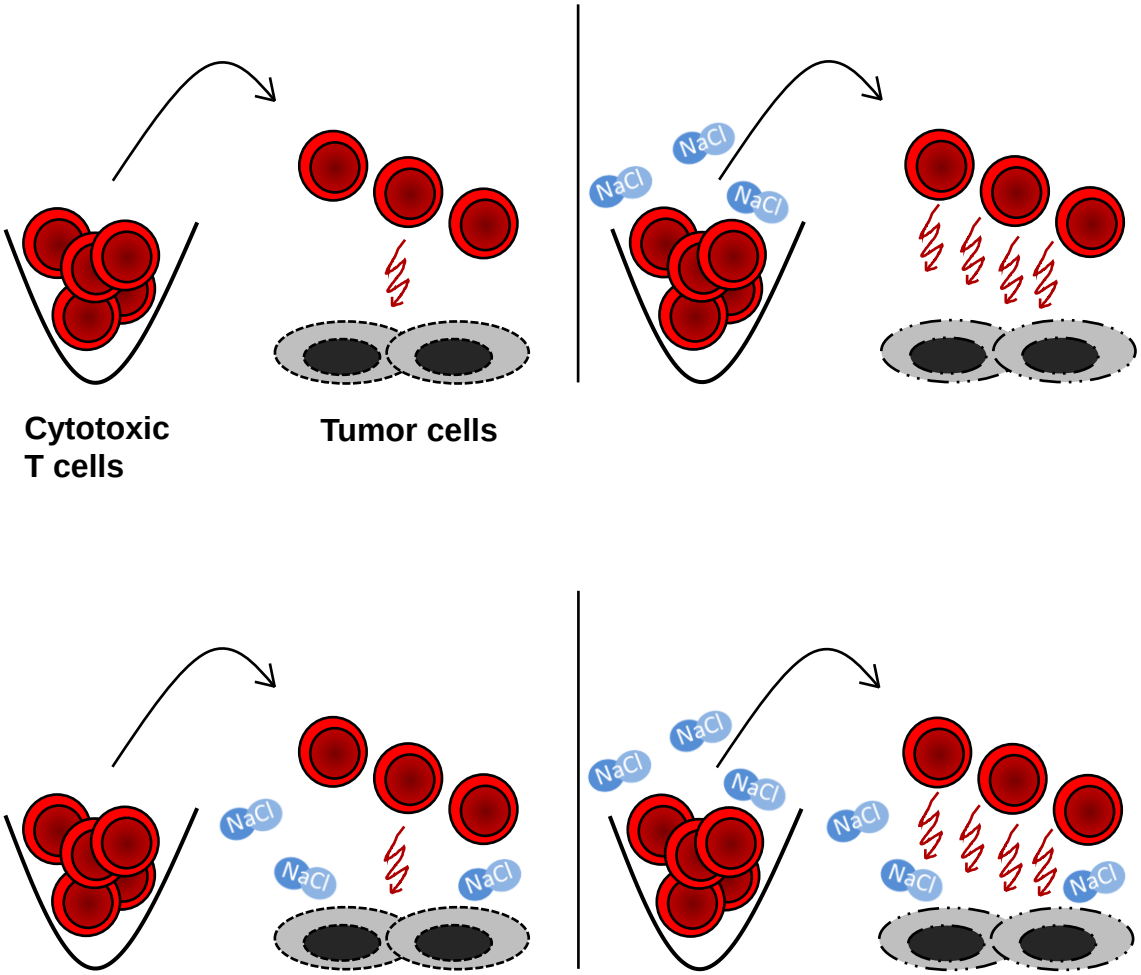


**Figure 4.3. Schematic representation of the changes in cytolytic capability in cytotoxic T cells in hyperosmotic environments.**
Cytotoxic T cells show cytolytic capability to kill tumor cells. Increased tumor cell clearance can be observed when the CTLs are stimulated under hypertonic conditions before co-culture and the subsequent co-culture takes place in a hypertonic environment. Similarly increased clearance is demonstrated when only the CTL stimulation before co-culture takes place in hypertonicity but the co-culture takes place in an isotonic environment. However, co-culture under hypertonic conditions when the CTLs were not exposed to hypertonicity before does not result in enhanced cytolytic potential of the CTLs.

## 4.1. Tonicity signals shape $T_h17$ cell differentiation and plasticity

### 4.1.1. Hypertonicity accentuates anti-inflammatory features in $T_h17$ cells

In the main, the findings from my studies on memory T cells seem to be in line with the results from Kleinewietfeld et al. and Wu et al. (Kleinewietfeld et al., 2013; Wu et al., 2013): under hypertonic conditions, $T_h17$ show augmented RORγt and IL-17 expression and this increase is similarly mediated by the NFAT5 and SGK1. I can confirm that the effects of hypertonicity on T cell differentiation can to some extent be transferred to T cell plasticity in $T_h17$ cells, even though the induction of RORγt expression was significant but in its extent hardly relevant. However, though I propose that the $T_h17$ phenotype is promoted by hypertonicity, my findings question whether this represents a mere boost of the pro-inflammatory phenotype in $T_h17$ cells as proposed by Kleinewietfeld et al.

Recently, it has been shown that $T_h17$ cells do not only exhibit pro-inflammatory features but may also be capable of regulatory functions (O'Connor et al., 2010). Zielinski et al. have found that the differentiation of naïve T cells using different pathogens leads to different species of $T_h17$ cells. *Candida albicans*-specific $T_h17$ cells produce IL-17 and the pro-inflammatory cytokine IFN-γ. In contrast, *Staphylococcus aureus*-specific $T_h17$ cells are able to produce IL-17 and the anti-inflammatory cytokine IL-10, after restimulation. The presence or absence of IL-1β in the milieu of differentiation, which is pathogen-dependent, was found to be responsible for this duality, emphasizing the importance of the composition of the micromilieu during T cell differentiation. (Zielinski et al., 2012) Although my work focused on memory T cells, which are already differentiated, $T_h17$ cells represent a highly plastic T cell subset with the ability to transdifferentiate into different lineages (Weaver et al., 2006). Moreover, $T_h17$ cells are not only able to co-produce hallmark cytokines of other lineages but also co-express the respective master regulator. The lineage frontiers seem to be especially flexible between $T_h17$ cells with the master regulator RORγt and $T_{reg}$ cells with the respective FOXP3 (Zhou et al., 2009).

I found that $T_h17$ cells stimulated under hypertonic conditions strongly co-express IL-17 and FOXP3 and produce higher levels TGF-β. This finding suggests that the function of the arising $T_h17$ cells under hypertonic conditions cannot be fully pro-inflammatory. Interestingly, a $FOXP3^+$ $ROR\gamma t^+$ regulatory T cell population has recently been described to co-produce high levels of TGF-β and IL-17 on the one hand, but to induce enhanced mast cell degranulation on the other hand (Chellappa et al., 2015). Similarly, $T_h17$ cells may exhibit a dual phenotype in hyperosmolarity, with a complex behavior combining pro- and anti-inflammatory properties.

The profile of relevant cytokine expressions in $T_h17$ cells in hypertonicity gives an ambiguous picture: the production of the anti-inflammatory IL-10 is reduced and the expression of the pro-inflammatory IFN-γ remains almost unaltered. The increase in FOXP3 expression would suggest an anti-inflammatory cytokine profile. Recent results from Hernandez et al. demonstrate that under hypertonic conditions, $FOXP3^+$ regulatory T cells produce IFN-γ and consequently lose their suppressive function towards other T cells (Hernandez et al., 2015). In the end, the definite role of FOXP3 in suppressive functions of T cells is currently under investigation since recent findings question the mere function as master regulator for regulatory T cells, but also describe FOXP3 expression in response to T cell activation (Kmieciak et al., 2009; Wang et al., 2007). Thus, it is imaginable that the demonstrated elevated FOXP3 levels under hypertonic conditions represent rather an activated than an anti-inflammatory state of $T_h17$ cells.

Remarkably, Gagliani et al. have recently discovered that in the course of an inflammation and mediated by TGF-β, $T_h17$ cells can change their functional phenotype into $FOXP3^-$ type 1 regulatory T cells that express IL-10 (Gagliani et al., 2015). This shows that an anti-inflammatory phenotype is not dependent on continuous FOXP3 expression. Similar to their findings that the new phenotype develops during resolution of the inflammation, I also discovered alterations in the $T_h17$ cells that depend on the temporal aspects of environmental changes: the induction of FOXP3 expression in $T_h17$ cells in hypertonicity is dependent on persistent osmotic stress and will regress as soon as the cells enter an isotonic environment. This suggests that the longer the inflammation lasts and keeps a hypertonic micromilieu, the more dominant the anti-inflammatory features in $T_h17$ cells may become, possibly in order to prevent overshooting immune responses. Nevertheless, once the immune reaction is finished and the cells leave the hypertonic environment they could return to their original phenotype. However, in order to improve our understanding of these cellular processes, additional research on the function of $T_h17$ cells during spatiotemporal changes of tonicity is necessary.

On the molecular level, enhanced FOXP3 expression in hypertonicity was dependent on NFAT5 as well as SGK1. SGK1 has previously been shown to play an important role in FOXO1 phosphorylation and its elimination from the nucleus (Wu et al., 2013). FOXO1 is known to have a crucial role in the differentiation of $FOXP3^+$ regulatory T cells by binding to the *FOXP3* locus and activating its promoter (Ouyang et al., 2010). In addition to FOXO1, findings from the literature suggest that SGK1 might also downregulate FOXP3 expression (Wu et al., 2018). However, my findings show that SGK1 may be important for FOXP3 upregulation in hypertonicity. Therefore, an alternative pathway for FOXP3 induction by SGK1 can be anticipated

and should be subject of further investigation. In this regard, Matthias et al. have recently demonstrated the importance of NFAT5 and SGK1 in hypertonicity by emphasizing their roles in the promotion of the $T_h2$ phenotype by inducing the expression of the transcription factor GATA3 and mediating the depletion of T-bet (Matthias et al., 2019). While novel insights emerge frequently, the interplay of sodium, p38 MAP kinase, NFAT5 and SGK1 in T helper cells is complex and remains not fully understood.

Additionally, it must be noticed, that many knockout and knockdown experiments greatly interfere with multiple cell functions. T cell survival is restricted in hyperosmolarity if NFAT5 is artificially downregulated in the cells (Go et al., 2004). Therefore, selection of surviving cells might have influenced my findings using shRNA.

Furthermore, there are several other mechanisms that influence T helper cell differentiation. For example, certain microRNAs have been found to inhibit or accelerate $T_h17$ differentiation. Their response to tonicity signals has not yet been studied in T cells and could be a target of future research. (Montoya et al., 2017)

### 4.1.2. Influence of hypertonicity on $T_h17$ cells in immunological diseases

$T_h17$ cells are known to be major players in a large number of autoimmune diseases like psoriasis and MS (Fitch et al., 2007; Fletcher et al., 2010; Rostami and Ciric, 2013). Kleinewietfeld et al. proposed that high salt intake in mice led to more pathogenic $T_h17$ cells and consequently to more severe types of EAE, an animal model of MS (Kleinewietfeld et al., 2013). However, the transferability of these findings to the human situations was put into question due to far-from-real-life amounts of salt used in the mice (comment #65409 in Kleinewietfeld et al., 2013). Nevertheless, pathogenic behavior in $T_h17$ or $T_{reg}$ cells in hyperosmotic culture has been described repeatedly (Hernandez et al., 2015; Wu et al., 2013). Recently, a subsequent study demonstrated that a high salt diet affected and changed the gut microbiota by depletion of certain strains of Lactobacilli in mice. Restoring them alleviated the effect of the high salt intake on EAE. (Wilck et al., 2017) These findings suggest that hyperosmolarity can accelerate immunological disorders, which are based on $T_h17$ cell response, even though the disorder's localization may not necessarily be hypertonic. The high salt diet has also recently been shown to affect the gut homeostasis itself: in mice, a high salt diet induced IL-23 and IL-17 production together with increased SGK1 expression in the colon aggravating an artificially induced colitis (Aguiar et al., 2018).

Paling et al. have shown that, in patients suffering from MS, sodium concentrations are increased not only within lesions but also within normal appearing white and cortical grey matter. Moreover, higher levels of sodium accumulation in the tissue were associated with greater disability (Paling et al., 2013). Sodium based MRI examinations are currently under discussion for the monitoring of neuroinflammation in MS (Huhn et al., 2019). An observational study by Farez et al. has demonstrated that high salt (here above 2 g per day) intake may be associated with higher exacerbation rates and a higher number of lesions in MRI in patients suffering from MS (Farez et al., 2015). However, the significance of this study is questionable as salt intake was not measured directly, but calculated based on spot measurements of urinary sodium excretion. A recent publication by Rakova et al. casts doubt on this method due to the fact that urinary sodium excretion is not directly linked to sodium intake but follows infradian rhythms (Rakova et al., 2013). Thus, conclusions about daily salt intake based on spot measurements of urinary sodium excretion may be methodically problematic. Furthermore, another observational study questioned the salt's effect on MS by finding no association between salt intake and MS incidence (Cortese et al., 2017). However, salt intake might not be the only variable to take into consideration when assessing the effect of nutrition on autoimmune diseases: certain fatty acids have been disclosed to influence the effects of sodium and have distinct effects on $T_h17$ properties (Bartolomaeus et al., 2019; Hammer et al., 2017). Hence, while animal experiments already give some insight, the extent to which sodium affects MS is still not fully understood.

Most aforementioned publications emphasize the pathogenic effects of $T_h17$ cells and consequently increased severity of related diseases in a hypertonic environment. In contrast, my findings suggest enhancement of anti-inflammatory features in the $T_h17$ cells in hyperosmotic surroundings. Therefore, it might be relevant to assess in which settings the immune system conducts pro- and anti-inflammatory reactions at the same time and place. It is known that in certain situations (e.g. during local infection) pro- and anti-inflammatory reactions coexist within a compartment. Imbalance in the ratio between $T_{reg}$ and $T_h17$ cells seems to be a relevant factor in the development of autoimmune diseases like rheumatoid arthritis (Wang et al., 2012). While there still is conflicting data starting from whether sodium intake in general is higher in patients or not, the role of sodium in the pathogenesis of rheumatoid arthritis is currently under investigation (Marouen et al., 2017; Scrivo et al., 2019; Vitales-Noyola et al., 2018). $T_{reg}$ cells are present in sites of inflammation and control the immune response by modulating antigen presenting cells and directly regulating other T cells (Belkaid, 2007). The regulation of other innate and adaptive immune cells plays a significant role in protecting the surrounding tissue (Lei et al., 2015;

Weirather et al., 2014). Both, indirect and direct functions are often mediated by TGF-β (Belkaid, 2007; Weirather et al., 2014). Similar regulatory functions may be assumed for $T_h17$ cells in a hypertonic environment. There, FOXP3 expression is induced during the course of the inflammation, potentially to limit over-activation while concurrent inflammatory signals provide clearance of the pathogen.

Immune homeostasis is not only important during an infection but also in the prevention of autoimmune diseases. It can be hypothesized that the hypertonic environment of an inflammation induces not only pro-inflammatory characteristics but also an regulatory behavior in $T_h17$ cells. Thus, hyperosmolarity would be a crucial factor to execute a local immune response but also to contain it. Nevertheless, the definite role of hypertonicity during T helper cell-mediated inflammation remains to be fully understood. Since our models can represent neither the complex compositions nor all relevant cell interactions within the human body, further *in vivo* studies are necessary to unravel the greater picture.

## 4.2. Cytotoxic T cells gain momentum in the hypertonicity present in relevant immunological compartments

While T helper cells have been in the focus of recent investigations, the osmotic influence on cytotoxic T cells has not yet been analyzed. This is surprising as there is high promise for applications in this area, ranging from potential manipulation of cytotoxic T cells in the course of autoimmune diseases to using tonicity signals to improve adoptive T cell therapy. Only a single study by Popovic et al. investigated how antigen-presenting cells are affected by hyperosmolarity and shortly discussed what consequences this might have for $CD8^+$ T cells (Popovic et al., 2017). Thus, my findings give novel insights into the function of cytotoxic T cells and their dependence on environmental factors.

Of all findings presented in this thesis, the most remarkable one may be cytotoxic T cells demonstrating higher killing efficiency in hypertonicity. This effect is based on the phenotypical changes the cells undergo. Noteworthy, this effect does only occur when the cells enter the hypertonic environment before recognition of the target cell. It is conceivable that the intracellular mechanisms need some time to adapt to the new milieu resulting in cytotoxic T cells that are more effective. Further studies on the kinetics of the effects of hyperosmolarity are necessary to determine the exact temporal setting.

In the physiological setting of the human body, it is very plausible that cytotoxic T cells are more active and potent in hypertonic environments. Hyperosmolarity prevails especially in immunologically active compartments such as skin and infection sites (Brocker et al., 2012; Jantsch et al., 2015; Schwartz et al., 2009). These locations comprise the body spaces where immune responses should be the fiercest due to high chance of pathogen encounter. In consequence, the finding of highly active and potent cytotoxic T cells in a hypertonic environment can be anticipated. The human body may respond to increased hazards in sites of high osmolarity by augmenting cytotoxic functions of T cells to support successful protection. Likewise, increased cytolytic T cell function is not required and may actually be counterproductive in isosmotic environments like the plasma where increased immunological response can lead to severe disorders such as the systemic inflammatory response syndrome (Davies and Hagen, 1997). Similarly, this finding may contribute to the understanding how the immune system prevents tumor growth. As indicated before, tumor sites also show increased osmolarity (Baronzio et al., 2012; McGrail et al., 2015). Thus, advanced cytotoxic T cell function may analogously contribute to the eradication of most tumor cells before their definitive settlement. A very recent study demonstrated that feeding mice a high salt diet inhibited their tumor growth. Even though higher amounts of TNF-α and IFN-γ have been found in the high salt diet tumors, the corresponding effect was shown to be independent of T cell responses but was apparently mediated by inhibition of myeloid-derived suppressor cells. Unfortunately, functional analysis of the impact of cytotoxic T cells to the tumor suppression was not undertaken. (Willebrand et al., 2019) Consequently, my finding of highly active and potent cytotoxic T cells in hypertonicity may contribute to the understanding how the immune system can enhance its response when needed.

The interaction between lymphocyte function and cell metabolism is one of the main interests of current research underlining the importance of metabolic changes as a driver of cell function. In the resting state, T cells mainly rely on fatty acid β-oxidation and oxidative phosphorylation. However, upon initiation of TCR-mediated signaling, cells perform a metabolic switch towards T cell activation based essentially on aerobic glycolysis while fatty acid β-oxidation is largely reduced. (Pearce et al., 2013) Wang et al. suggested that oxidative phosphorylation remains engaged and is in fact a critical factor for T cell activation (Wang et al., 2011). However, in the microenvironment of a tumor, access to glucose may be reduced. Tumor cells, in contrast to most of other body cells, use mainly anaerobic glycolysis and fermentation to produce ATP. This phenomenon is called the Warburg effect. (Liberti and Locasale, 2016) Thus, tumors deprive glucose from their surroundings. Consequently, the limited availability of glucose in the tumor

microenvironment dampens cytolytic T cell functions by modifying T cell metabolism and the ability to produce relevant cytokines (Chang et al., 2015). Among other things, this may represent a part of a tumor evasion mechanism used to escape immune responses. Still, recent findings suggest that cytotoxic T cells can regain tumor killing functionality by promoting fatty acid β-oxidation after having limited access to glucose and oxygen (Zhang et al., 2017). My findings demonstrate that cytotoxic T cells augment their metabolic throughput in hypertonicity by upregulating glycolysis as well as oxidative phosphorylation. This does not only reflect the higher states of activation in the T cells but may also illustrate adaptations of the immune system to overcome immune evasion and regain functionality even in a setting where T cell functions are being suppressed. If T cells can at least partially rely on fatty acid β-oxidation to remain functional, increased oxidative phosphorylation in the hypertonic tumor microenvironment may provide a relevant source of energy.

Unfortunately, detailed analysis of the mechanism leading to the effects of hypertonicity on $CD8^+$ T cells is still unresolved. In 2012, a study by Lee et al. found that the nematode homolog of RUNX3, RNT-1, is regulated and stabilized by p38 MAP kinase (Lee et al., 2012). A similar pathway is conceivable in humans, where p38 MAP kinase is known to regulate cellular adaption to extracellular stress (Obata et al., 2000). I have shown that NFAT5 and SGK1 are significantly upregulated in cytotoxic T cells in hypertonicity. Both molecules are positioned downstream of p38 MAP kinase which has been shown to play a pivotal role in mediating the effects of hyperosmolarity on $CD4^+$ T cells (Kleinewietfeld et al., 2013). Hence, a comparable pathway for inducing T cell activation and boosting cytotoxic functions via RUNX3 in $CD8^+$ T cells is possible. Unfortunately, the direct roles of p38 MAP kinase, NFAT5 and SGK1 in regulating the tonicity's effects on $CD8^+$ T cells were not determinable in my studies because the application of shRNA altered the cells' response, in general. Future studies in this regard may include animal models with application of respective knockouts.

### 4.2.1. Enhancement of cytotoxic features in hypertonicity can be beneficial or maleficent

As aforementioned, increased functionality of cytolytic T cells in certain hyperosmotic compartments may be part of the natural defense mechanisms against pathogens and cell malignancies. While sensitive compartments should be protected from overwhelming immune reactions, strong responses are necessary to fight off infections in some tissues such as lymphoid tissue and skin. The antimicrobial barrier function of the skin has already been described to be

expanded by a hypertonicity-mediated functional activation of macrophages (Jantsch et al., 2015). A hypertonic environment increases NO release in macrophages challenged with lipopolysaccharides or cytokines leading to macrophage activation. Consequently, mice fed with high salt diet show facilitated clearance of cutaneous leishmanial infection which depends on macrophage functionality (Jantsch et al., 2015). Since my findings demonstrate increased cytotoxic function of $CD8^+$ T cells in hypertonicity, they may similarly help to improve the skin barrier with its hyperosmotic microenvironment. Among others, the prominent cytolytic function of $CD8^+$ T cells is especially relevant in viral infections. The strong activation of both, cytotoxic T cells and macrophages, in hyperosmotic environments may contribute to an enhanced barrier function of the skin against various kinds of pathogens.

A recent study investigated the effects of osmolarity on dendritic cells and their ability to activate $CD8^+$ T cells (Popovic et al., 2017). They found that hypertonicity affects the behavior of dendritic cells and diminishes their ability to activate $CD8^+$ T cells in a NFAT5-independent manner. However, the conductors of the study only examined the behavior of dendritic cells and analyzed their reaction to hyperosmolarity while the cytotoxic T cells were not exposed to this hypertonic environment. Thus, this did not reflect the physiological setting where both cell types reside within a hyperosmotic micromilieu during an inflammation. Furthermore, the T cell reaction was evaluated by measuring levels of IFN-γ which I have found to remain unaltered in hypertonicity even though the cytotoxic function of the $CD8^+$ T cells is highly induced. Therefore, the overall effect of changes in dendritic cells by tonicity signals and its impact on T cell function remain unclear.

Nevertheless, there are increasing indications suggesting that enhanced cytolytic function of $CD8^+$ T cells in hypertonicity might very well be problematic in the course of autoimmune diseases. There is growing interest in the role of cytotoxic T cells in numerous autoimmune diseases, such as diabetes mellitus type 1, rheumatoid arthritis and MS (Bulek et al., 2012; Walter and Santamaria, 2005). Since the osmolarity is increased in lesions of patients suffering from MS (Paling et al., 2013), it is conceivable that the hyperosmolarity-based enhancement of cytotoxic T cell functions may be involved in the disease's pathophysiology. Indeed, it is known that $CD8^+$ T cells outnumber the $CD4^+$ T cells in MS lesions (Babbe et al., 2000). MHC class I genes in neurons and glia cells are highly upregulated within MS lesions (Höftberger et al., 2004). Consequently, the magnitude of acute axonal injury in MS has been shown to be correlated with the number of infiltrating $CD8^+$ T cells (Bitsch et al., 2000). The infiltrating $CD8^+$ T cells have been found to express high levels of granzyme B as well as IFN-γ (Salou et al., 2015). Increased expression of

granzyme B in hyperosmolarity represents one of my findings building the basis for the enhanced cytolytic function of $CD8^+$ T cells. Thus, it is plausible to relate increased cytotoxic functions in hypertonicity with the hypertonic milieu in MS lesions. It is, however, relevant to notice that the definite role of cytotoxic T cells in MS is still unclear (Sinha et al., 2015). Further investigation in mouse models should reveal the role of tonicity in MS/EAE influencing cytotoxic T cells reactions in order to unlock the understanding of its pathophysiology and subsequently to help prevent its occurrence.

### 4.2.2. Considering tonicity in T cell therapy

Adoptive T cell transfer represents a novel approach in cancer immunotherapy. In its most simple setup, T cells are taken from a patient suffering from cancer. The cells are then searched for tumor antigen-specific T cells that are subsequently stimulated and expanded *ex vivo* for days to weeks, typically using αCD3/αCD28 signals as well as IL-2-stimuli. After sufficient expansion, the tumor-specific T cells are transfused back into the patient where they exert curative effects on different kinds of cancer like leukemia and melanoma (Rosenberg, 2012). Many different tested techniques exist when it comes to T cell selection or expansion. To obtain tumor-specific T cells, these can either be taken from resected tumor tissue, sorted from PBMCs or transduced to express artificial TCRs or chimeric antigen receptors (CARs) (Brenner and Heslop, 2010). Based on the selection method, different expansion protocols can be applied with considerable consequences for the resulting T cells (Ghaffari et al., 2019). Short-term *ex vivo* expansion is desired to keep the cells both functional and proliferative (Rasmussen et al., 2010).

My findings demonstrate that lysis rates of target tumor cells can be boosted by up to 30 % if the tumor-specific cytotoxic T cells are stimulated in hyperosmotic medium. This may not only lead to improved remission rates but also decrease the time necessary for cell expansion. However, to estimate the practicability, it will be essential to determine the durability of the demonstrated effects. Furthermore, the influence of hyperosmolarity on memory T cell formation behavior has to be analyzed since the composition of central memory and effector memory T cells is highly relevant for the long-term outcome (Rasmussen et al., 2010; Sallusto et al., 2004). Nevertheless, my findings endorse the idea to use hyperosmotic medium during *ex vivo* expansion in order to boost cytotoxic T cell functions for adoptive T cell therapy.

In conclusion, I was able to show that cytotoxic T cells demonstrate higher levels of activation and express more effector cytokines in hyperosmotic environments, resulting in increased immune

function and enhanced cytolytic capacity. This effect may be part of the defense mechanisms against pathogens in immunologically active tissue and on body surfaces. Possible applications of this finding range from relief of autoimmune disease to adoptive T cell therapy. Together with the findings in $T_h17$ cells, my results indicate that *in vitro* studies solely performed in isotonic environments are insufficient to reproduce natural conditions making the consideration of tonicity highly relevant to obtain reliable and translational results.

## 5. Abbreviations

| | |
|---|---|
| ATP | Adenosine triphosphate |
| BSA | Bovine serum albumin |
| CAR | chimeric antigen receptors |
| CCCP | Carbonyl cyanide 3-chlorophenyl hydrazone |
| CCR | Chemokine receptor |
| CD | Cluster of differentiation |
| CF | Cystic fibrosis |
| CFSE | Carboxyfluorescein succinimidyl ester |
| CI | Cell index |
| $C_t$ | Cycle threshold |
| CTL | Cytotoxic T cell |
| CXCR | CXC chemokine receptor |
| DMEM | Dulbecco's modified eagle's medium |
| DMSO | Dimethyl sulphoxide |
| DNA | Deoxyribonucleic acid |
| EAE | Experimental autoimmune encephalomyelitis |
| ECAR | Extracellular acidification rate |
| EDTA | Ethylenediaminetetraacetic acid |
| FACS | Fluorescence-activated cell sorting |
| FasL (*FASLG*) | Fas ligand |
| FCS | Fetal calf serum / fetal bovine serum |
| FOXP3 | Forkhead box P3 |
| Grz | Granzyme |
| HIV | Human immunodeficiency virus |
| HS | Human serum |
| IFN | Interferon |
| IL | Interleukin |
| LAMP1 (CD107a) | Lysosome-associated membrane protein 1 |
| LB | Lysogeny broth |
| mAbs | Monoclonal antibodies |
| MACS | Magnetic cell separation |

| | |
|---|---|
| MAP | Mitogen-activated protein |
| MART-1 | Melanoma antigen recognized by T cells 1 |
| MFI | Mean fluorescence intensity |
| MHC | Major histocompatibility complex |
| MS | Multiple sclerosis |
| NaCl | Sodium chloride |
| nCI | Normalized cell index |
| NFAT5 | Nuclear factor of activated T cells 5 |
| NFκB | Nuclear factor kappa of activated B cells |
| ns | Not significant |
| OCR | Oxygen consumption rate |
| PBMCs | Peripheral blood mononuclear cells |
| PBS | Phosphate buffered saline |
| PD-1 | Programmed cell death protein 1 |
| PHA | Phytohemagglutinin |
| PMA | Phorbol 12-myristate 13-acetate |
| qPCR | Quantitative real-time polymerase chain reaction |
| RNA | Ribonucleic acid |
| RORγt (*RORC*) | RAR-related orphan receptor-γt |
| RPMI | Roswell Park memorial institute medium |
| RUNX3 | Runt-related transcription factor 3 |
| SGK1 | Serum and glucocorticoid-regulated kinase 1 |
| shRNA | Small hairpin RNA |
| TCR | T cell receptor |
| TGF | Transforming growth factor |
| $T_h1$ cell | T helper 1 cell |
| $T_h17$ cell | T helper 17 cell |
| $T_h2$ cell | T helper 2 cells |
| TNF | Tumor necrosis factor |
| TRAIL (*TNFSF10*) | TNF-related apoptosis-inducing ligand |
| $T_{reg}$ | Regulatory T cell |
| α | Anti |

## 6. Bibliography

Abbey, J.L., O'Neill, H.C., 2007. Expression of T-cell receptor genes during early T-cell development. Immunol. Cell Biol. 86, 166–174.

Acosta-Rodriguez, E.V., Rivino, L., Geginat, J., Jarrossay, D., Gattorno, M., Lanzavecchia, A., Sallusto, F., Napolitani, G., 2007. Surface phenotype and antigenic specificity of human interleukin 17–producing T helper memory cells. Nat. Immunol. 8, 639–646.

Agata, Y., Kawasaki, A., Nishimura, H., Ishida, Y., Tsubata, T., Yagita, H., Honjo, T., 1996. Expression of the PD-1 antigen on the surface of stimulated mouse T and B lymphocytes. Int. Immunol. 8, 765–772.

Aguiar, S.L.F., Miranda, M.C.G., Guimarães, M.A.F., Santiago, H.C., Queiroz, C.P., Cunha, P. da S., Cara, D.C., Foureaux, G., Ferreira, A.J., Cardoso, V.N., Barros, P.A., Maioli, T.U., Faria, A.M.C., 2018. High-Salt Diet Induces IL-17-Dependent Gut Inflammation and Exacerbates Colitis in Mice. Front. Immunol. 8, 1969.

Aktas, E., Kucuksezer, U.C., Bilgic, S., Erten, G., Deniz, G., 2009. Relationship between CD107a expression and cytotoxic activity. Cell. Immunol. 254, 149–154.

Allenspach, E., Rawlings, D.J., Scharenberg, A.M., 1993-2016. X-Linked Severe Combined Immunodeficiency, in: Adam, M.P., Ardinger, H.H., Pagon, R.A., Wallace, S.E., Bean, L.J., Mefford, H.C., Stephens, K., Amemiya, A., Ledbetter, N. (Eds.), GeneReviews(®). University of Washington, Seattle, Seattle (WA). (Accessed November 05 2017, at https://www.ncbi.nlm.nih.gov/books/NBK1410/)

Altman, J.D., Moss, P.A., Goulder, P.J., Barouch, D.H., McHeyzer-Williams, M.G., Bell, J.I., McMichael, A.J., Davis, M.M., 1996. Phenotypic analysis of antigen-specific T lymphocytes. Science 274, 94–96.

Annunziato, F., Romagnani, S., 2009. Heterogeneity of human effector CD4+ T cells. Arthritis Res. Ther. 11, 257.

Babbe, H., Roers, A., Waisman, A., Lassmann, H., Goebels, N., Hohlfeld, R., Friese, M., Schröder, R., Deckert, M., Schmidt, S., Ravid, R., Rajewsky, K., 2000. Clonal Expansions of Cd8+ T Cells Dominate the T Cell Infiltrate in Active Multiple Sclerosis Lesions as Shown by Micromanipulation and Single Cell Polymerase Chain Reaction. J. Exp. Med. 192, 393–404.

Baronzio, G., Schwartz, L., Kiselevsky, M., Guais, A., Sanders, E., Milanesi, G., Baronzio, M., Freitas, I., 2012. Tumor interstitial fluid as modulator of cancer inflammation, thrombosis, immunity and angiogenesis. Anticancer Res. 32, 405–414.

Barry, M., Bleackley, R.C., 2002. Cytotoxic T lymphocytes: all roads lead to death. Nat. Rev. Immunol. 2, 401–409.

Bartolomaeus, H., Balogh, A., Yakoub, M., Homann, S., Markó, L., Höges, S., Tsvetkov, D., Krannich, A., Wundersitz, S., Avery, E.G., Haase, N., Kräker, K., Hering, L., Maase, M., Kusche-Vihrog, K., Grandoch, M., Fielitz, J., Kempa, S., Gollasch, M., Zhumadilov, Z., Kozhakhmetov, S., Kushugulova, A., Eckardt, K.-U., Dechend, R., Rump, L.C., Forslund, S.K., Müller, D.N., Stegbauer, J., Wilck, N., 2019. Short-Chain Fatty Acid Propionate Protects From Hypertensive Cardiovascular Damage. Circulation 139, 1407–1421.

Belkaid, Y., 2007. Regulatory T cells and infection: a dangerous necessity. Nat. Rev. Immunol. 7, 875-888.

Bitsch, A., Schuchardt, J., Bunkowski, S., Kuhlmann, T., Brück, W., 2000. Acute axonal injury in multiple sclerosisCorrelation with demyelination and inflammation. Brain 123, 1174–1183.

Boehm, U., Klamp, T., Groot, M., Howard, J.C., 1997. Cellular responses to interferon-gamma. Annu. Rev. Immunol. 15, 749–795.

Brenner, M.K., Heslop, H.E., 2010. Adoptive T Cell Therapy of Cancer. Curr. Opin. Immunol. 22, 251–257.

Brocker, C., Thompson, D.C., Vasiliou, V., 2012. The role of hyperosmotic stress in inflammation and disease. Biomol. Concepts 3, 345–364.

Bulek, A.M., Cole, D.K., Skowera, A., Dolton, G., Gras, S., Madura, F., Fuller, A., Miles, J.J., Gostick, E., Price, D.A., Drijfhout, J.W., Knight, R.R., Huang, G.C., Lissin, N., Molloy, P.E., Wooldridge, L., Jakobsen, B.K., Rossjohn, J., Peakman, M., Rizkallah, P.J., Sewell, A.K., 2012. Structural basis for the killing of human beta cells by $CD8^+$ T cells in type 1 diabetes. Nat. Immunol. 13, 283-289.

Busam, K.J., Chen, Y.T., Old, L.J., Stockert, E., Iversen, K., Coplan, K.A., Rosai, J., Barnhill, R.L., Jungbluth, A.A., 1998. Expression of melan-A (MART1) in benign melanocytic nevi and primary cutaneous malignant melanoma. Am. J. Surg. Pathol. 22, 976–982.

Busch, D.H., Pilip, I., Pamer, E.G., 1998. Evolution of a complex T cell receptor repertoire during primary and recall bacterial infection. J. Exp. Med. 188, 61–70.

Chang, C.-H., Qiu, J., O'Sullivan, D., Buck, M.D., Noguchi, T., Curtis, J.D., Chen, Q., Gindin, M., Gubin, M.M., van der Windt, G.J.W., Tonc, E., Schreiber, R.D., Pearce, E.J., Pearce, E.L., 2015. Metabolic Competition in the Tumor Microenvironment Is a Driver of Cancer Progression. Cell 162, 1229–1241.

Chellappa, S., Hugenschmidt, H., Hagness, M., Line, P.D., Labori, K.J., Wiedswang, G., Taskén, K., Aandahl, E.M., 2015. Regulatory T cells that co-express RORγt and FOXP3 are pro-inflammatory and immunosuppressive and expand in human pancreatic cancer. Oncoimmunology 5, e1102828.

Chicaybam, L., Sodre, A.L., Curzio, B.A., Bonamino, M.H., 2013. An efficient low cost method for gene transfer to T lymphocytes. PloS One 8, e60298.

Cortese, M., Yuan, C., Chitnis, T., Ascherio, A., Munger, K.L., 2017. No association between dietary sodium intake and the risk of multiple sclerosis. Neurology 89, 1322–1329.

Cruz-Guilloty, F., Pipkin, M.E., Djuretic, I.M., Levanon, D., Lotem, J., Lichtenheld, M.G., Groner, Y., Rao, A., 2009. Runx3 and T-box proteins cooperate to establish the transcriptional program of effector CTLs. J. Exp. Med. 206, 51–59.

Curtis, M.M., Way, S.S., 2009. Interleukin-17 in host defence against bacterial, mycobacterial and fungal pathogens. Immunology 126, 177–185.

Davies, M.G., Hagen, P.O., 1997. Systemic inflammatory response syndrome. Br. J. Surg. 84, 920–935.

Divakaruni, A.S., Paradyse, A., Ferrick, D.A., Murphy, A.N., Jastroch, M., 2014. Analysis and Interpretation of Microplate-Based Oxygen Consumption and pH Data, in: Methods in Enzymology. Elsevier, pp. 309–354.

Falschlehner, C., Emmerich, C.H., Gerlach, B., Walczak, H., 2007. TRAIL signalling: decisions between life and death. Int. J. Biochem. Cell Biol. 39, 1462–1475.

Farez, M.F., Fiol, M.P., Gaitán, M.I., Quintana, F.J., Correale, J., 2015. Sodium intake is associated with increased disease activity in multiple sclerosis. J. Neurol. Neurosurg. Psychiatry 86, 26–31.

Feng, D., Nagy, J.A., Dvorak, A.M., Dvorak, H.F., 2000. Different pathways of macromolecule extravasation from hyperpermeable tumor vessels. Microvasc. Res. 59, 24–37.

Fitch, E., Harper, E., Skorcheva, I., Kurtz, S.E., Blauvelt, A., 2007. Pathophysiology of Psoriasis: Recent Advances on IL-23 and Th17 Cytokines. Curr. Rheumatol. Rep. 9, 461–467.

Fletcher, J., Lalor, S., Sweeney, C., Tubridy, N., Mills, K., 2010. T cells in multiple sclerosis and experimental autoimmune encephalomyelitis: T cells in MS and EAE. Clin Exp Immunol. 162, 1-11.

Gagliani, N., Vesely, M.C.A., Iseppon, A., Brockmann, L., Xu, H., Palm, N.W., de Zoete, M.R., Licona-Limón, P., Paiva, R.S., Ching, T., Weaver, C., Zi, X., Pan, X., Fan, R., Garmire, L.X., Cotton, M.J., Drier, Y., Bernstein, B., Geginat, J., Stockinger, B., Esplugues, E., Huber, S., Flavell, R.A., 2015. Th17 cells transdifferentiate into regulatory T cells during resolution of inflammation. Nature 523, 221–225.

Garboczi, D.N., Ghosh, P., Utz, U., Fan, Q.R., Biddison, W.E., Wiley, D.C., 1996a. Structure of the complex between human T-cell receptor, viral peptide and HLA-A2. Nature 384, 134–141.

Garboczi, D.N., Utz, U., Ghosh, P., Seth, A., Kim, J., VanTienhoven, E.A., Biddison, W.E., Wiley, D.C., 1996b. Assembly, specific binding, and crystallization of a human TCR-alphabeta with an antigenic Tax peptide from human T lymphotropic virus type 1 and the class I MHC molecule HLA-A2. J. Immunol. Baltim. Md 1950 157, 5403–5410.

Ghaffari, S., Torabi-Rahvar, M., Omidkhoda, A., Ahmadbeigi, N., 2019. Impact of Various Culture Conditions on Ex Vivo Expansion of Polyclonal T-cells for Adoptive Immunotherapy. APMIS Acta Pathol. Microbiol. Immunol. Scand. https://doi.org/10.1111/apm.12981 [Epub ahead of print]

Go, W.Y., Liu, X., Roti, M.A., Liu, F., Ho, S.N., 2004. NFAT5/TonEBP mutant mice define osmotic stress as a critical feature of the lymphoid microenvironment. Proc. Natl. Acad. Sci. U. S. A. 101, 10673–10678.

Guicciardi, M.E., Gores, G.J., 2009. Life and death by death receptors. FASEB J. 23, 1625–1637.

Gutcher, I., Donkor, M.K., Ma, Q., Rudensky, A.Y., Flavell, R.A., Li, M.O., 2011. Autocrine Transforming Growth Factor-β1 Promotes in vivo Th17 Cell Differentiation. Immunity 34, 396–408.

Halle, S., Keyser, K.A., Stahl, F.R., Busche, A., Marquardt, A., Zheng, X., Galla, M., Heissmeyer, V., Heller, K., Boelter, J., Wagner, K., Bischoff, Y., Martens, R., Braun, A., Werth, K., Uvarovskii, A., Kempf, H., Meyer-Hermann, M., Arens, R., Kremer, M., Sutter, G., Messerle, M., Förster, R., 2016. In Vivo Killing Capacity of Cytotoxic T Cells Is Limited and Involves Dynamic Interactions and T Cell Cooperativity. Immunity 44, 233–245.

Hammer, A., Schliep, A., Jörg, S., Haghikia, A., Gold, R., Kleinewietfeld, M., Müller, D.N., Linker, R.A., 2017. Impact of combined sodium chloride and saturated long-chain fatty acid challenge on the differentiation of T helper cells in neuroinflammation. J. Neuroinflammation 14, 184.

Harrington, L.E., Hatton, R.D., Mangan, P.R., Turner, H., Murphy, T.L., Murphy, K.M., Weaver, C.T., 2005. Interleukin 17–producing CD4+ effector T cells develop via a lineage distinct from the T helper type 1 and 2 lineages. Nat. Immunol. 6, 1123–1132.

Hernandez, A.L., Kitz, A., Wu, C., Lowther, D.E., Rodriguez, D.M., Vudattu, N., Deng, S., Herold, K.C., Kuchroo, V.K., Kleinewietfeld, M., Hafler, D.A., 2015. Sodium chloride inhibits the suppressive function of FOXP3+ regulatory T cells. J. Clin. Invest. 125, 4212–4222.

Höftberger, R., Aboul-Enein, F., Brueck, W., Lucchinetti, C., Rodriguez, M., Schmidbauer, M., Jellinger, K., Lassmann, H., 2004. Expression of major histocompatibility complex class I molecules on the different cell types in multiple sclerosis lesions. Brain Pathol. Zurich Switz. 14, 43–50.

Huang, L., Crothers, K.A., 2009. HIV-associated Opportunistic Pneumonias. Respirol. Carlton Vic 14, 474–485.

Huhn, K., Engelhorn, T., Linker, R.A., Nagel, A.M., 2019. Potential of Sodium MRI as a Biomarker for Neurodegeneration and Neuroinflammation in Multiple Sclerosis. Front. Neurol. 10, 84.

Inglese, M., Madelin, G., Oesingmann, N., Babb, J.S., Wu, W., Stoeckel, B., Herbert, J., Johnson, G., 2010. Brain tissue sodium concentration in multiple sclerosis: a sodium imaging study at 3 tesla. Brain 133, 847–857.

Ishimura, N., Isomoto, H., Bronk, S.F., Gores, G.J., 2006. Trail induces cell migration and invasion in apoptosis-resistant cholangiocarcinoma cells. Am. J. Physiol. Gastrointest. Liver Physiol. 290, G129-136.

Janeway, C., Travers, P., Walport, M., Shlomchik, M.J., 2001a. The recognition and effector mechanisms of adaptive immunity, in Immunobiology: The Immune System in Health and Disease. 5th edition. New York: Garland Science. (Accessed November 4 2017 at https://www.ncbi.nlm.nih.gov/books/NBK27124/)

Janeway, C., Travers, P., Walport, M., Shlomchik, M.J., 2001b. Principles of innate and adaptive immunity, in Immunobiology: The Immune System in Health and Disease. 5th edition. New York: Garland Science. (Accessed November 4 2017 at https://www.ncbi.nlm.nih.gov/books/NBK27090/)

Janeway, C., Travers, P., Walport, M., Shlomchik, M.J., 2001c. T cell-mediated cytotoxicity, in Immunobiology: The Immune System in Health and Disease. 5th edition. New York: Garland Science. (Accessed November 14 2017 at https://www.ncbi.nlm.nih.gov/books/NBK27101/)

Jantsch, J., Schatz, V., Friedrich, D., Schröder, A., Kopp, C., Siegert, I., Maronna, A., Wendelborn, D., Linz, P., Binger, K.J., Gebhardt, M., Heinig, M., Neubert, P., Fischer, F., Teufel, S., David, J.-P., Neufert, C., Cavallaro, A., Rakova, N., Küper, C., Beck, F.-X., Neuhofer, W., Muller, D.N., Schuler, G., Uder, M., Bogdan, C., Luft, F.C., Titze, J., 2015. Cutaneous Na+ Storage Strengthens the Antimicrobial Barrier Function of the Skin and Boosts Macrophage-Driven Host Defense. Cell Metab. 21, 493–501.

Kagami, S., Rizzo, H.L., Lee, J.J., Koguchi, Y., Blauvelt, A., 2010. Circulating Th17, Th22, and Th1 cells are increased in psoriasis. J. Invest. Dermatol. 130, 1373–1383.

Kalliolias, G.D., Ivashkiv, L.B., 2016. TNF biology, pathogenic mechanisms and emerging therapeutic strategies. Nat. Rev. Rheumatol. 12, 49–62.

Kebir, H., Kreymborg, K., Ifergan, I., Dodelet-Devillers, A., Cayrol, R., Bernard, M., Giuliani, F., Arbour, N., Becher, B., Prat, A., 2007. Human TH17 lymphocytes promote blood-brain barrier disruption and central nervous system inflammation. Nat. Med. 13, 1173–1175.

Kim, Jimyung, Kang, S., Kim, Jinhyun, Kwon, G., Koo, S., 2013. Elevated Levels of T Helper 17 Cells Are Associated with Disease Activity in Patients with Rheumatoid Arthritis. Ann. Lab. Med. 33, 52–59.

Kim, M.T., Harty, J.T., 2014. Impact of Inflammatory Cytokines on Effector and Memory CD8+ T Cells. Front. Immunol. 5, 295.

Kimura, A., Kishimoto, T., 2010. IL-6: Regulator of Treg/Th17 balance. Eur. J. Immunol. 40, 1830–1835.

Kleinewietfeld, M., Manzel, A., Titze, J., Kvakan, H., Yosef, N., Linker, R.A., Muller, D.N., Hafler, D.A., 2013. Sodium chloride drives autoimmune disease by the induction of pathogenic TH17 cells. Nature 496, 518–522.

Kmieciak, M., Gowda, M., Graham, L., Godder, K., Bear, H.D., Marincola, F.M., Manjili, M.H., 2009. Human T cells express CD25 and Foxp3 upon activation and exhibit effector/memory phenotypes without any regulatory/suppressor function. J. Transl. Med. 7, 89.

Kopp, C., Linz, P., Dahlmann, A., Hammon, M., Jantsch, J., Müller, D.N., Schmieder, R.E., Cavallaro, A., Eckardt, K.-U., Uder, M., Luft, F.C., Titze, J., 2013. 23Na magnetic resonance imaging-determined tissue sodium in healthy subjects and hypertensive patients. Hypertens. Dallas Tex 1979 61, 635–640.

Kopp, C., Linz, P., Wachsmuth, L., Dahlmann, A., Horbach, T., Schöfl, C., Renz, W., Santoro, D., Niendorf, T., Müller, D.N., Neininger, M., Cavallaro, A., Eckardt, K.-U., Schmieder, R.E., Luft, F.C., Uder, M., Titze, J., 2012. 23Na Magnetic Resonance Imaging of Tissue Sodium. Hypertension 59, 167–172.

Kotake, S., Udagawa, N., Takahashi, N., Matsuzaki, K., Itoh, K., Ishiyama, S., Saito, S., Inoue, K., Kamatani, N., Gillespie, M.T., Martin, T.J., Suda, T., 1999. IL-17 in synovial fluids from patients with rheumatoid arthritis is a potent stimulator of osteoclastogenesis. J. Clin. Invest. 103, 1345–1352.

Lee, K., Shim, J., Bae, J., Kim, Y.-J., Lee, J., 2012. Stabilization of RNT-1 Protein, Runt-related Transcription Factor (RUNX) Protein Homolog of Caenorhabditis elegans, by Oxidative Stress through Mitogen-activated Protein Kinase Pathway. J. Biol. Chem. 287, 10444–10452.

Legembre, P., Barnhart, B.C., Peter, M.E., 2004. The relevance of NF-kappaB for CD95 signaling in tumor cells. Cell Cycle Georget. Tex 3, 1235–1239.

Lei, H., Schmidt-Bleek, K., Dienelt, A., Reinke, P., Volk, H.-D., 2015. Regulatory T cell-mediated anti-inflammatory effects promote successful tissue repair in both indirect and direct manners. Front. Pharmacol. 6, 184.

Li, Y., Wang, H., Long, Y., Lu, Z., Hu, X., 2011. Increased memory Th17 cells in patients with neuromyelitis optica and multiple sclerosis. J. Neuroimmunol. 234, 155–160.

Liberti, M.V., Locasale, J.W., 2016. The Warburg Effect: How Does it Benefit Cancer Cells? Trends Biochem. Sci. 41, 211–218.

Lock, C., Hermans, G., Pedotti, R., Brendolan, A., Schadt, E., Garren, H., Langer-Gould, A., Strober, S., Cannella, B., Allard, J., Klonowski, P., Austin, A., Lad, N., Kaminski, N., Galli, S.J., Oksenberg, J.R., Raine, C.S., Heller, R., Steinman, L., 2002. Gene-microarray analysis of multiple sclerosis lesions yields new targets validated in autoimmune encephalomyelitis. Nat. Med. 8, 500–508.

Lombard, J., 2014. Once upon a time the cell membranes: 175 years of cell boundary research. Biol. Direct 9, 32.

Lowes, M.A., Kikuchi, T., Fuentes-Duculan, J., Cardinale, I., Zaba, L.C., Haider, A.S., Bowman, E.P., Krueger, J.G., 2008. Psoriasis vulgaris lesions contain discrete populations of Th1 and Th17 T cells. J. Invest. Dermatol. 128, 1207–1211.

Marouen, S., du Cailar, G., Audo, R., Lukas, C., Vial, G., Tournadre, A., Barrat, E., Ribstein, J., Combe, B., Morel, J., Daien, C.I., 2017. Sodium excretion is higher in patients with rheumatoid arthritis than in matched controls. PloS One 12, e0186157.

Matthias, J., Maul, J., Noster, R., Meinl, H., Chao, Y.-Y., Gerstenberg, H., Jeschke, F., Gasparoni, G., Welle, A., Walter, J., Nordström, K., Eberhardt, K., Renisch, D., Donakonda, S., Knolle, P., Soll, D., Grabbe, S., Garzorz-Stark, N., Eyerich, K., Biedermann, T., Baumjohann, D., Zielinski, C.E., 2019. Sodium chloride is an ionic checkpoint for human TH2 cells and shapes the atopic skin microenvironment. Sci. Transl. Med. 11, eaau0683.

Matusevicius, D., Kivisäkk, P., He, B., Kostulas, N., Ozenci, V., Fredrikson, S., Link, H., 1999. Interleukin-17 mRNA expression in blood and CSF mononuclear cells is augmented in multiple sclerosis. Mult. Scler. Houndmills Basingstoke Engl. 5, 101–104.

McGrail, D.J., McAndrews, K.M., Brandenburg, C.P., Ravikumar, N., Kieu, Q.M.N., Dawson, M.R., 2015. Osmotic Regulation Is Required for Cancer Cell Survival under Solid Stress. Biophys. J. 109, 1334–1337.

Montoya, M.M., Maul, J., Singh, P.B., Pua, H.H., Dahlström, F., Wu, N., Huang, X., Ansel, K.M., Baumjohann, D., 2017. A Distinct Inhibitory Function for miR-18a in Th17 Cell Differentiation. J. Immunol. 199, 559–569.

Noster, R., de Koning, H., Sallusto, F., Zielinski, C., 2015. Two types of human Th17 cells with pro- and anti-inflammatory properties and distinct roles in autoinflammation. Pediatr. Rheumatol. Online J. 13, O49.

Noster, R., de Koning, H.D., Maier, E., Prelog, M., Lainka, E., Zielinski, C.E., 2016. Dysregulation of proinflammatory versus anti-inflammatory human TH17 cell functionalities in the autoinflammatory Schnitzler syndrome. J. Allergy Clin. Immunol. 138, 1161-1169.

Noubade, R., Krementsov, D.N., Del Rio, R., Thornton, T., Nagaleekar, V., Saligrama, N., Spitzack, A., Spach, K., Sabio, G., Davis, R.J., Rincon, M., Teuscher, C., 2011. Activation of p38 MAPK in CD4 T cells controls IL-17 production and autoimmune encephalomyelitis. Blood 118, 3290–3300.

Obata, T., Brown, G.E., Yaffe, M.B., 2000. MAP kinase pathways activated by stress: the p38 MAPK pathway. Crit. Care Med. 28, N67-77.

O'Connor, W., Zenewicz, L.A., Flavell, R.A., 2010. The dual nature of T(H)17 cells: shifting the focus to function. Nat. Immunol. 11, 471–476.

Oestreich, K.J., Weinmann, A.S., 2012. Master regulators or lineage-specifying? Changing views on CD4+ T cell transcription factors. Nat. Rev. Immunol. 12, 799–804.

Ouyang, W., Beckett, O., Ma, Q., Paik, J., DePinho, R.A., Li, M.O., 2010. Foxo proteins cooperatively control the differentiation of Foxp3+ regulatory T cells. Nat. Immunol. 11, 618–627.

Paling, D., Solanky, B.S., Riemer, F., Tozer, D.J., Wheeler-Kingshott, C.A.M., Kapoor, R., Golay, X., Miller, D.H., 2013. Sodium accumulation is associated with disability and a progressive course in multiple sclerosis. Brain J. Neurol. 136, 2305–2317.

Pearce, E.L., Poffenberger, M.C., Chang, C.-H., Jones, R.G., 2013. Fueling Immunity: Insights into Metabolism and Lymphocyte Function. Science 342, 1242454.

Peper, J.K., Schuster, H., Löffler, M.W., Schmid-Horch, B., Rammensee, H.-G., Stevanović, S., 2014. An impedance-based cytotoxicity assay for real-time and label-free assessment of T-cell-mediated killing of adherent cells. J. Immunol. Methods 405, 192–198.

Pepper, M., Jenkins, M.K., 2011. Origins of CD4+ effector and central memory T cells. Nat. Immunol. 12, 467-471.

Pinkoski, M.J., Hobman, M., Heibein, J.A., Tomaselli, K., Li, F., Seth, P., Froelich, C.J., Bleackley, R.C., 1998. Entry and trafficking of granzyme B in target cells during granzyme B-perforin-mediated apoptosis. Blood 92, 1044–1054.

Pittet, M.J., Valmori, D., Dunbar, P.R., Speiser, D.E., Liénard, D., Lejeune, F., Fleischhauer, K., Cerundolo, V., Cerottini, J.-C., Romero, P., 1999. High Frequencies of Naive Melan-a/Mart-1–Specific Cd8+ T Cells in a Large Proportion of Human Histocompatibility Leukocyte Antigen (Hla)-A2 Individuals. J. Exp. Med. 190, 705–716.

Popovic, Z.V., Embgenbroich, M., Chessa, F., Nordström, V., Bonrouhi, M., Hielscher, T., Gretz, N., Wang, S., Mathow, D., Quast, T., Schloetel, J.-G., Kolanus, W., Burgdorf, S., Gröne, H.-J., 2017. Hyperosmolarity impedes the cross-priming competence of dendritic cells in a TRIF-dependent manner. Sci. Rep. 7, 311.

Rakova, N., Jüttner, K., Dahlmann, A., Schröder, A., Linz, P., Kopp, C., Rauh, M., Goller, U., Beck, L., Agureev, A., Vassilieva, G., Lenkova, L., Johannes, B., Wabel, P., Moissl, U., Vienken, J., Gerzer, R., Eckardt, K.-U., Müller, D.N., Kirsch, K., Morukov, B., Luft, F.C., Titze, J., 2013. Long-term space flight simulation reveals infradian rhythmicity in human Na(+) balance. Cell Metab. 17, 125–131.

Raphael, I., Nalawade, S., Eagar, T.N., Forsthuber, T.G., 2015. T cell subsets and their signature cytokines in autoimmune and inflammatory diseases. Cytokine 74, 5–17.

Rasmussen, A.-M., Borelli, G., Hoel, H.J., Lislerud, K., Gaudernack, G., Kvalheim, G., Aarvak, T., 2010. Ex vivo expansion protocol for human tumor specific T cells for adoptive T cell therapy. J. Immunol. Methods 355, 52–60.

Ratner, A., Clark, W.R., 1993. Role of TNF-alpha in CD8+ cytotoxic T lymphocyte-mediated lysis. J. Immunol. Baltim. Md 1950 150, 4303–4314.

Richer, M.J., Nolz, J.C., Harty, J.T., 2013. Pathogen-specific inflammatory milieux tune the antigen sensitivity of CD8(+) T cells by enhancing T cell receptor signaling. Immunity 38, 140–152.

Rosenberg, S.A., 2012. Raising the bar: the curative potential of human cancer immunotherapy. Sci. Transl. Med. 4, 127ps8.

Rostami, A., Ciric, B., 2013. Role of Th17 cells in the pathogenesis of CNS inflammatory demyelination. J. Neurol. Sci. 333, 76–87.

Sallusto, F., Geginat, J., Lanzavecchia, A., 2004. Central memory and effector memory T cell subsets: function, generation, and maintenance. Annu. Rev. Immunol. 22, 745–763.

Salou, M., Nicol, B., Garcia, A., Laplaud, D.-A., 2015. Involvement of CD8+ T Cells in Multiple Sclerosis. Front. Immunol. 6, 604.

Sands, J.M., Layton, H.E., 2009. The Physiology of Urinary Concentration: an Update. Semin. Nephrol. 29, 178–195.

Sato, K., Suematsu, A., Okamoto, K., Yamaguchi, A., Morishita, Y., Kadono, Y., Tanaka, S., Kodama, T., Akira, S., Iwakura, Y., Cua, D.J., Takayanagi, H., 2006. Th17 functions as an osteoclastogenic helper T cell subset that links T cell activation and bone destruction. J. Exp. Med. 203, 2673–2682.

Schwartz, L., Guais, A., Pooya, M., Abolhassani, M., 2009. Is inflammation a consequence of extracellular hyperosmolarity? J. Inflamm. Lond. Engl. 6, 21.

Scrivo, R., Perricone, C., Altobelli, A., Castellani, C., Tinti, L., Conti, F., Valesini, G., 2019. Dietary Habits Bursting into the Complex Pathogenesis of Autoimmune Diseases: The Emerging Role of Salt from Experimental and Clinical Studies. Nutrients 11, 1013.

Sinha, S., Boyden, A.W., Itani, F.R., Crawford, M.P., Karandikar, N.J., 2015. CD8+ T-Cells as Immune Regulators of Multiple Sclerosis. Front. Immunol. 6, 619.

Takeuchi, A., Saito, T., 2017. CD4 CTL, a Cytotoxic Subset of CD4+ T Cells, Their Differentiation and Function. Front. Immunol. 8, 194.

Titze, J., 2004. Glycosaminoglycan polymerization may enable osmotically inactive Na+ storage in the skin. AJP Heart Circ. Physiol. 287, H203–H208.

Titze, J., Maillet, A., Lang, R., Gunga, H.C., Johannes, B., Gauquelin-Koch, G., Kihm, E., Larina, I., Gharib, C., Kirsch, K.A., 2002. Long-term sodium balance in humans in a terrestrial space station simulation study. Am. J. Kidney Dis. Off. J. Natl. Kidney Found. 40, 508–516.

Vignali, D.A.A., Collison, L.W., Workman, C.J., 2008. How regulatory T cells work. Nat. Rev. Immunol. 8, 523–532.

Vitales-Noyola, M., Layseca-Espinosa, E., Baranda, L., Abud-Mendoza, C., Niño-Moreno, P., Monsiváis-Urenda, A., Rosenstein, Y., González-Amaro, R., 2018. Analysis of Sodium Chloride

Intake and Treg/Th17 Lymphocytes in Healthy Individuals and Patients with Rheumatoid Arthritis or Systemic Lupus Erythematosus. J. Immunol. Res. Article ID 9627806.

Voo, K.S., Wang, Yui-Hsi, Santori, F.R., Boggiano, C., Wang, Yi-Hong, Arima, K., Bover, L., Hanabuchi, S., Khalili, J., Marinova, E., Zheng, B., Littman, D.R., Liu, Y.-J., 2009. Identification of IL-17-producing FOXP3+ regulatory T cells in humans. Proc. Natl. Acad. Sci. U. S. A. 106, 4793–4798.

Voskoboinik, I., Whisstock, J.C., Trapani, J.A., 2015. Perforin and granzymes: function, dysfunction and human pathology. Nat. Rev. Immunol. 15, 388–400.

Walter, U., Santamaria, P., 2005. CD8+ T cells in autoimmunity. Curr. Opin. Immunol. 17, 624–631.

Wang, J., Ioan-Facsinay, A., van der Voort, E.I.H., Huizinga, T.W.J., Toes, R.E.M., 2007. Transient expression of FOXP3 in human activated nonregulatory CD4+ T cells. Eur. J. Immunol. 37, 129–138.

Wang, R., Dillon, C.P., Shi, L.Z., Milasta, S., Carter, R., Finkelstein, D., McCormick, L.L., Fitzgerald, P., Chi, H., Munger, J., Green, D.R., 2011. The transcription factor Myc controls metabolic reprogramming upon T lymphocyte activation. Immunity 35, 871–882.

Wang, W., Shao, S., Jiao, Z., Guo, M., Xu, H., Wang, S., 2012. The Th17/Treg imbalance and cytokine environment in peripheral blood of patients with rheumatoid arthritis. Rheumatol. Int. 32, 887–893.

Weaver, C.T., Harrington, L.E., Mangan, P.R., Gavrieli, M., Murphy, K.M., 2006. Th17: An Effector CD4 T Cell Lineage with Regulatory T Cell Ties. Immunity 24, 677–688.

Weirather, J., Hofmann, U.D.W., Beyersdorf, N., Ramos, G.C., Vogel, B., Frey, A., Ertl, G., Kerkau, T., Frantz, S., 2014. Foxp3+ CD4+ T cells improve healing after myocardial infarction by modulating monocyte/macrophage differentiation. Circ. Res. 115, 55–67.

Wilck, N., Matus, M.G., Kearney, S.M., Olesen, S.W., Forslund, K., Bartolomaeus, H., Haase, S., Mähler, A., Balogh, A., Markó, L., Vvedenskaya, O., Kleiner, F.H., Tsvetkov, D., Klug, L., Costea, P.I., Sunagawa, S., Maier, L., Rakova, N., Schatz, V., Neubert, P., Frätzer, C., Krannich, A., Gollasch, M., Grohme, D.A., Côrte-Real, B.F., Gerlach, R.G., Basic, M., Typas, A., Wu, C., Titze, J.M., Jantsch, J., Boschmann, M., Dechend, R., Kleinewietfeld, M., Kempa, S., Bork, P.,

Linker, R.A., Alm, E.J., Müller, D.N., 2017. Salt-responsive gut commensal modulates $T_H17$ axis and disease. Nature 551, 585–589.

Willebrand, R., Hamad, I., Van Zeebroeck, L., Kiss, M., Bruderek, K., Geuzens, A., Swinnen, D., Côrte-Real, B.F., Markó, L., Lebegge, E., Laoui, D., Kemna, J., Kammertoens, T., Brandau, S., Van Ginderachter, J.A., Kleinewietfeld, M., 2019. High Salt Inhibits Tumor Growth by Enhancing Anti-tumor Immunity. Front. Immunol. 10, 1141.

Wong, C.K., Lit, L.C.W., Tam, L.S., Li, E.K.M., Wong, P.T.Y., Lam, C.W.K., 2008. Hyperproduction of IL-23 and IL-17 in patients with systemic lupus erythematosus: implications for Th17-mediated inflammation in auto-immunity. Clin. Immunol. Orlando Fla 127, 385–393.

Wu, C., Chen, Z., Xiao, S., Thalhamer, T., Madi, A., Han, T., Kuchroo, V., 2018. SGK1 Governs the Reciprocal Development of Th17 and Regulatory T Cells. Cell Rep. 22, 653-665.

Wu, C., Yosef, N., Thalhamer, T., Zhu, C., Xiao, S., Kishi, Y., Regev, A., Kuchroo, V.K., 2013. Induction of pathogenic TH17 cells by inducible salt-sensing kinase SGK1. Nature 496, 513–517.

Zhang, Y., Kurupati, R., Liu, L., Zhou, X.Y., Zhang, G., Hudaihed, A., Filisio, F., Giles-Davis, W., Xu, X., Karakousis, G.C., Schuchter, L.M., Xu, W., Amaravadi, R., Xiao, M., Sadek, N., Krepler, C., Herlyn, M., Freeman, G.J., Rabinowitz, J.D., Ertl, H.C.J., 2017. Enhancing CD8(+) T Cell Fatty Acid Catabolism within a Metabolically Challenging Tumor Microenvironment Increases the Efficacy of Melanoma Immunotherapy. Cancer Cell 32, 377-391.

Zheng, S.G., 2013. Regulatory T cells vs Th17: differentiation of Th17 versus Treg, are the mutually exclusive? Am. J. Clin. Exp. Immunol. 2, 94–106.

Zhou, L., Chong, M.M.W., Littman, D.R., 2009. Plasticity of CD4+ T Cell Lineage Differentiation. Immunity 30, 646–655.

Ziegler, S.F., Ramsdell, F., Alderson, M.R., 1994. The activation antigen CD69. Stem Cells Dayt. Ohio 12, 456–465.

Zielinski, C.E., Mele, F., Aschenbrenner, D., Jarrossay, D., Ronchi, F., Gattorno, M., Monticelli, S., Lanzavecchia, A., Sallusto, F., 2012. Pathogen-induced human TH17 cells produce IFN-γ or IL-10 and are regulated by IL-1β. Nature 484, 514–518.

## 7. Declaration of authorship / Eidesstattliche Versicherung

„Ich, Dominik Soll, versichere an Eides statt durch meine eigenhändige Unterschrift, dass ich die vorgelegte Dissertation mit dem Thema: ‚Regulation of human T cell properties by the micromilieu' selbstständig und ohne nicht offengelegte Hilfe Dritter verfasst und keine anderen als die angegebenen Quellen und Hilfsmittel genutzt habe.

Alle Stellen, die wörtlich oder dem Sinne nach auf Publikationen oder Vorträgen anderer Autoren beruhen, sind als solche in korrekter Zitierung (siehe „Uniform Requirements for Manuscripts (URM)" des ICMJE -www.icmje.org) kenntlich gemacht. Die Abschnitte zu Methodik (insbesondere praktische Arbeiten, Laborbestimmungen, statistische Aufarbeitung) und Resultaten (insbesondere Abbildungen, Graphiken und Tabellen) entsprechen den URM (s.o.) und werden von mir verantwortet.

Meine Anteile an etwaigen Publikationen zu dieser Dissertation entsprechen denen, die in der untenstehenden gemeinsamen Erklärung mit dem/der Betreuer/in angegeben sind. Sämtliche Publikationen, die aus dieser Dissertation hervorgegangen sind und bei denen ich Autor bin, entsprechen den URM (s.o.) und werden von mir verantwortet.

Die Bedeutung dieser eidesstattlichen Versicherung und die strafrechtlichen Folgen einer unwahren eidesstattlichen Versicherung (§156,161 des Strafgesetzbuches) sind mir bekannt und bewusst."

Datum Unterschrift

## 8. Curriculum vitae

Mein Lebenslauf wird aus datenschutzrechtlichen Gründen in der elektronischen Version meiner Arbeit nicht veröffentlicht.

## 9. List of publications

Berker, M., Frank, L.J., Geßner, A.L., Grassl, N., Holtermann, A.V., Höppner, S., Kraef, C., Leclaire, M.D., Maier, P., Messerer, D.A., Möhrmann, L., Nieke, J.P., Schoch, D., **Soll, D.**, Woopen, C.M., 2016. Allergies - A T cells perspective in the era beyond the TH1/TH2 paradigm. Clin Immunol. 174, 73-83.

Matthias, J., Maul, J., Noster, R., Meinl, H., Chao, Y.-Y., Gerstenberg, H., Jeschke, F., Gasparoni, G., Welle, A., Walter, J., Nordström, K., Eberhardt, K., Renisch, D., Donakonda, S., Knolle, P., **Soll, D**., Grabbe, S., Garzorz-Stark, N., Eyerich, K., Biedermann, T., Baumjohann, D., Zielinski, C.E., 2019. Sodium chloride is an ionic checkpoint for human TH2 cells and shapes the atopic skin microenvironment. Sci. Transl. Med. 11, eaau0683.

**Soll, D.**, Spira, D., Hollstein, T., Haberbosch, L., Demuth, I., Steinhagen-Thiessen, E., Bobbert, T., Spranger, J., Kassner, U., 2019. Clinical outcome of a patient with lysosomal acid lipase deficiency and first results after initiation of treatment with Sebelipase alfa: A case report. Mol Genet Metab Rep. 20, 100479.

Andrä, I., Ulrich, H., Dürr, S., **Soll, D.**, Henkel, L., Angerpointner, C., Ritter, J., Przibilla, S., Stadler, H., Effenberger, M., Busch, D.H., Schiemann, M., 2020. An Evaluation of T-Cell Functionality After Flow Cytometry Sorting Revealed p38 MAPK Activation. Cytometry A 97, 171-183.

**Soll, D.**, Guraiib, M.M., Rollins, N.C., Reis, A.A., 2020. Improving assent in health research: a rapid systematic review. BMC Med. Res. Methodol. 20, 114.

Matthias, J., Heink, S., Picard, F., Zeiträg, J., Kolz, A., Chao, Y.Y., **Soll, D.**, de Almeida, G.P., Glasmacher, E., Jacobsen, I.D., Riedel, T., Peters, A., Floess, S., Huehn, J., Baumjohann, D., Huber, M., Korn, T., Zielinski, C.E., 2020. Salt generates antiinflammatory Th17 cells but amplifies pathogenicity in proinflammatory cytokine microenvironments. J. Clin. Invest., 137786.

## 10. Acknowledgements

Im Folgenden möchte ich mich bei allen Personen bedanken, die mich bei der Erstellung dieser Dissertation unterstützt haben.

Meiner Doktormutter Prof. Dr. Christina Zielinski danke ich für die Aufnahme in die Arbeitsgruppe in München und die Bereitstellung des äußerst interessanten Themas. Mein Dank gilt ihrer Unterstützung, die mir während meiner Zeit als Doktorand entgegengebracht wurde.

Bei meinem Charité-internen Betreuer Prof. Dr. Lutz Harms möchte ich mich für die sehr hilfsbereite Betreuung aus Berlin sowie für die großartige Unterstützung bei der Eröffnung des Promotionsverfahrens bedanken.

Ebenso danke ich den Gutachterinnen und Gutachtern dieser Arbeit.

Zudem bedanke ich mich bei allen Kolleginnen und Kollegen der AG Zielinski für die fachliche und persönliche Unterstützung während meiner Zeit im Labor. Julia Matthias gilt besonderer Dank für ihre hervorragende vorausgegangene Arbeit an dem $T_h17$-Salz-Projekt. Mein herausragender Dank gebührt Dr. Mateusz Poltorak, der mich als betreuender Post-Doc und als Kollege professionell und auch persönlich unterstützt und gefördert hat. Ich danke außerdem Dr. Patrick Rämer für die Unterstützung beim lentiviralen Gene silencing, Manuel Effenberger für die Hilfe bei der Durchführung der T cell nucleofection sowie der Tetramer sorts, Dr. Kerstin Lohr für die Einführung in die Arbeit mit dem Seahorse device und Dr. Nina Böttinger für die Einführung in das xCELLigence device. Den Genannten danke ich ebenso für die Diskussion meiner Ergebnisse aus den jeweiligen Methoden. Für die Hilfe bei allen Cell Sortings danke ich Lynette Henkel sowie Immanuel Andrä. Meinen Berliner Kommilitonen Philip, Martin und Jan danke ich für die immerwährenden, kritischen Auseinandersetzungen über die letzten gemeinsamen Jahre.

Abschließend gilt mein besonderer Dank meinen Eltern, Winfried und Petra, die mich auf meinem bisherigen Weg immer in großem Vertrauen unterstützt und gefördert haben. Meinem Bruder Sebastian, meiner Schwägerin Marie und meinem Neffen Leonard danke ich für die vielen schönen Zeiten während der Arbeit an dieser Dissertation.